EARTHQUAKE ENGINEERING RESEARCH CENTER

EVALUATION OF SEISMIC PERFORMANCE OF A TEN-STORY RC BUILDING DURING THE WHITTIER NARROWS EARTHQUAKE

by

EDUARDO MIRANDA
VITELMO V. BERTERO
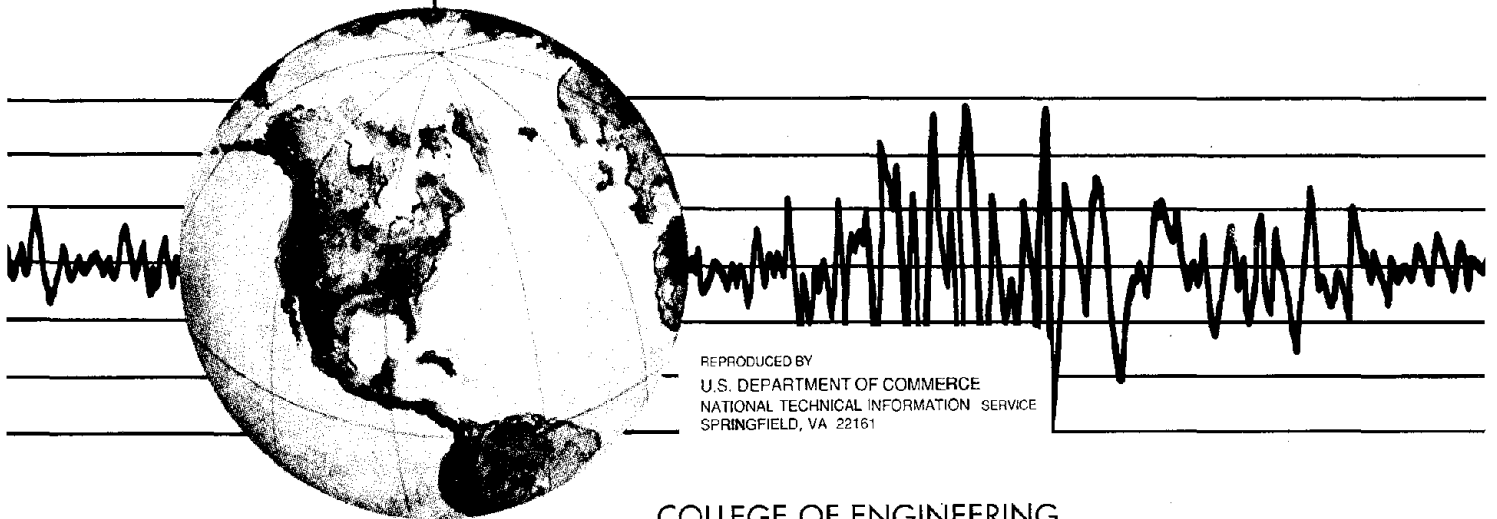
COLLEGE OF ENGINEERING

UNIVERSITY OF CALIFORNIA AT BERKELEY

EVALUATION OF THE SEISMIC PERFORMANCE
OF A TEN-STORY RC BUILDING
DURING THE WHITTIER NARROWS EARTHQUAKE

by

Eduardo Miranda
and
Vitelmo V. Bertero

ABSTRACT

This report summarizes the main results of studies evaluating the response of an existing instrumented ten-story Reinforced Concrete (RC) building, which was subjected to earthquake ground motions of what can be considered moderate damage potential during the 1987 Whittier Narrows earthquake. The seismically laterally resistant structural system consists of moment-resisting frames in the N-S (longitudinal) direction and RC shear walls in the E-W (transverse) direction. It was designed according to the 1970 edition of the Uniform Building Code (UBC). The ultimate goal of the studies reported herein has been to evaluate the reliability of present methods of estimating the performance of existing buildings. To achieve this goal the following objectives were pursued: (1) evaluation of the reliability of presently available system identification techniques for inferring the dynamic characteristics of a building from its recorded responses; (2) assessment of the reliability of analytical models and methods presently available for conducting analyses of the seismic performance of buildings; (3) evaluation, through static and dynamic (time-history) analyses, of the strength and deformation capacity of the building as well as its response, overall and local, and particularly the damage that the building could suffer when subjected to future critical ground motions; and (4) assessment of the implications for present EQ-resistant design practice of the results obtained.

After collecting all of the necessary data regarding design, construction and instrumentation of the building; the records of the ground motions at its foundation; and its response to such ground motions in the past, the following studies were undertaken: (1) analysis of the recorded responses of the building during the most demanding motions that it had experienced, and an attempt to identify from these records its dynamic characteristics using different available system identification techniques; (2) development of analytical models and calibration of these models with the identified dynamic characteristics; (3) analytical prediction of the behavior of the building when subjected to the recorded earthquake ground motions, and comparison of these predictions with the recorded responses in order to evaluate the reliability of the analytical models used in the prediction; (4) evaluation of the capacities supplied to the building in order to evaluate its possible overstrength; (5) analysis of the probable performance of the building under more demanding seismic motions than those

recorded; (6) study of the possibility of using a simpler methodology than one requiring nonlinear time-history analyses to attain reliable estimates of the magnitude and distribution of local demands on buildings; and (7) assessment of the implications for present EQ-resistant design practice of the results obtained.

These studies showed the following. (1) Large peak ground accelerations were recorded in both directions (0.60g and 0.40g, respectively, in the transverse and longitudinal directions). (2) In spite of the apparent severity of the recorded ground motions, there was only a small change in fundamental period during the earthquake for the transverse direction of the building. This indicates that some extra damage (extra cracking or small foundation movement or both) had occurred. No changes in the longitudinal direction fundamental period were observed, indicating that no significant damage could have occurred in this direction during the response of the building to the earthquake ground motions. (3) For both directions, the analyses that took into account only the fundamental mode failed to reproduce the recorded accelerations. When the first nine modes of vibration were considered, very good correlation between the measured and computed responses was obtained for both directions. Maximum computed interstory drifts of 0.34% in the longitudinal direction and 0.21% in the transverse direction explain the absence of significant damage in the building. These results confirm once more that Peak Ground Accelerations of recorded ground motions are not a reliable parameter by which to judge the damage potential of an earthquake ground motion to a specific structure. (4) From static-to-collapse lateral loading, using both a triangular and a rectangular loading pattern, significant overstrengths were computed, particularly in the transverse direction. For the longitudinal direction, the ratio between the base shear at first significant yielding and the design base shear (0.052W) was about 3.06 for the case of triangular lateral loading pattern, and about 3.62 for the rectangular loading. For the transverse direction the overstrength ratios were higher than for the longitudinal direction. Base shear strengths corresponding to first significant yielding of the shear walls were 0.32W and 0.43W, respectively, for the triangular and the rectangular load patterns. Considering that the structural system according to code requirements has to be designed for 0.073W, the resulting strength ratios are 4.38 and 5.89. The maximum base shear strengths were computed as 0.42W and 0.51W, respectively, for the triangular and rectangular load patterns,

with the result that their ratios with the code requirement of 0.073W were 5.75 and 6.99. These overstrengths were obtained assuming that the shear wall systems can develop a global displacement ductility ratio larger than 3 and near 2.5 for the triangular and rectangular patterns respectively. It is doubtful that the detailing of the reinforcement in the coupling girders and walls could allow such a high global displacement ductility ratio to develop. (5) Nonlinear time-history analyses were carried out for the longitudinal direction of the building when subjected to the Hollister and James Road records, which were selected as the most demanding earthquake ground motions that have been recorded in the U.S. on site conditions similar to that of the building site. The maximum displacement for this particular building was 7.71 inches, and the maximum interstory drift index was 0.016, resulting in a maximum demanded story displacement ductility ratio of 3.15 in the 4th story. The number of yielding reversals was small, only four. (6) Simplified earthquake analyses were conducted, using a proposed approximate method, under the James Road and Hollister records. For both records, the simplified analysis method produced very good estimates of story displacement ductility demands. (7) Attempts have been made to estimate the maximum displacement at the roof and the maximum Interstory Displacement (IDI) of the building when subjected to the James Road record, using the results from the proposed simplified analysis: while the estimates of the maximum IDI agreed very well with the value obtained from the time-history analysis, the estimated value of the maximum displacement at the roof was larger.

These studies confirm once more that there are large uncertainties in predicting the seismic performance of existing buildings, and point out clearly the advantages of having very well instrumented buildings. Any recorded response can be used effectively to identify the actual dynamic characteristics of the whole building system. These characteristics can then be used to calibrate the analytical models of the building. The results also show that RC structures designed according to present building regulations have significant first yielding and maximum resistance overstrengths. These overstrengths need to be considered in the design. In order to attain in practice realistic estimations of the real strength and deformation capacity of existing or newly designed buildings it is necessary to develop simple but reliable analytical methods such as the one proposed and used in the studies reported herein.

ACKNOWLEDGEMENTS

TABLE OF CONTENTS

LIST OF TABLES

LIST OF FIGURES

1. INTRODUCTION

1.1 INTRODUCTORY REMARKS

The studies reported herein are a part of an ongoing research program at the University of California at Berkeley on the seismic performance of existing building structures. This program has continued over several years, with the ultimate objectives of developing reliable methods for the design of new buildings and aiding in the vulnerability assessment of existing buildings and the selection of efficient strategies and techniques for the seismic upgrading of existing hazardous buildings. To achieve these goals it was considered necessary to carry out case studies on seismically instrumented real buildings which have survived recent moderate earthquake excitations. One of the buildings selected for these case studies was a ten-story Reinforced Concrete (RC) building which survived the ground excitations induced by the 1987 Whittier Narrows earthquake. The studies conducted on this particular building have the following objectives.

1.2 OBJECTIVES

Although the main objective is to determine how reliable are present methods of estimating the seismic performance of existing buildings, the studies conducted herein also have the following objectives:

(1) Evaluation of the reliability of present system identification techniques of inferring the dynamic characteristics of the building from its recorded responses.

(2) Assessment of the reliability of analytical models and methods that are presently available for conducting analyses of the seismic performance of buildings.

(3) Evaluation, through static and dynamic (time-history) analyses, of the strength and deformation capacities of the building, of its response, and particularly of the damage that the building can suffer when subjected to future critical ground motions.

(4) Development of a simplified method of analysis to estimate the expected overall and local deformation, particularly the local ductility ratios of the building.

(5)   Assessment of the implications of the results obtained regarding the reliability of present code regulations for the earthquake-resistant design of buildings similar to the one studied.

1.3 SCOPE

To achieve the above objectives the following tasks were undertaken.

(1)   Collection of all the necessary data regarding the design of the structure and construction of the building, how the building is instrumented, and the records of the responses of the building to the earthquake motions it has experienced in the past. A brief description of the selected building, its seismic design criteria, its instrumentation and its recorded responses is presented in Chapter 2 of this report.

(2)   Analysis of the recorded response of the building during the most demanding earthquake ground motions that it has experienced, and an attempt to identify from the recorded accelerations, through system identification techniques, its dynamic characteristics. The description of the recorded response during the October 1987 Whittier Narrows earthquake and the system identification of the dynamic characteristics are summarized in Chapter 3 of this report.

(3)   Analytical prediction of the behavior of the building when subjected to the recorded earthquake ground motions, followed by comparison of such predictions with the recorded response during the Whittier Narrows earthquake. This comparison was planned in order to evaluate the reliability of the analytical methods used in the prediction. A description of the three-dimensional linear elastic model used in the time-history prediction of the response of the building, as well as of the results obtained and the comparison of these results with the recorded response, is contained in Chapter 4.

(4)   Evaluation of the capacities supplied to the building, particularly in order to find out its possible overstrength, i.e., its strength beyond that required by the code. This evaluation was conducted using static lateral load-to-collapse analyses of the

analytical model developed for the building. The results of this study are presented in Chapter 5.

(5)   Analysis of the probable performance of the building under more demanding earthquake ground motions than those which occurred at its foundation during the 1987 Whittier Narrows earthquake. To achieve this, nonlinear time-history analyses under two severe recorded ground motions, Hollister and James Road records, were conducted, and are reported in Chapter 6.

(6)   Study of the possibility of using a simpler methodology than that requiring nonlinear time-history analyses for obtaining estimates of the magnitude and distribution of local ductility ratio demands in the building when subjected to a number of previously recorded ground motions on similar sites and geological conditions. The simplified nonlinear analysis, conducted with the objective of evaluating the response of the building in the longitudinal direction when subjected to the Hollister and James Road records, is presented in Chapter 6.

(7)   The drawing of conclusions, the assessment of the implications of the results obtained regarding present earthquake-resistant design practice, and the formulation of recommendations for future research to improve the state of the art in evaluating seismic performance of existing buildings. The main conclusions drawn from the studies reported, the assessment of the implications of the results, and the recommendations for future research are presented in the final chapter of this report.

2. DESCRIPTION OF THE BUILDING, ITS INSTRUMENTATION AND DESIGN CRITERIA

2.1 GENERAL DESCRIPTION OF THE BUILDING SYSTEM

The building selected for this case study is a ten-story RC building located at latitude 33.98°N and longitude 118.04°W. A photograph of the building is shown in Fig. 2.1. The building was designed and constructed in 1972. Plan views of the foundation and first floors are shown in Fig. 2.2. Plan views of the second floor and the fourth through tenth floors are shown in Fig. 2.3. The structural system in the transverse (E-W) direction is a dual system composed of RC coupled shear walls in the north and south ends of the building (lines 2 and 13 in Figs. 2.2 and 2.3), two smaller shear walls surrounding the elevators (lines 7 and 8) and a very flexible frame (columns and flat plate) on the remaining lines. There are additional shear walls at the second story on all E-W lines between lines G and E [Fig. 2.3 (A)].

In the longitudinal (N-S) direction the structural system of the building comprises a moment-resisting frame designed to carry most of the lateral loads in the exterior frames. The interior frames (lines D and E) consist of 16 in.x16 in. RC columns and a cast-in-place 6 1/2 in. thick concrete slab (flat plate). The exterior frames (C and F) consist of 20 in.x20 in. columns and 24 in.x24 in. beams.

The foundation of the building consists of spread footings [Fig. 2.2 (A)] with a design bearing pressure of 5,000 psf. The parking structure consists of a prestressed floor and columns as shown in Fig. 2.2 (B). The building is 183 ft.-4 in. by 52 ft.-8 in. in plan from the third level to the roof level and is 183 ft.-4 in. by 64 ft.-2 in. from the first floor up to the third floor, while the parking deck is 205 ft.-4 in. by 50 ft.-6 in. in plan. The building extends 90 feet above the ground level. Fig. 2.4 shows an elevation of the transverse direction of the building. Interstory heights are 12 ft.-0 in. in the first story and 8 ft.-8 in. for the second through tenth stories.

The specified 28-day strength of the concrete (f'_c) was 4,000 psi for the first floor and columns up to the 6th floor, and 3,000 psi for the rest of the structure. All reinforcing steel was grade 60, conforming to ASTM specification A-615.

Longitudinal and transverse reinforcement details of typical columns are shown in Fig. 2.5. Reinforcement details of typical beams are shown in Fig. 2.6. It is important to note that the amount of specified transverse reinforcement exceeds the minimum requirements of the 1970 UBC (the specification used in the design of the building). However, reinforcement at the beam-column joints is still minimal and transverse reinforcement in the columns consists of ties with 90° hooks at the corners. Similarly, ties in the beams are not closed, instead consisting of U-shaped ties with alternating caps. By today's standards these details are considered unacceptable. A summary of the steel reinforcement in the structural members of the building is presented in Table 2.1.

2.2 INSTRUMENTATION

The building forms part of the National Strong-Motion Instrumentation Network (NSMIN) operated by the U.S. Geological Survey (USGS). The building instrumentation consists of three SMA-1 analog accelerographs (each capable of recording three components of motion) located at the basement, 5th floor and 10th floor. The location of these instruments is shown in Figs. 2.2, 2.3, and 2.4.

The first set of earthquake records obtained from the building was obtained in the January 1, 1976 Whittier earthquake. The epicenter of this magnitude 4.2 (M_L) earthquake was approximately 8.6 miles (13.8 km) east of the building [1]. In the transverse (E-W) direction peak accelerations of 0.16g, 0.23g, and 0.18g were recorded at the basement, 5th floor, and 10th floor, respectively. In the longitudinal (N-S) direction peak accelerations of 0.06g, 0.06g, and 0.04g were recorded at the basement, 5th floor, and 10th floor, respectively.

At the time of writing, the largest magnitude earthquake to shake the building was the October 1, 1987 Whittier Narrows earthquake. The epicenter of this magnitude 5.9 (M_L) earthquake was approximately 10 km (6.2 miles) north of the building. Among more than 250 strong-motions accelerograph stations (operated by USGS, CSMIP, and the University

of Southern California) that were triggered in the earthquake, the largest peak ground acceleration was recorded in the basement of this building. In the transverse (E-W) direction peak accelerations of 0.63g, 0.62g, and 0.53g were recorded in the basement, 5th floor, and 10th floor, respectively. In the longitudinal (N-S) direction peak accelerations of 0.43g, 0.55g, and 0.40g were obtained on the 10th floor, 5th floor, and the basement, respectively [2].

A magnitude 5.3 (M_L) aftershock which occurred on October 4, 1987 produced peak accelerations of 0.33g, 0.58g, and 0.43g in the transverse direction in the basement, 5th floor and 10th floor, respectively. Recorded peak accelerations in the longitudinal direction were 0.30g, 0.30g, and 0.17g in the basement, 5th floor, and 10th floor respectively [3].

Peak accelerations recorded in the building during these three earthquakes are summarized in Table 2.2. Two general trends can be observed from this table: (a) the largest acceleration has always been recorded at the 5th floor and not at the 10th floor, indicating a possible strong participation of the second mode; and (b) larger accelerations have been recorded in the transverse (stiff) direction than in the longitudinal (flexible) direction.

Besides the earthquakes listed in Table 2.2, instruments in the building were also triggered during the July 8, 1986 North Palm Springs Earthquake (M_L = 5.9) and the February 28, 1990 Upland, California earthquake (M_L = 5.5). The epicenter of the North Palm Springs earthquake was 9.3 miles (15 km) north of Palm Springs, approximately 81 miles (131 km) east of the building. Maximum ground and building accelerations recorded in this event were 0.03g and 0.08g, respectively [4]. The epicenter of the Uplands earthquake was 3.1 miles (5 km) northwest of downtown Upland, approximately 22.4 miles (36 km) east of the building. Owing to a malfunction of the 5th floor instrument, records were only obtained in the basement and 10th floor during this earthquake. At both locations peak accelerations were smaller than 0.05g [5].

2.3 SEISMIC DESIGN CRITERIA

The building was designed according to the 1970 edition of the Uniform Building Code [6]. Under these design recommendations the building had to be designed to resist the lateral forces given by the following expression

$$V = Z K C W \tag{2.1}$$

where V is the total horizontal force to be resisted, Z is a factor which depends on the seismic zone, K is a factor that is a function of the structural system of the building, and W is the total dead load of the building. C is given by

$$C = \frac{0.05}{T^{\frac{1}{3}}} \tag{2.2}$$

where T is the fundamental period of the building, which shall be determined by

$$T = \frac{0.05 \, h_n}{D^{\frac{1}{2}}} \tag{2.3}$$

where h_n is the height of the roof above the ground level (in feet), and D is the dimension of the building (in feet) parallel to the applied forces. Formula 2.3 shall be used for all buildings except for buildings where 100% of the lateral forces were resisted by moment-resisting space frames, in which case the period shall be estimated by

$$T = 0.1 \, N \tag{2.4}$$

where N is the number of stories.

The use of Eq. 2.3 leads to an unrealistically low period of 0.33 second for the longitudinal direction, while for the transverse direction the same expression leads to a very reasonable approximation of 0.62 second. Equation 2.4 predicts a more realistic fundamental period for the longitudinal direction (1.0 second).

For the transverse (dual system) direction, the use of Eqs. 2.1 to 2.3 along with corresponding load and strength reduction factors lead to the following minimum factored (ultimate) strength:

$$\frac{V}{W} = \frac{(0.75 \times 1.7 \times 1.1)ZKC}{0.9} = \frac{(0.75 \times 1.7 \times 1.1)(1.0)(0.8)(0.0586)}{0.9} = 0.073 \quad (2.5)$$

For the longitudinal (moment-resisting frame) direction, Eqs. 2.1, 2.2, and 2.4 and corresponding load and strength reduction factors lead to a minimum lateral factored (ultimate) strength of

$$\frac{V}{W} = \frac{(0.75 \times 1.7 \times 1.1)ZKC}{0.9} = \frac{(0.75 \times 1.7 \times 1.1)(1.0)(0.67)(0.0335))}{0.9} = 0.052 \quad (2.6)$$

(A) COLUMNS

FLOOR	INTERIOR COLUMN	EXTERIOR COLUMN	CORNER COLUMN
1 - 2	4 #11	10 #11	14 #11
2 - 3	4 #8	6 #11	14 #11
3 - 4	4 #8	4 #11	14 #11
4 - 6	4 #8	4 #10	10 #11
6 - 7	4 #8	4 #10	8 #11
7 - 8	4 #8	4 #9	6 #11
8 - 9	4 #8	4 #9	6 #10
9 - R	4 #8	4 #9	4 #9

(B) BEAMS

FLOOR	LONGITUDINAL REINFORCEMENT	
	TOP	BOTTOM
1 - 3	6 #10	6 #10
3 - 6	6 #8	6 #8
6 - 8	6 #7	6 #7
8 - R	6 #6	6 #6

(C) SHEAR WALLS

FLOOR	BOUNDARY ELEMENT LONG. REINFORCEMENT	WEB REINFORCEMENT
B - 1	16 #11	#4 @ 18" vert. #5 @ 13" horiz.
1 - 4	14 #11	#4 @ 18" vert. #4 @ 16" horiz.
4 - 6	10 #11	#4 @ 16" vert. #5 @ 12" horiz.
6 - 7	8 #11	#4 @ 16" vert. #5 @ 12" horiz.
7 - 8	6 #11	#4 @ 16" vert. #5 @ 12" horiz.
8 - 9	6 #10	#4 @ 16" vert. #5 @ 12" horiz.
9 - R	4 #9	#4 @ 16" vert. #5 @ 12" horiz.

Table 2. 1 - Summary of the steel reinforcement of the structural members of the building.

FLOOR	DIRECTION	1/1/76 EVENT ($M_L \approx 4.2$)	1/10/87 EVENT ($M_L \approx 5.9$)	4/10/87 EVENT ($M_L \approx 5.3$)
10th Floor	90° (A)	0.18	0.53	0.43
5th Floor	90°	0.23	0.62	0.58
Basement	90°	0.16	0.60	0.33
10th Floor	180° (B)	0.04	0.43	0.17
5th Floor	180°	0.06	0.55	0.30
Basement	180°	0.06	0.40	0.30

(A) Dual system (shear walls & moment-resisting frame)

(B) Moment-resisting frame

All values in g's

Table 2. 2 - Peak accelerations in the building during three earthquakes.
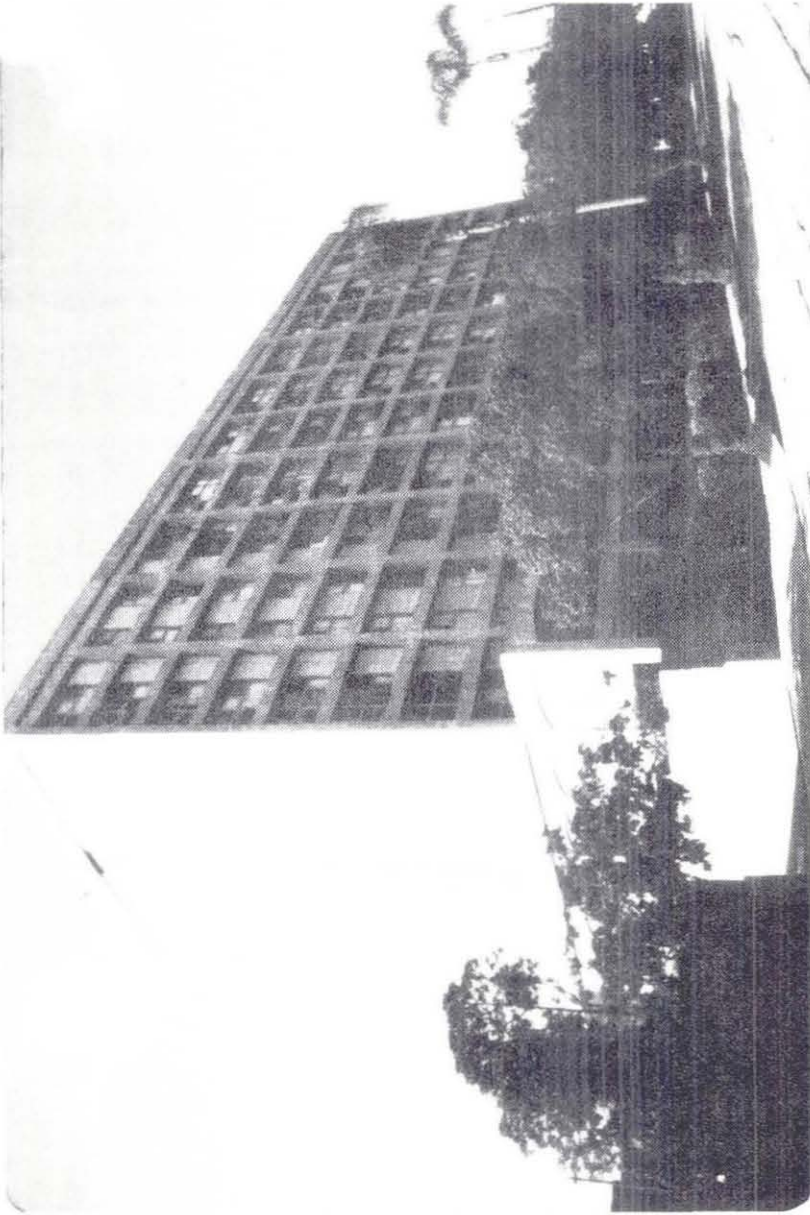
Figure 2. 1 - General view of the ten-story RC building
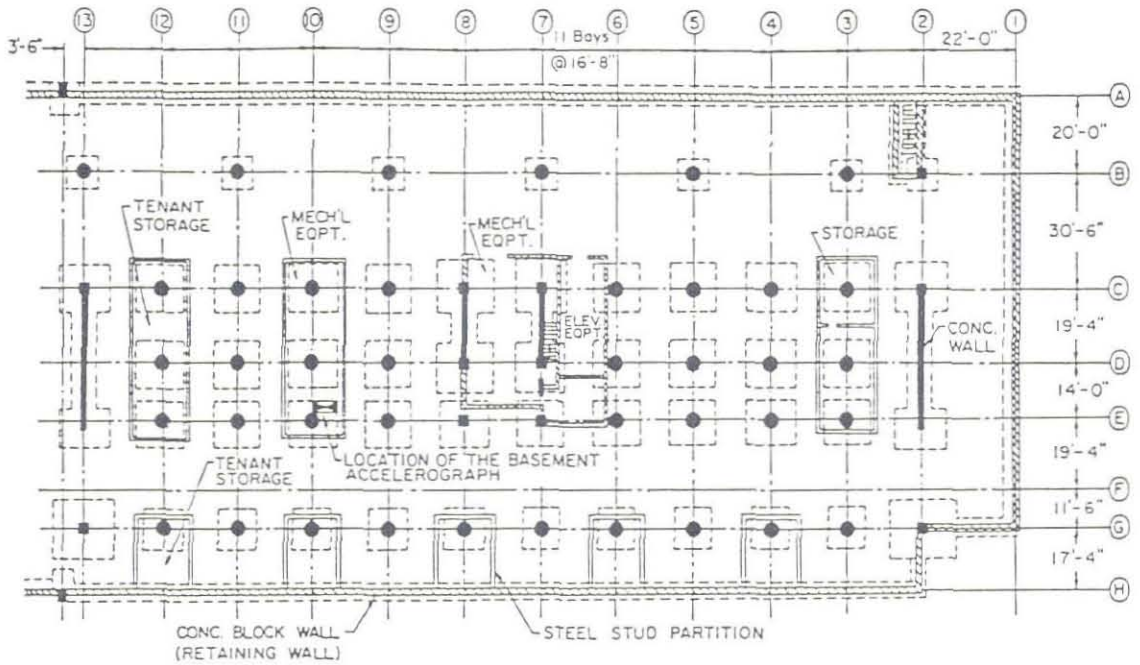
(A) BASEMENT - FOUNDATION PLAN ⊕ N
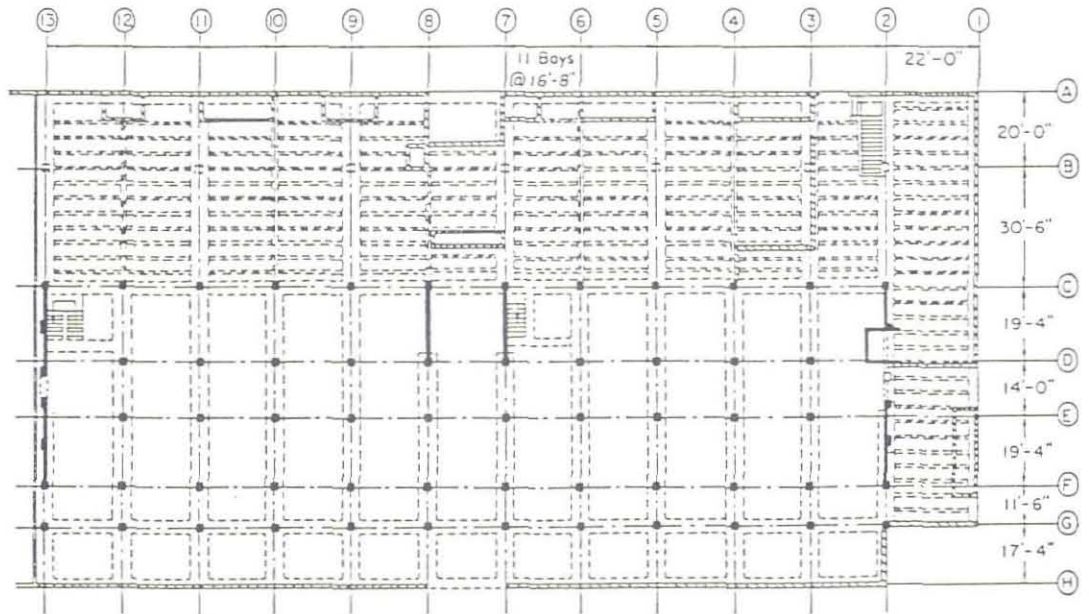
(B) FIRST FLOOR FRAMING PLAN ⊕ N

Figure 2. 2 - Floor plans of basement and first floor [1]
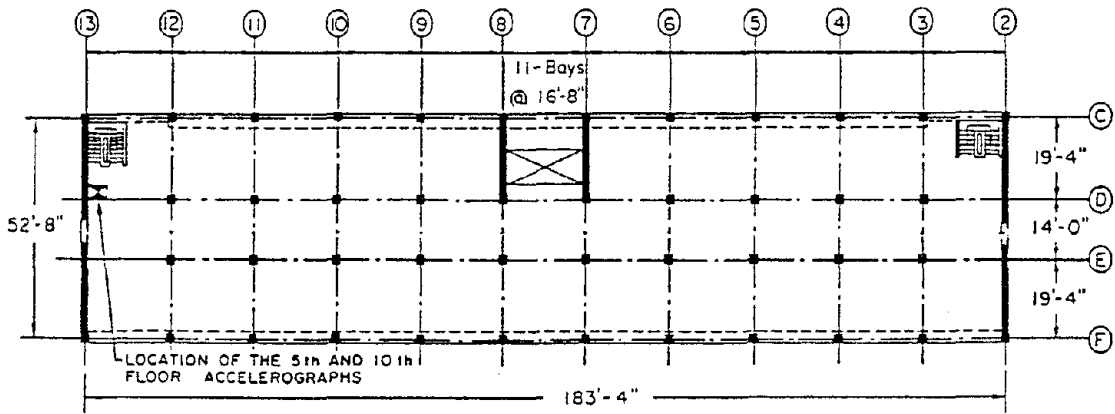
Figure 2. 3 - Floor plans of second and fourth through tenth floors [1]
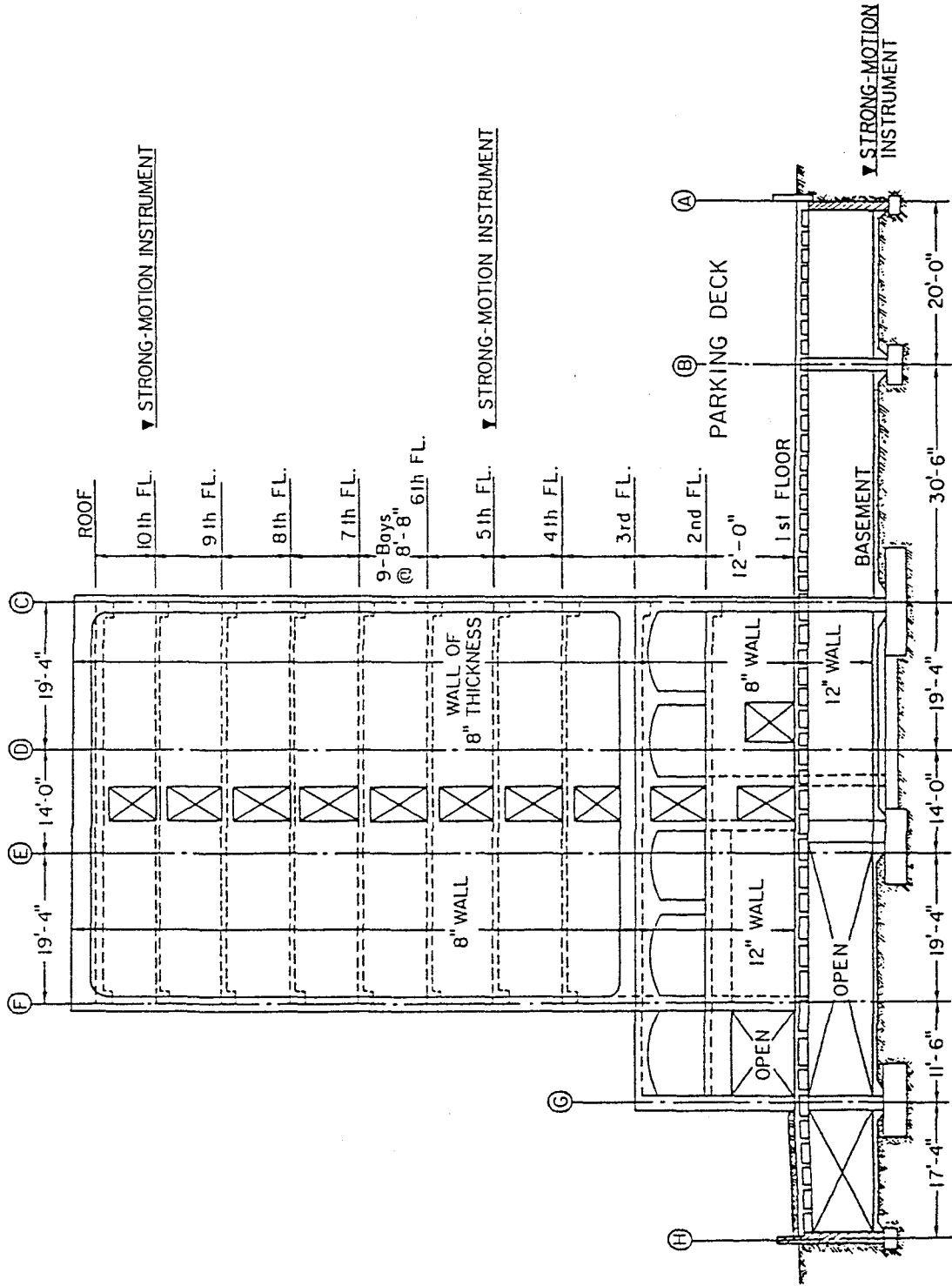
Figure 2. 4 - Elevation of the transverse direction of the building

TYPICAL INTERIOR COLUMN

TYPICAL EXTERIOR COLUMN

2"

16"

16"

#4

4 # 8

2"

20"

20"

#4

4 # 10

COLUMN TIES
2 @ 4" o.c.
5 @ 6" o.c.
top & bott.
rem. @ 10" o.c.

2"

30 Ø (2' min.)
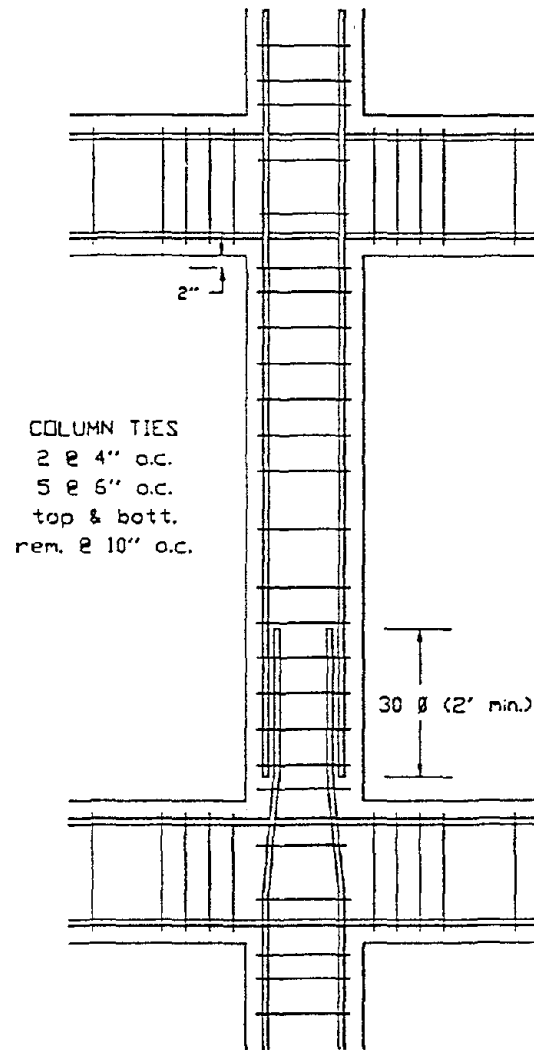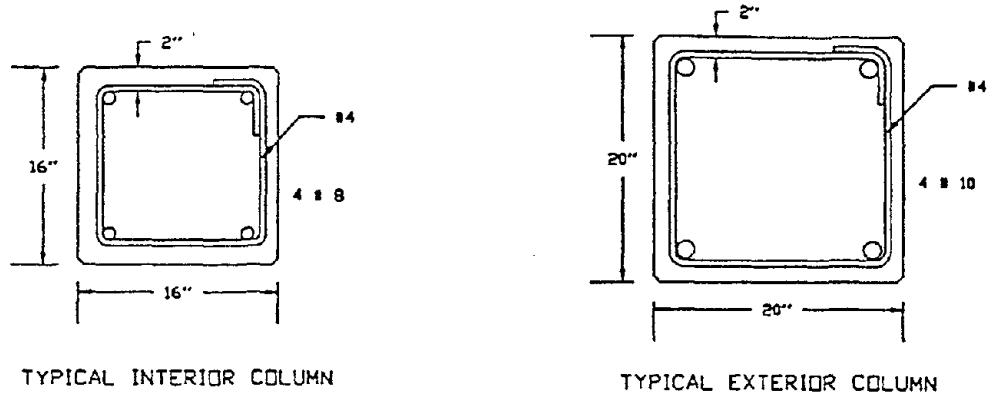
Figure 2. 5 - Column reinforcing details

TYPICAL COUPLING BEAM

TYPICAL EXTERIOR BEAM
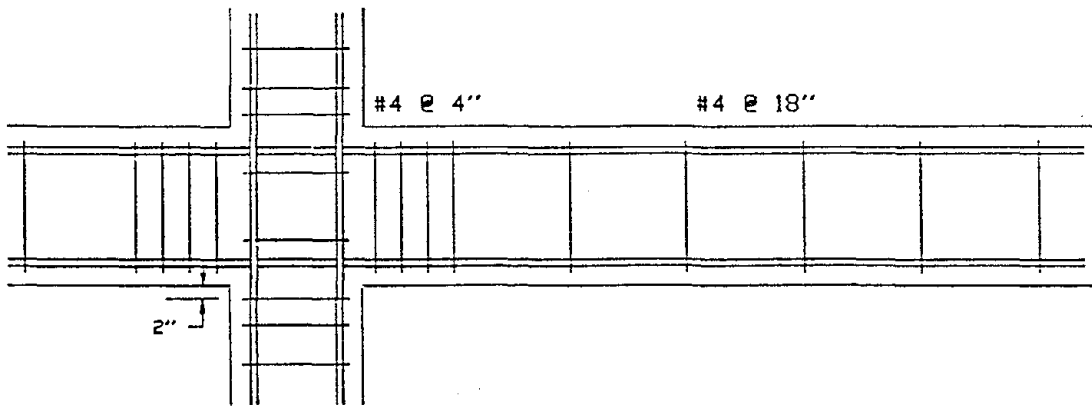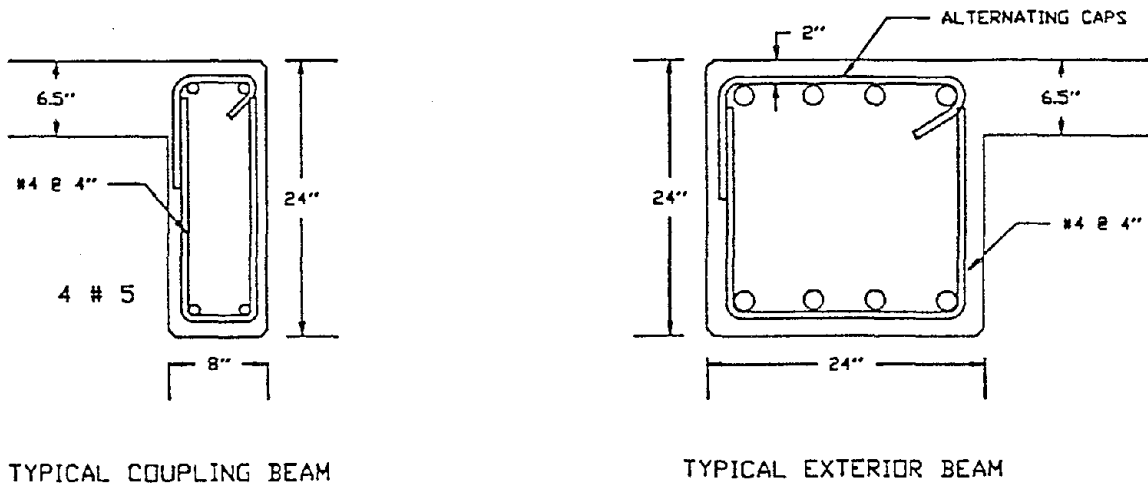
TYPICAL EXTERIOR BEAM AND JOINT

Figure 2. 6 - Beam reinforcing details

3. RECORDED RESPONSE DURING THE WHITTIER NARROWS EARTHQUAKE

3.1 THE WHITTIER NARROWS EARTHQUAKE

The October 1, 1987 Whittier Narrows earthquake (M_L = 5.9) occurred at 7:42 A.M., Pacific Daylight Time (PDT) at 34° 3.0' N, 118° 4.8' W, about 9.3 miles (15 km) northeast of downtown Los Angeles, at a focal depth of about 8.7 miles (14 km). The earthquake ruptured a small part, 4 km by 5 km, of a previously unidentified buried thrust fault that strikes east-west and dips 25° down to the north [7]. This earthquake caused 3 deaths, 932 earthquake-related injuries, 385 million dollars in property damage, and displaced (made homeless) 10,400 persons [8].

Major damage occurred within 3 miles (5 km) of the building, including several partial collapses in the Whittier downtown shopping area (Whittier Village). A Modified Mercalli Intensity (MMI) of VII was assigned to the area where the building is located [9]. No damage was found in the ten-story building during two different post-earthquake visual inspections [10, 11].

3.2 DESCRIPTION OF THE RECORDED RESPONSE DURING THE WHITTIER NARROWS EARTHQUAKE

Acceleration time-histories recorded in the building are shown in Figs. 3.1 and 3.2. All records are plotted with the same time and intensity scales to facilitate their direct comparison. Although the duration of the digitized records is 30 seconds, the duration of the strong motion is only about 4 seconds. As mentioned before, motions recorded in the transverse direction have a larger intensity than those recorded in the longitudinal direction. Peak acceleration values are summarized in Table 2.2.

Relative velocity and displacement time histories at the 5th and 10th floors were computed by numerical integration, high-pass filtering, and base-line correction of recorded accelerations [12, 13]. Peak values are summarized in Table 3.1.

Linear elastic response spectra of the horizontal motions recorded in the basement were calculated by direct integration [14]. Figure 3.3 shows the computed linear elastic spectra for 0, 2, 5, 10, and 20% damping.

3.3 SYSTEM IDENTIFICATION OF THE DYNAMIC CHARACTERISTICS OF THE BUILDING

The dynamic characteristics of the building were inferred from the acceleration records obtained in the October 1, 1987 Whittier Narrows earthquake, using the same three identification techniques that were used for a thirty-story RC Y-shaped building [15, 16].

Fourier amplitude spectra of acceleration records in the longitudinal direction of the building are shown in Fig. 3.4. Results are only shown for a 0 to 5 Hz window for easy identification of the first few modes of vibration. It can be seen that the ground has its strongest input in a band between 2 and 3 Hz (predominant period between 0.33 and 0.5 second). Motion in this frequency band is amplified in the structure, particularly at the 5th floor. Figure 3.5 shows Fourier amplitude spectra of accelerations recorded in the transverse direction of the building. The input motion (basement) is particularly strong for frequencies between 2 and 3 Hz (as in the longitudinal direction) and around 3.5 Hz. Differences in the frequency content of the orthogonal motions recorded in the basement may be indicative of soil-structure interaction; however, this hypothesis cannot be verified due to the absence of free-field records in the vicinity of the building.

Transfer functions for the longitudinal motion (moment-resisting frame) direction are shown in Fig. 3.6. From this figure, the 1st, 2nd, and 3rd mode frequencies were identified to be 0.70, 2.03, and 3.15 Hz, respectively. The ratios between these frequencies ($F_2/F_1 = 2.9$, $F_3/F_1 = 4.5$) agree reasonably well with what could be expected for moment-resisting frame buildings [17]. However, the fundamental period (1.43 seconds) is significantly longer than what could be expected for U.S. reinforced-concrete, moment-resisting frame buildings [18, 19], or assumed by the code used in the design of the building [6].

Figure 3.7 shows the transfer functions for the motions recorded in the transverse (dual system) direction of the building. The largest amplitude peak (at 1.64 Hz) corresponds to the fundamental mode. The second peak (at 4.1 Hz), and the vibrational mode shape associated with it, corresponds to the second mode. The ratio of second to first modal frequencies is 2.5, which is low for what could be expected for this structural system in this direction. A summary of translational frequencies and periods of vibration identified from the recorded earthquake motions are presented in Tables 3.2 and 3.3.

Since the response of each instrumented floor was recorded at only one location, torsional modes could not be reliably identified. Computed damping ratios varied depending on the resolution, smoothing, and filter used in computing the Fourier amplitude spectra. For the first mode the damping varied between 4.9% and 7.3% for the longitudinal direction and between 3.3% and 4.2% for the transverse direction.

Moving-window Fourier analyses were conducted using windows of 5 seconds for the transverse direction and 7.5 seconds for the longitudinal direction, moving at 2.5 second intervals. An increase of 4.2% in the fundamental period was observed in the transverse direction between the 2.5 and 5.0 second marks. This increase in period could be the result of some nonstructural or structural damage, or of some movement (rocking) of the foundation of the shear walls, or of some combination of these. No change in fundamental period was observed in the longitudinal direction.

It should be noted that Abdel-Ghaffar [1] conducted a detailed analysis of the accelerations recorded in the building as a consequence of the January 1, 1976 Whittier earthquake. Table 3.4 summarizes the different vibration periods of the building that have been identified by Abdel-Ghaffar. From comparison of these identified values with the values identified in the studies reported herein, which are also summarized in Table 3.4, it is clear that the values of the vibration periods of the building identified from the 1987 records are larger than those identified from the 1976 records. This should be expected, because in general the stiffness of RC building structures decrease with their service age and because the stiffness also depends on the intensity (amplitude) of the response. Although the observed increase in the

periods of the modes in the longitudinal (N-S) direction, 81% for the first mode, is very high, similar increases have been reported for other existing RC buildings [15 and 16]. These observed increases deserve further investigation.

FLOOR	DIRECTION	MAX. REL. VELOCITY[A] [cm/sec]	MAX. REL. DISPL.[B] [cm]
10th	90° [C]	55.87	2.94
5th	90°	22.07	1.18
10th	180° [D]	46.04	7.14
5th	180°	39.55	4.11

(A) Velocities obtained from highpassed, baseline corrected integral with respect to time of recorded accelerations.

(B) Displacements obtained from highpassed, baseline corrected integral with respect to time of computed velocities.

(C) Dual system (shear walls & moment-resisting frame)

(D) Moment-resisting frame

Table 3. 1 - Peak responses in the building during the October 1, 1987 Whittier Narrows earthquake.

DIRECTION	MODAL FREQUENCIES [Hz]		
	1st MODE	2nd MODE	3rd MODE
East-West 90° [A]	1.64	4.12	-
North-South 180° [B]	0.70	2.03	3.15

(A) Dual system (shear walls & moment-resisting frame)

(B) Moment-resisting frame

Table 3. 2 - Translational modal frequencies identified from the earthquake records.

DIRECTION	PERIODS OF VIBRATION [sec]		
	1st MODE	2nd MODE	3rd MODE
East-West 90° (A)	0.61	0.24	-
North-South 180° (B)	1.43	0.48	0.31

(A) Dual system (shear walls & moment-resisting frame)
(B) Moment-resisting frame

Table 3. 3 - Translational periods of vibration identified from earthquake records.

RECORDS ANALYZED	IDENTIFIED VIBRATION PERIODS (SECS) IN THE DIRECTIONS						
	LONGITUDINAL (N-S)			TRANSVERSE (E-W)		TORSIONAL	
	T_1	T_2	T_3	T_1	T_2	T_1	T_2
(1) 1976 WHITTIER	0.79	0.27	0.14	0.60	0.18	0.43	0.17
(2)1987 WHITTIER NARROWS	1.43	0.48	0.31	0.61	0.24	0.44	____
(3) RATIOS (1)/(2)	1.81	1.78	2.21	1.02	1.33	1.02	____

Table 3. 4   Comparison of vibration periods identified from the 1976 Whittier and the 1987 Whittier Narrows records.
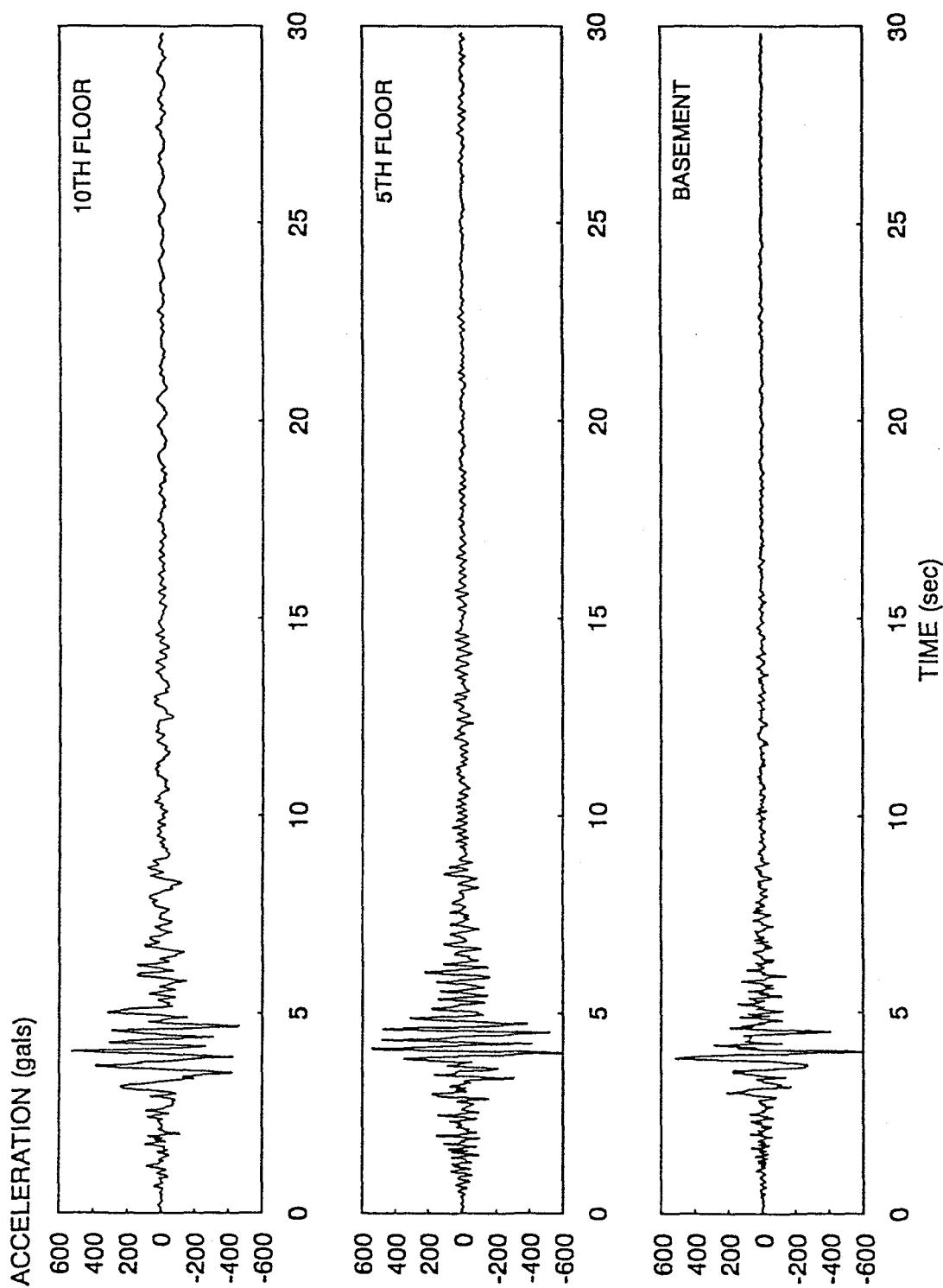
Figure 3. 1 - Transverse (East-West) acceleration time-histories recorded in the 1987 Whittier Narrows earthquake
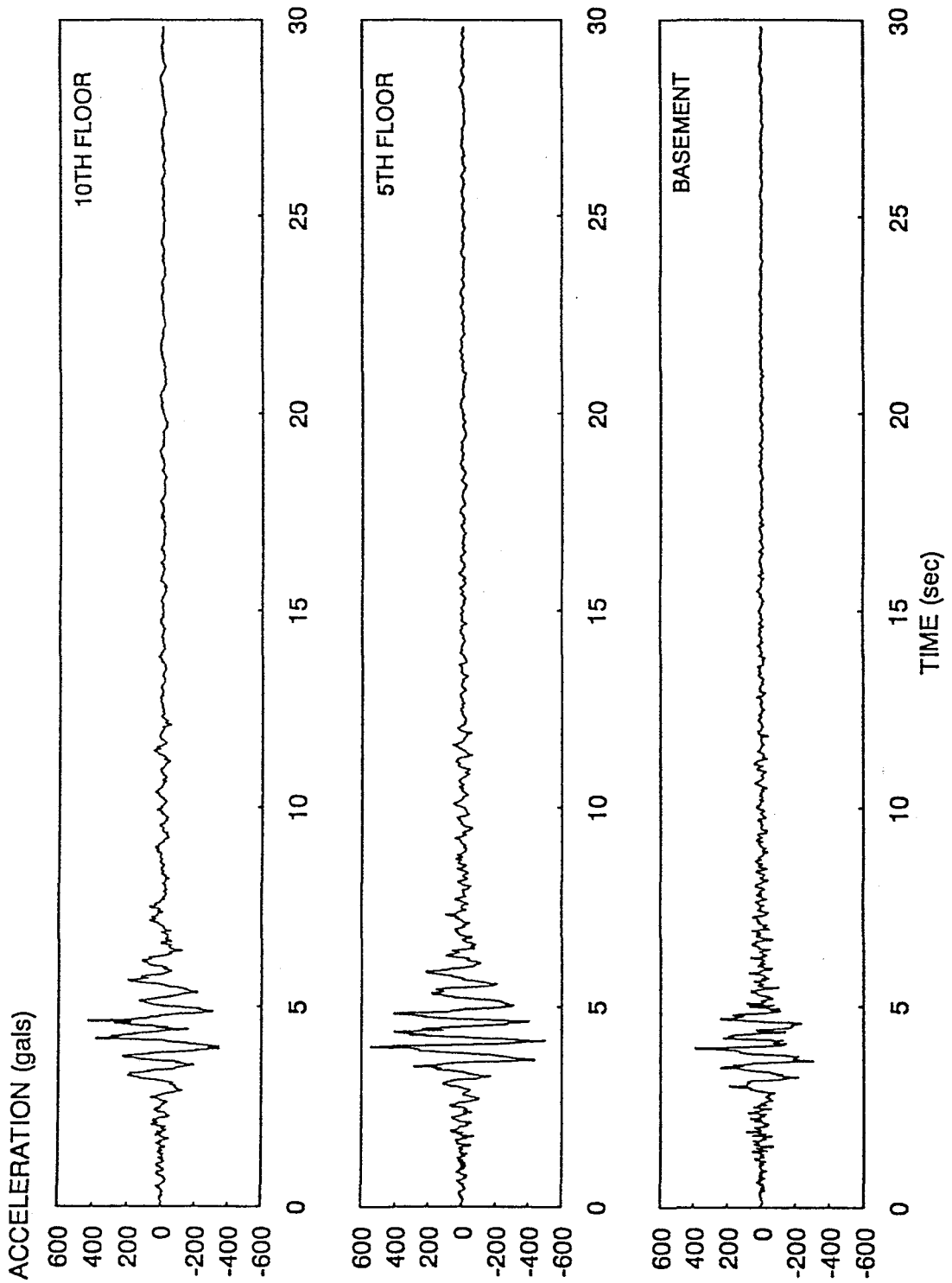
Figure 3. 2 - Longitudinal (North-South) acceleration time-histories recorded during the 1987 Whittier Narrows earthquake
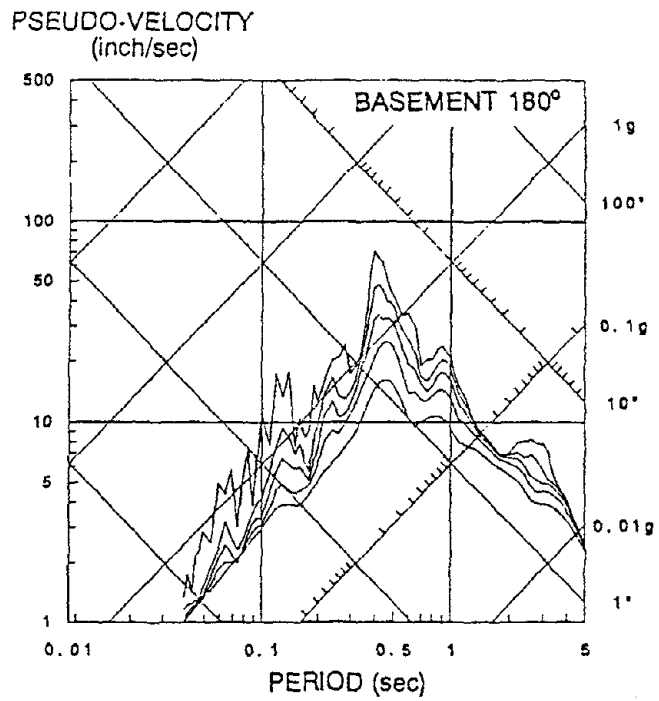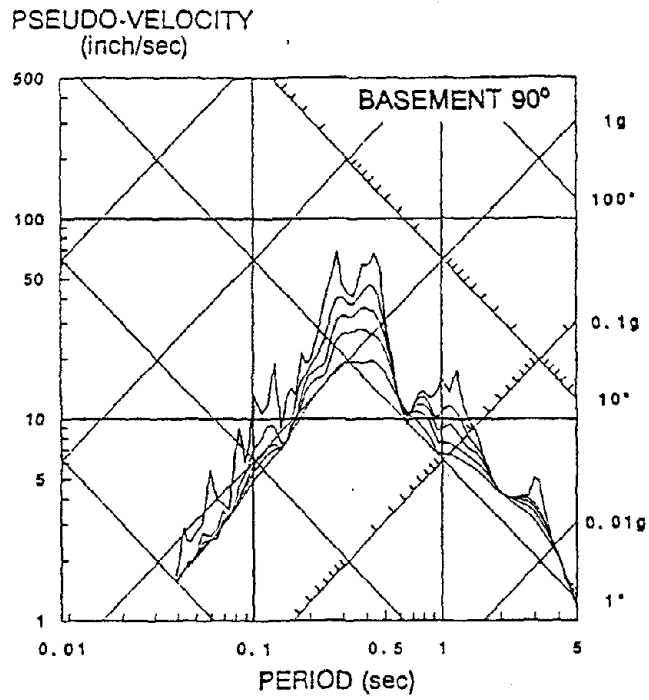
Figure 3. 3 - Linear-elastic response spectra of horizontal ground motions recorded in the basement of the building (0, 2, 5, 10, and 20% damping)
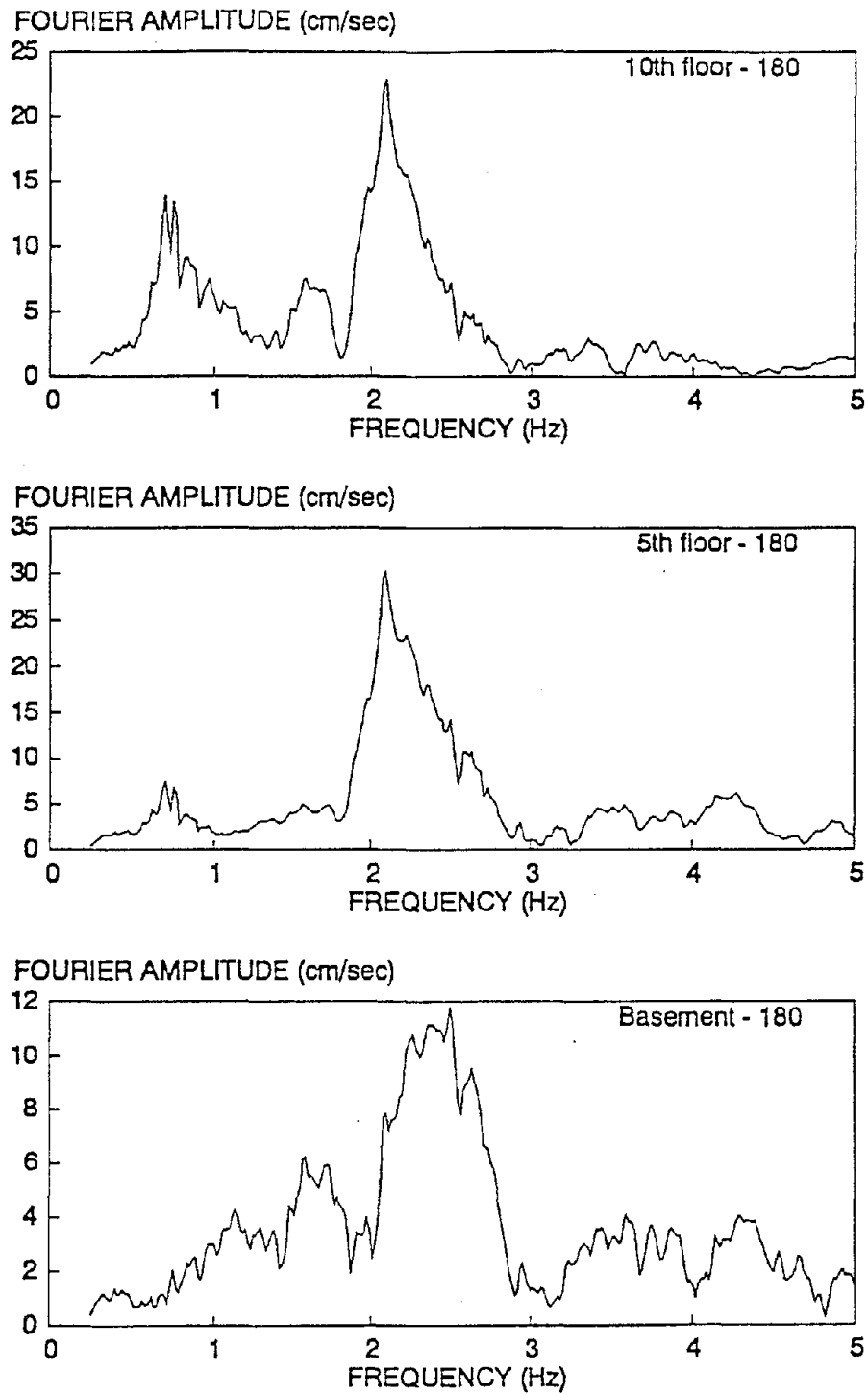
Figure 3. 4 - Fourier amplitude spectra of accelerations recorded in the longitudinal direction of the building

FOURIER AMPLITUDE (cm/sec)

10th floor - 90

FREQUENCY (Hz)

FOURIER AMPLITUDE (cm/sec)

5th floor - 90

FREQUENCY (Hz)

FOURIER AMPLITUDE (cm/sec)

Basement - 90

FREQUENCY (Hz)
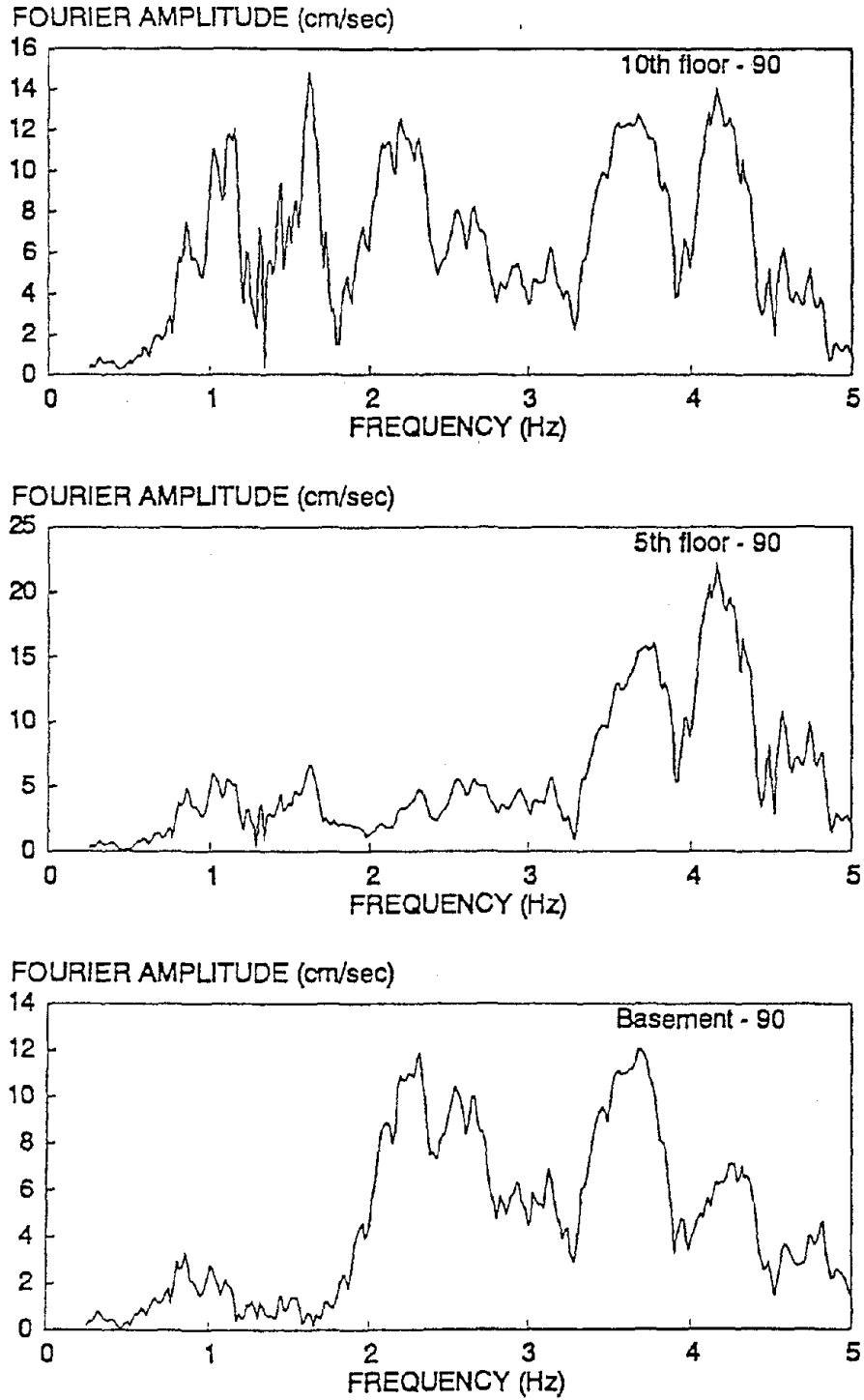
Figure 3. 5 - Fourier amplitude spectra of accelerations recorded in the transverse direction of the building
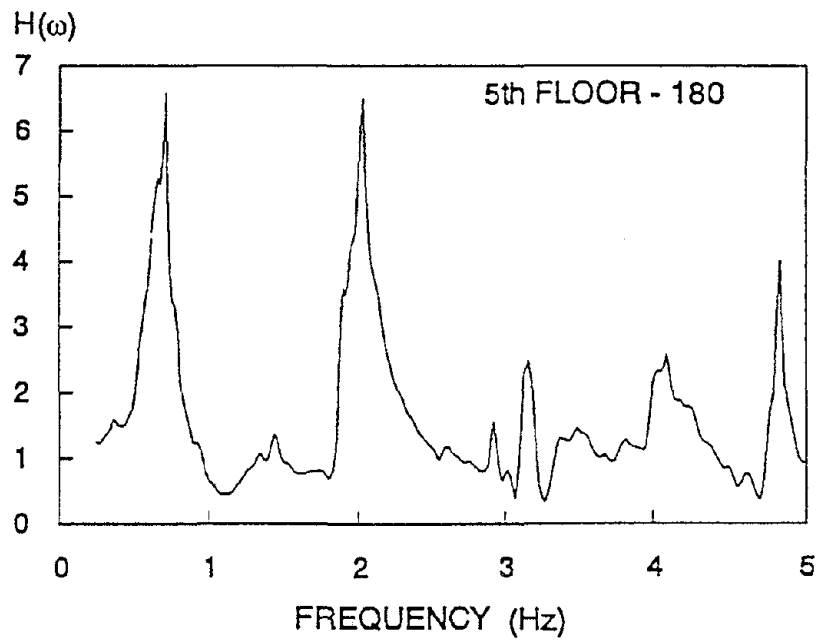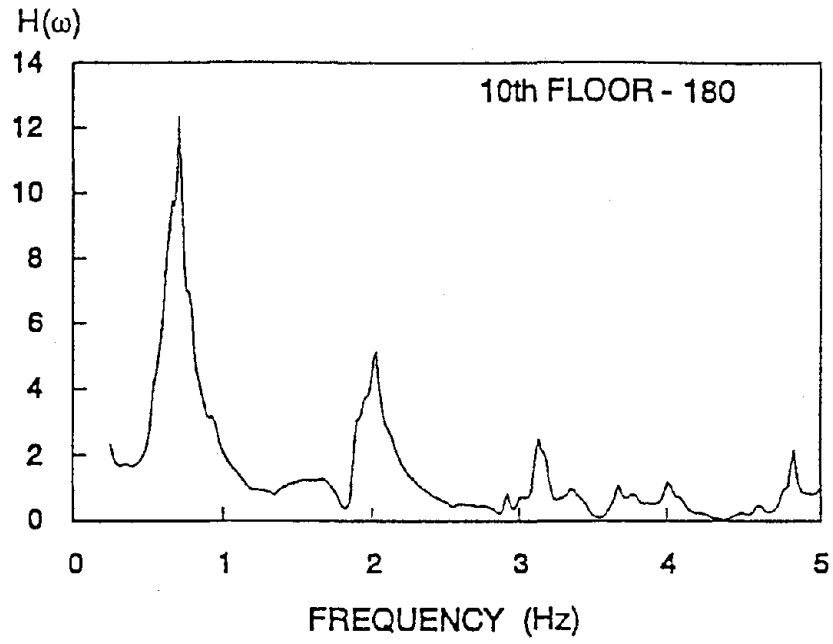
Figure 3. 6 - Transfer functions for the longitudinal direction of the building
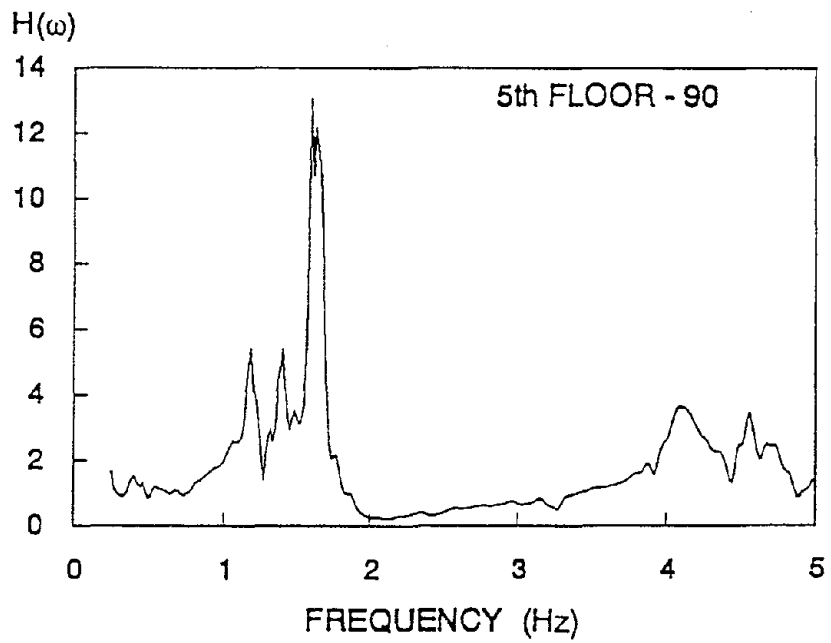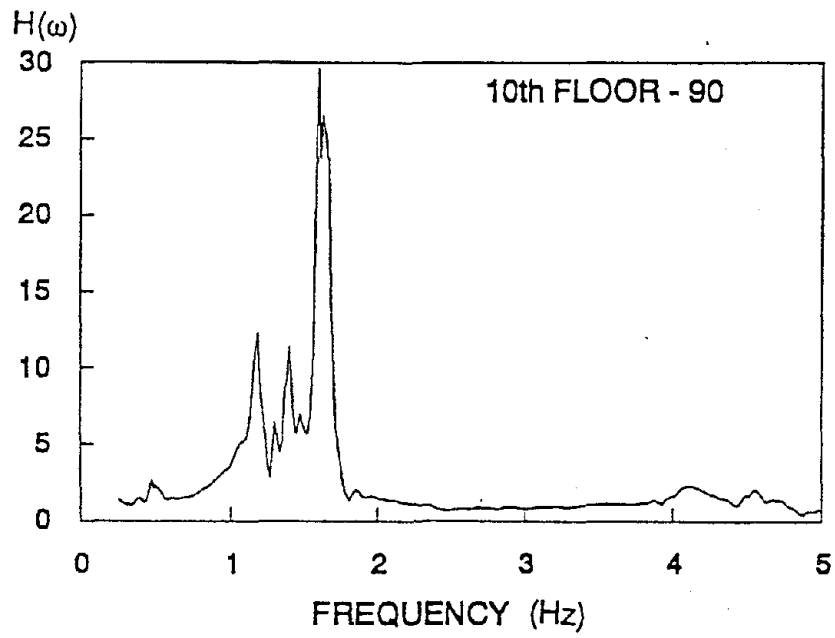
Figure 3. 7 - Transfer functions for the transverse direction of the building

4. EVALUATION OF THE PERFORMANCE OF THE BUILDING UNDER MODERATE EARTHQUAKE GROUND MOTIONS

4.1 INTRODUCTORY REMARKS

The assessment of the seismic vulnerability of any given structure requires the estimation of its mechanical (dynamic) characteristics and the prediction of its response to the seismic ground motions to which it could be subjected during its service life. Similar estimations and predictions are necessary for the analysis of the adequacy (soundness) of the preliminary design of a new structure. No matter for what purpose the analytical estimations and predictions are used, there are questions about the reliability of the analytical model, the estimation of the dynamic characteristics, and the method of analysis (computer programs) used. The occurrence of an earthquake and the recordings of the response of the structure to the resulting ground motions offer a unique opportunity to calibrate such reliability. It was decided to use the available records of the response of the ten-story building to find an answer to the question. For this purpose, the following analyses were conducted: eigenvalue analysis to determine the periods and mode shapes of the building, and time-history analyses using a three-dimensional linear elastic model of the building. Special emphasis was placed on studying the effectiveness of this kind of analysis at capturing the response of the building when subjected to moderate earthquake ground motions and evaluating the reasons for the absence of damage during the Whittier Narrows earthquake.

4.2 EIGENVALUE ANALYSIS

A widely-used finite element structural analysis program, SAP 90 [20], was used for this stage of the study. The building was modelled as a three-dimensional array of linear elements. The floor diaphragm was assumed to be rigid and the columns and shear walls were assumed to have fixed bases. Cracked, transformed sections were used for all structural elements, and the joints were assumed to be rigid over 75% of their dimensions. The complete model consisted of 899 nodes, 1642 members, and 2514 degrees of freedom. An isometric view of the three-dimensional model of the building is shown in Fig. 4.1.

An eigenvalue analysis was conducted in order to calibrate the model such that the fundamental periods (in both directions) agreed with those identified from the earthquake records. Keeping the computed masses constant, adjustments in member stiffnesses of less than 7% were necessary to calibrate the model. Computed periods and mode shapes for the dominant modes of vibration of the building are shown in Fig. 4.2. Except for the period for the second translational mode in the transverse direction, the computed periods agreed very well with those identified from the records (Tables 3.2 and 3.3).

Table 4.1 summarizes the participation of modal masses of the first two modes in each direction as a percentage of the total mass. For both directions, the first and second modal masses account for more than 80% of the total mass.

4.3 TIME-HISTORY ANALYSES

Time-history analyses were conducted using as input the acceleration time histories recorded in the basement of the building during the Whittier Narrows earthquake.

A time increment of 0.02 second and a damping ratio of 5% (for all modes) were used in the analyses. Accelerations recorded at the 5th floor of the building have been consistently higher in both translational directions than those at the 10th floor. This was confirmed by a quick analysis of the values of the spectral acceleration given in Fig. 3.3 together with the periods and mode shapes given in Fig. 4.2 and suggests an important participation of the second mode in past earthquakes. Two different analyses were therefore conducted to evaluate the contribution of higher modes to the total response. In the first analysis, only the first translational mode in each direction was considered. In the second analysis the first nine modes of vibration were considered, corresponding to all periods of vibration higher than 0.1 second.

A comparison of measured and calculated acceleration time histories in the transverse direction for the 5th and 10th floors is shown in Figs. 4.3 and 4.4. The correlation is poor between the measured accelerations and those calculated in the analysis, which only considered the fundamental mode. The correlation is especially poor at the 5th floor, where

the maximum acceleration is significantly underestimated. When the first 9 modes were considered the correlation is, in general, very good.

Figures 4.5 and 4.6 compare the measured and calculated acceleration time histories in the longitudinal direction of the building for the 5th and 10th floors, respectively. Again, the analysis that only took into account the fundamental mode failed to reproduce the recorded accelerations. When the first 9 modes of vibration were considered, the calculated accelerations agree well with the measured accelerations. In this case, the important contribution of the second mode is due to the fact that the second translational mode frequency in this direction (2.02 Hz) lies within the band of predominant frequencies of the ground motion (see Fig. 3.3 and particularly Fig. 3.4).

Comparisons of calculated (including 9 modes) and measured displacements (computed from recorded accelerations) for the transverse and longitudinal directions of the building are shown in Figs. 4.7 and 4.8, respectively. The correlation is relatively good. When comparing displacement time histories one must consider that differences are due not only to imperfect modelling assumptions but also to uncertainties in the computation of displacements from recorded acceleration time histories. The type of filter, and especially the selection of corner frequencies for the high-pass digital filter, may produce significant errors in the computation of displacements from strong-motion accelerograms [13, 21].

A summary of the results from the time-history analyses and a comparison with recorded motions is presented in Table 4.2.

The correlation attained by the present model is very good considering the uncertainties associated with the estimation of mechanical properties of the structural members, modelling assumptions, estimation of the masses, uncertainties associated with the structural damping, and contamination of the input motions due to soil-structure interaction.

The maximum base shears resulting from the time history analyses are 1524 kips and 3618 kips for the longitudinal and transverse directions, respectively. Normalized base shears with

respect to the total weight above this level are 9.9% and 23.6% for the longitudinal and transverse directions, respectively. These values are significantly higher than the values for which the building was designed, i.e., 5.2% and 7.3% (see Eqs. 2.5 and 2.6). In spite of the significantly higher computed shear values, there was no significant or even visible damage. This may be surprising, in view of the high recorded values of acceleration at the foundation (0.40g and 0.60g, see Table 2.2).

The absence of structural and nonstructural damage can be explained by first noting that the recorded accelerations in the 5th and 10th stories show that there was very small amplification of the input acceleration (see Table 2.2), and that there was actually deamplification at the roof. A second and perhaps even more convincing explanation is obtained by referring to the maximum interstory drifts computed in the time history analyses. The maximum computed interstory drift index for the longitudinal direction of the building (moment-resisting frame) was 0.0034, which occurred at the fourth story. For the transverse direction, the maximum computed interstory drift index was 0.0021. Both values are considered to be smaller than those which could cause visible damage to the building, as will be further discussed in the next chapter.

DIRECTION	PARTICIPATING MASS		
	1st MODE	2nd MODE	1st & 2nd MODES
East-West 90° (A)	62.4	19.5	81.9
North-South 180° (B)	75.3	13.4	88.8

(A) Dual system (shear walls & moment-resisting frame)

(B) Moment-resisting frame

Table 4. 1 Participating mass as a percentage of the total mass for the first two modes of the structure.

FLOOR	DIRECTION	PEAK ACCELERATION [cm/sec^2]		DIFFERENCE [%][C]
		ANALYTICAL	MEASURED	
10th	90° [A]	536.3	523.7	-2.4
5th	90°	587.9	612.2	4.0
10th	180° [B]	418.3	425.8	1.8
5th	180°	528.4	542.8	2.7

FLOOR	DIRECTION	PEAK REL. VELOCITY [cm/sec]		DIFFERENCE [%][C]
		ANALYTICAL	MEASURED	
10th	90° [A]	54.70	55.87	-2.1
5th	90°	21.10	22.07	-4.4
10th	180° [B]	46.55	46.04	1.1
5th	180°	40.82	39.55	3.2

FLOOR	DIRECTION	PEAK REL. DISPL. [cm]		DIFFERENCE [%][C]
		ANALYTICAL	MEASURED	
10th	90° [A]	2.92	2.94	0.7
5th	90°	1.22	1.18	-3.4
10th	180° [B]	7.12	7.14	0.3
5th	180°	4.33	4.11	-5.4

(A) Dual system (shear walls & moment-resisting frame)

(B) Moment-resisting frame

(C) (Measured - Analytical)*100/Measured

Table 4. 2 Comparison of analytical and measured responses of the building during the Whittier Narrows earthquake.
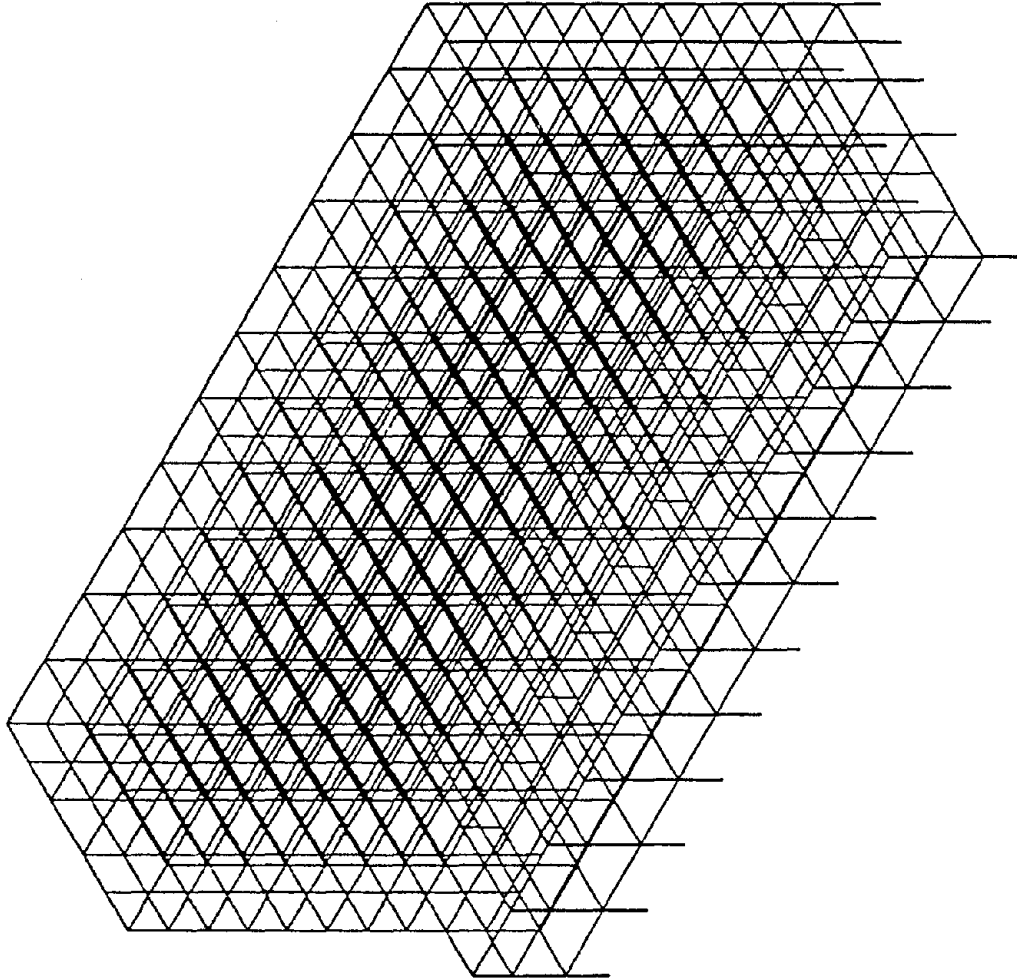
Figure 4. 1 - Three-dimensional finite element model of the building
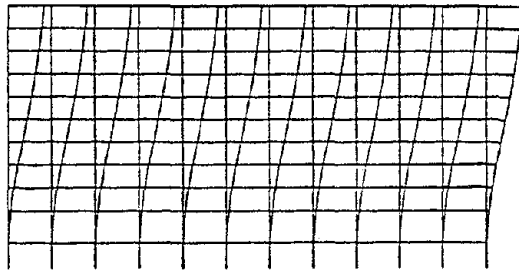
$T_1 = 1.42$ (1st long.)
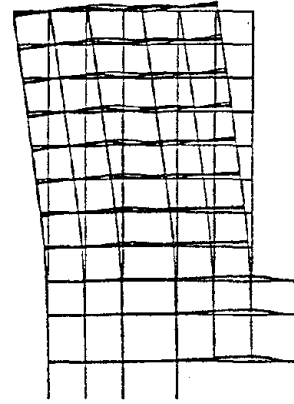
$T_2 = 0.62$ (1st trans.)
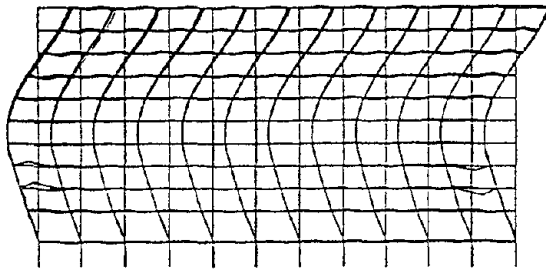
$T_3 = 0.49$ (2nd long.)
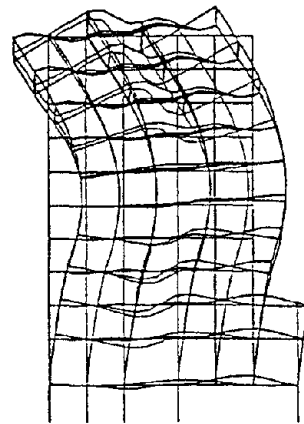
$T_8 = 0.13$ (2nd trans.)
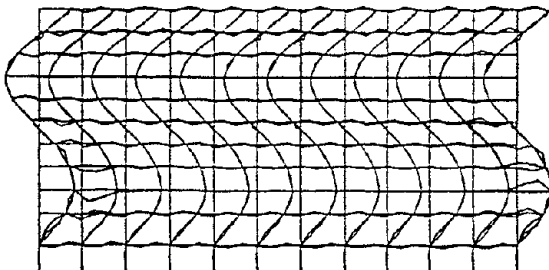
$T_5 = 0.29$ (3rd long.)
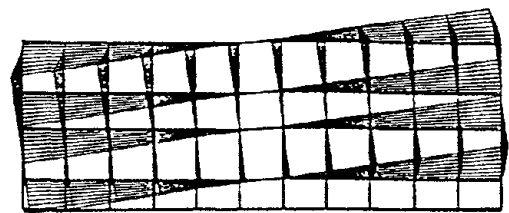
$T_4 = 0.44$ (1st tors.)

Figure 4. 2 - Results from the eigenvalue analysis of the building

ABSOLUTE ACCELERATION (gals)

MEASURED
CALCULATED: 1st MODE ONLY

ABSOLUTE ACCELERATION (gals)

MEASURED
CALCULATED: NINE MODES INCLUDED

TIME (sec)
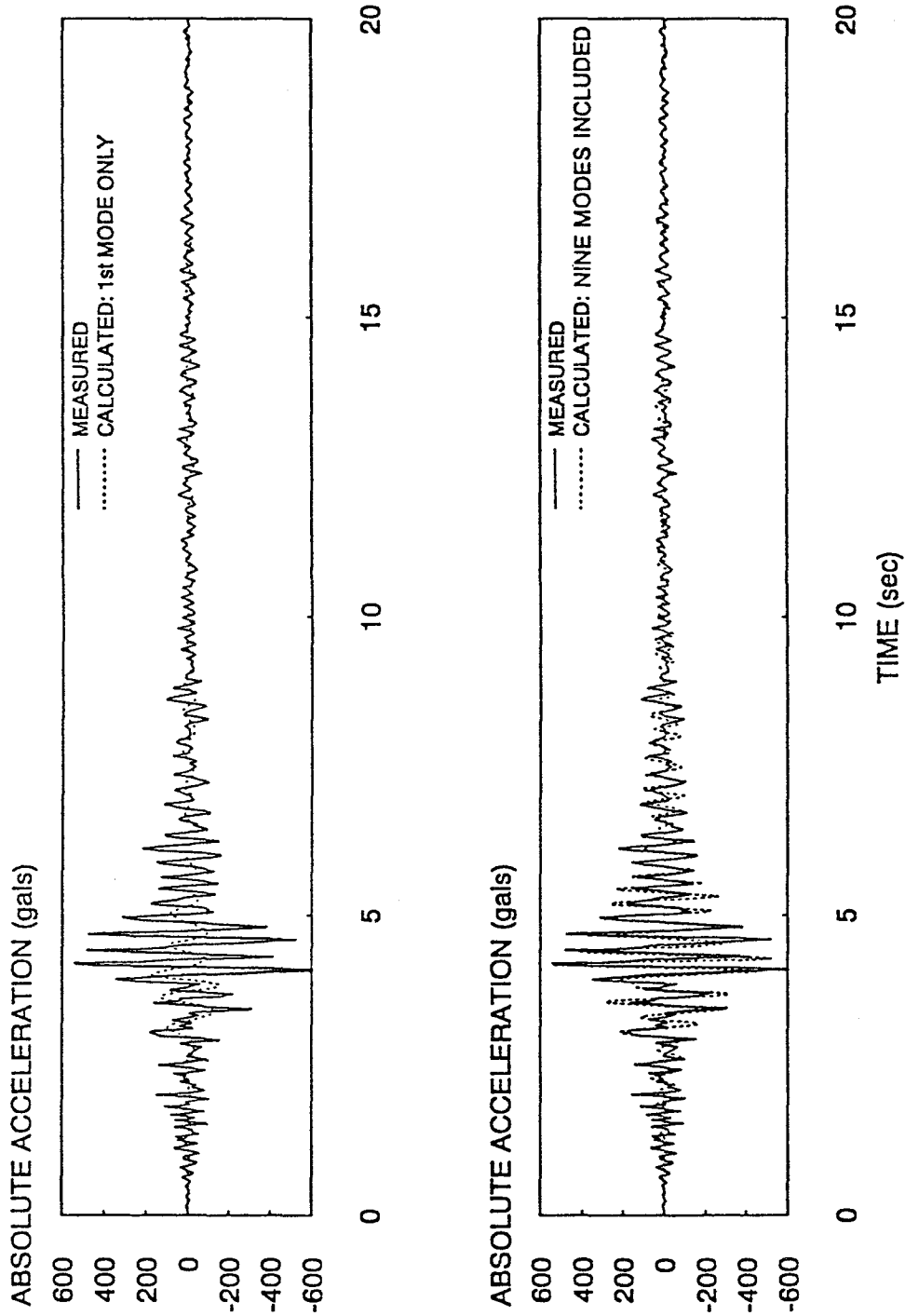
Figure 4. 3 - Comparison of measured and calculated acceleration
time histories at the 5th floor for the transverse direction of the building
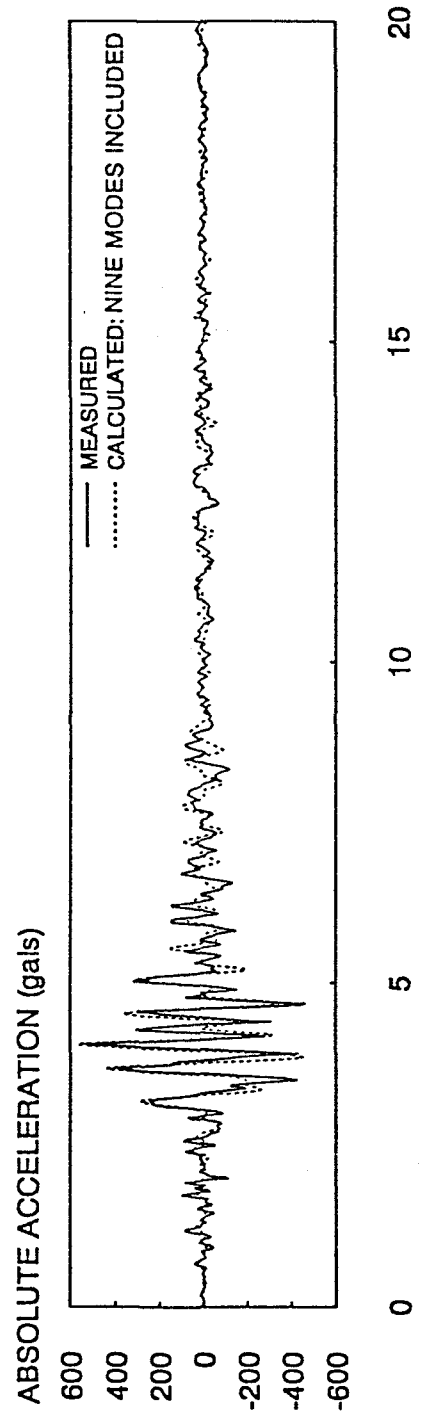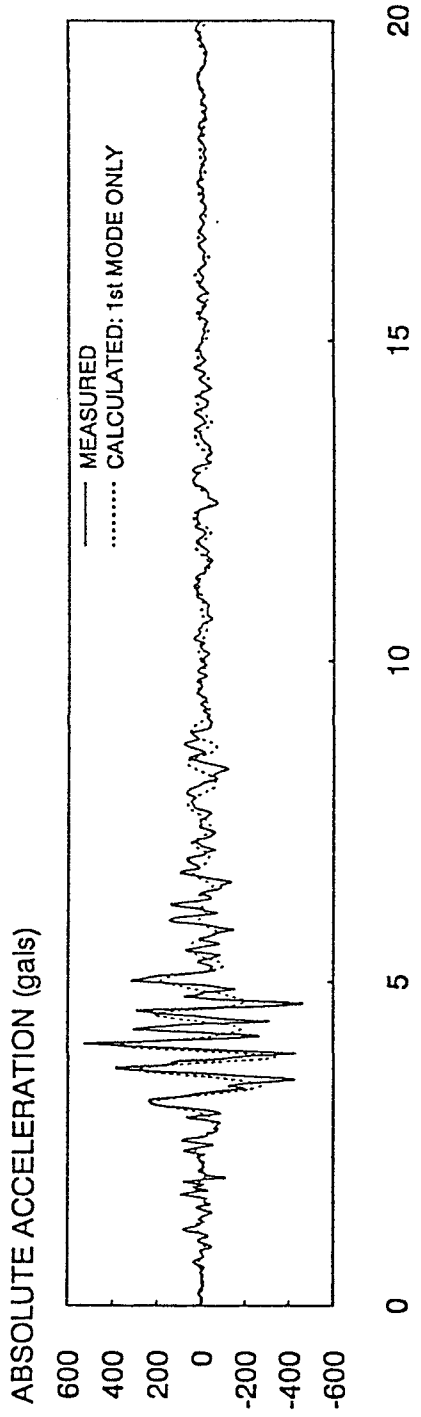
Figure 4. 4 – Comparison of measured and calculated acceleration time-histories at the 10th floor for the transverse direction of the building
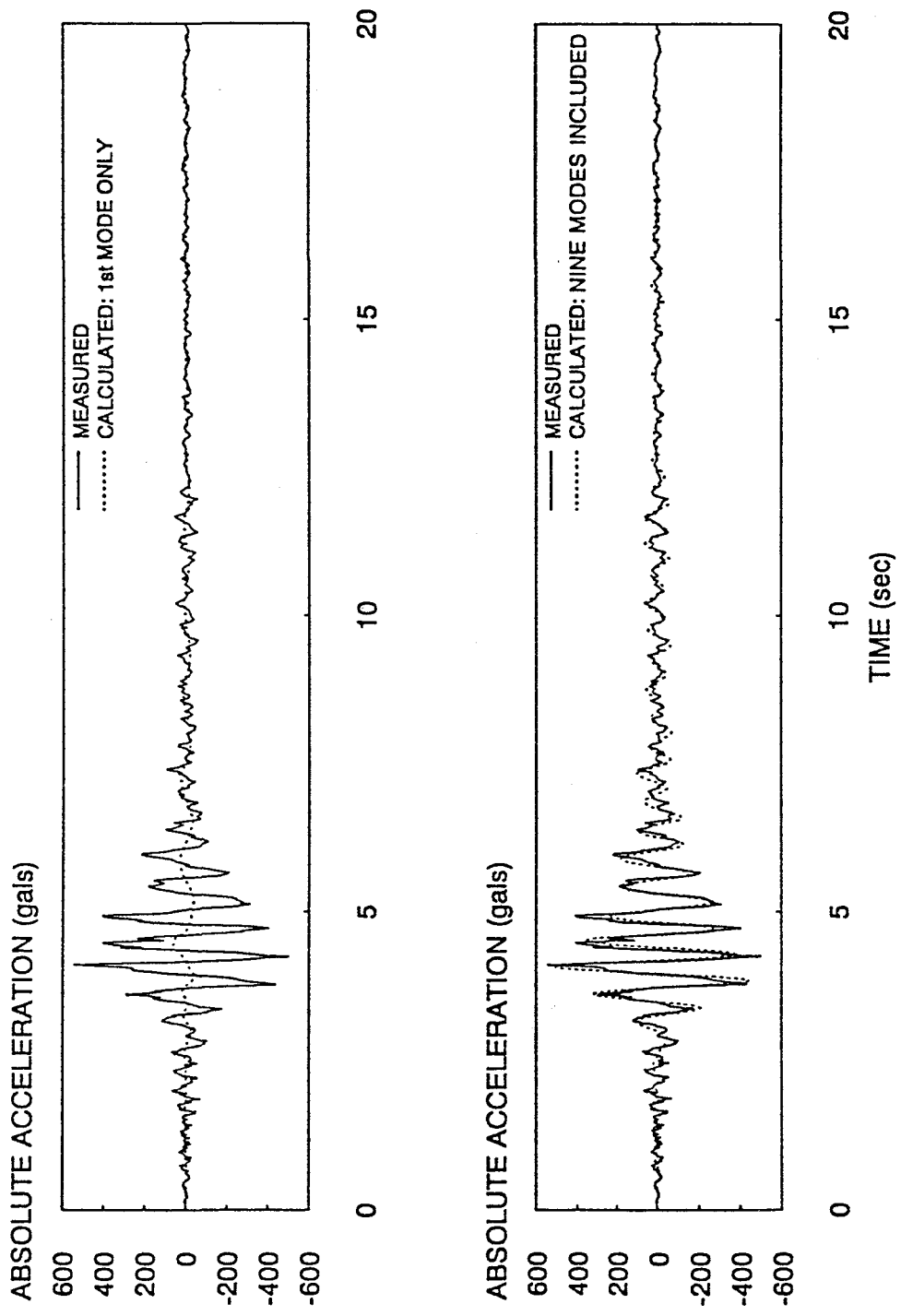
Figure 4. 5 - Comparison of measured and calculated acceleration time-histories at the 5th floor for the longitudinal direction of the building
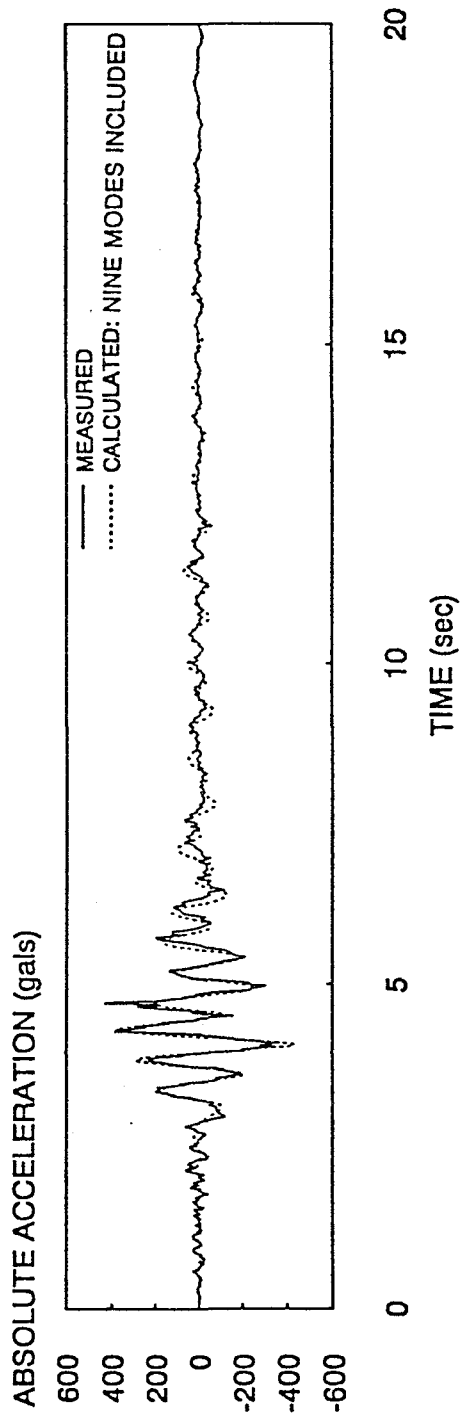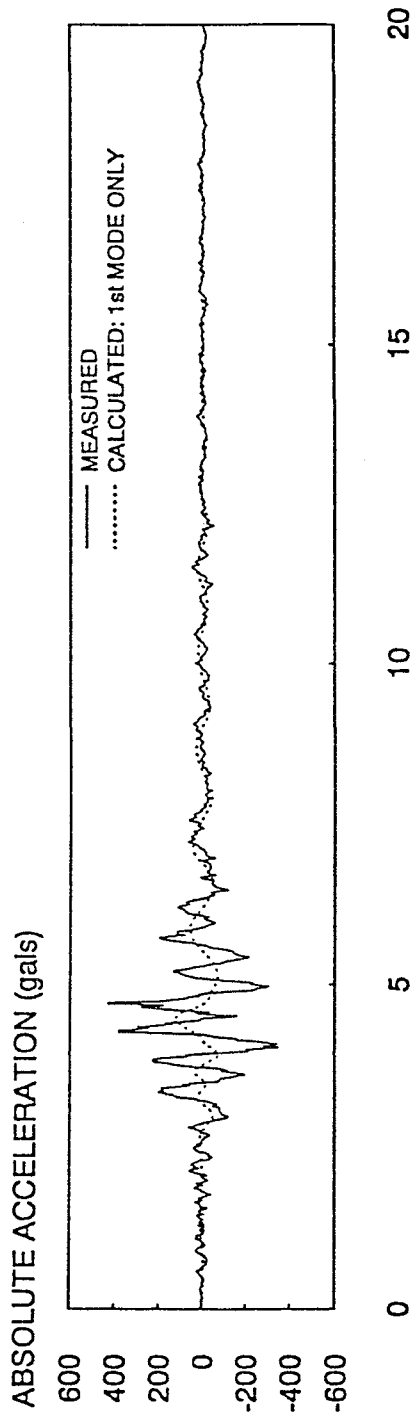
Figure 4. 6 - Comparison of measured and calculated acceleration
time-histories at the 10th floor for the longitudinal direction of the building
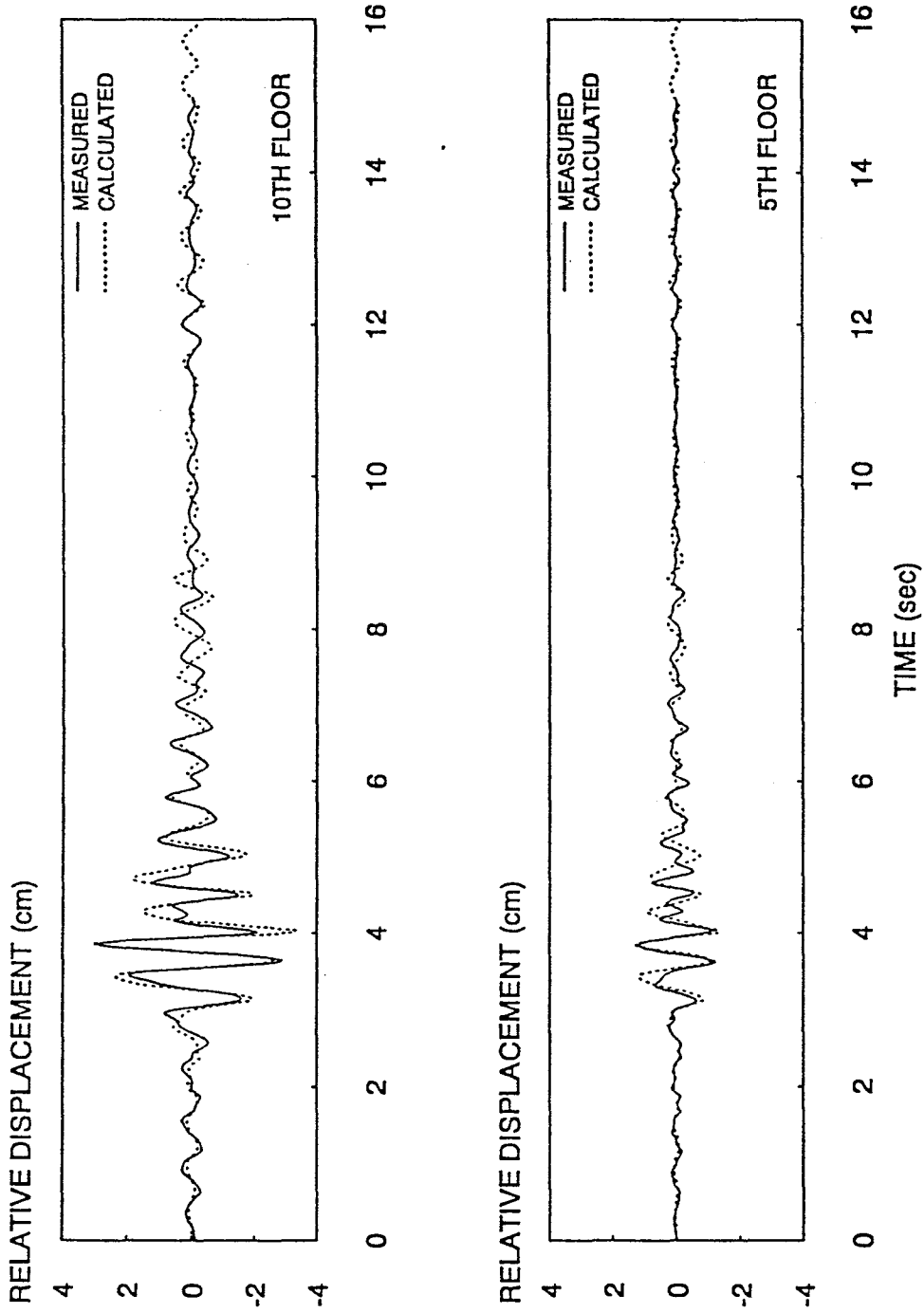
Figure 4. 7 - Comparison of measured and calculated displacement time-histories for the transverse direction of the building

RELATIVE DISPLACEMENT (cm)

MEASURED
CALCULATED

10TH FLOOR

RELATIVE DISPLACEMENT (cm)

MEASURED
CALCULATED

5TH FLOOR

TIME (sec)
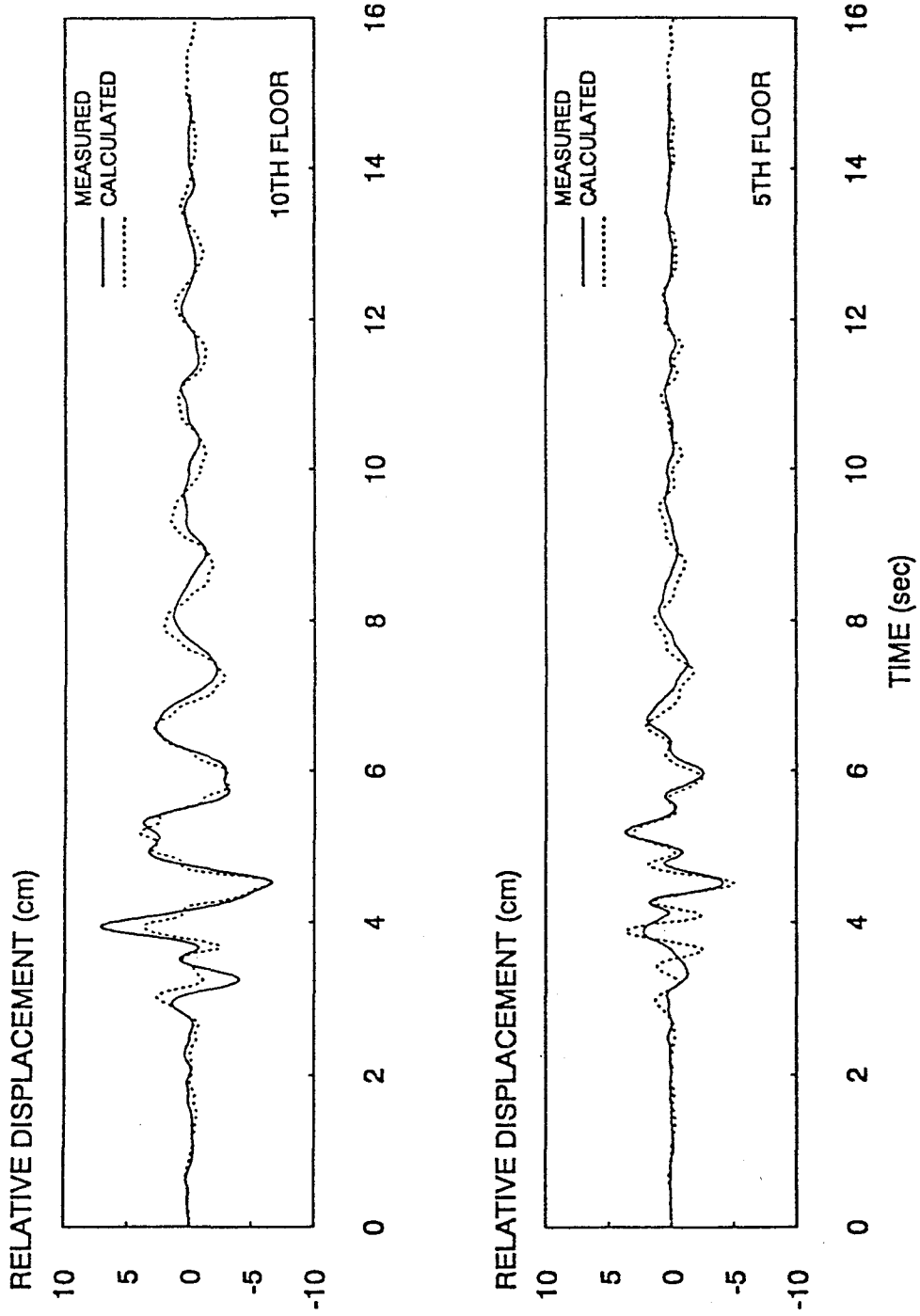
Figure 4. 8 - Comparison of measured and calculated displacement
time histories for the longitudinal direction of the building

5. EVALUATION OF THE SUPPLIED CAPACITIES TO THE BUILDING

5.1 GENERAL REMARKS

A series of nonlinear static-to-collapse analyses was conducted in order to investigate the supplied capacities (strength and deformability) to the building. The analyses were conducted using the DRAIN-2D computer program [23].

Nonlinear modelling of structural members was based on section analyses of their critical regions. For this purpose moment-curvature relations were computed for 18 different cross-sections. Additionally, moment-axial load interaction diagrams were computed for the critical cross-sections of 12 different column or shear wall elements.

5.2 NONLINEAR STATIC-TO-COLLAPSE ANALYSIS IN THE LONGITUDINAL (N-S) DIRECTION OF THE BUILDING

To model the longitudinal direction of the building, the exterior frames (frames C and F in Fig. 2.3) were lumped together, assuming a rigid floor diaphragm. Similarly, the interior frames (frames D and E in Fig. 2.3) were lumped together. The slab in the interior of the building was modelled by equivalent beams. These beams had a depth equal to the slab depth and width equal to the full slab width times an effective-width factor. Experimental research on flat-plate frame buildings has suggested that the effective width factor is a function of the level of lateral deformations, and that for drifts higher than 0.0025% the use of effective widths based on elastic plate theory produces significant overestimations of the stiffness of the system [23]. In order to account for the stiffness of the slab at large lateral drifts (IDI > 0.005), an equivalent width of 36 inches, equal to C + 3h (where C = column width and h = slab thickness), was used. The stiffness of the retaining walls in the basement was modelled by springs with zero tensile capacity. The mathematical nonlinear model consisted of 289 nodes, 519 members and 780 degrees of freedom.

Load-deformation relations were determined by imposing assumed shapes for lateral load distributions over the height of the structure and increasing the total load monotonically from

zero up to incipient collapse. For this purpose two loading patterns were used, triangular and rectangular (uniform). Figure 5.1 shows the relationship between the base shear (first story) and the roof displacement for the longitudinal direction of the building. The uniform loading pattern led to 24% higher initial stiffness and 19% higher maximum strength. From the figure it can be seen that the maximum longitudinal displacement of 7.14 cm (2.81 inches) experienced during the 1987 Whittier Narrows earthquake was not large enough to cause any yielding in the building. The ratio between the maximum base shear and the base shear at first significant yielding is 1.38 for both lateral loading patterns.

Figure 5.2 shows the relationship between the base shear (first story) normalized by the total weight (weight above the first story) and the roof displacement normalized by the roof height (above ground level). The maximum lateral strength of the building is 22% of its weight when subjected to a triangular load distribution and 26% for a uniform loading pattern. Structural damage is initiated in both cases for a normalized displacement of 0.004. Shown in this figure are the minimum strength requirements of the 1970 UBC (see Eq. 2.6). It can be observed that the building has a lateral strength significantly higher than that for which it was designed. The computed overstrengths of the building are 3.23 and 4.0 for the triangular and uniform loading patterns, respectively.

While base shear-roof displacement relationships provide a good picture of the global behavior of the building, they fail to provide information about the strength and deformation demands on specific stories of the building. Displacement profiles of the building at different levels of deformation are shown in Figs. 5.3 and 5.4 for triangular and uniform loading patterns, respectively. While the building remains elastic the displacement profile increases proportionally with the applied lateral load. However, when the structure becomes nonlinear (for roof displacements larger than approximately 4.3 inches) the displacement profiles are no longer proportional to the applied load. As shown in Figs. 5.5 and 5.6, where the profiles of the values of the interstory drift indices are presented, after yielding the lateral deformations tend to concentrate in certain stories. For a triangular loading pattern, large deformations concentrate in the 3rd to 7th stories, while for the uniform loading pattern, large deformations concentrate in the 3rd to 6th stories.

Figure 5.7 shows the contribution of interior and exterior frames to the strength and stiffness of the building when subjected to a triangular lateral loading pattern. It can be seen that because of the great flexibility of the interior frames (flat-plate), they make a relatively small contribution to the lateral strength and stiffness of the building. When the building remains elastic, the interior frames take 16.4% of the lateral forces. When the maximum strength of the building is reached, the contribution of the interior frames increases to 26.6% because of significant yielding in the exterior frames. The exterior frames start to yield at a roof displacement of 4.3 inches, while the first nonlinearity in the interior frames does not appear until a roof displacement of 7.5 inches is reached. This difference in yielding deformations results in a global (structure) post-yielding stiffness of approximately 22% of the original stiffness (for this range of deformations).

The location of plastic hinges in the building when subjected to triangular and uniform loading patterns at three different levels of deformation is shown in Figs. 5.8 and 5.9. As previously mentioned, deformations concentrate over the 3rd to 7th stories. Furthermore, because these stories of the exterior frames have stronger beams than columns (strong beam-weak column), yielding occurs in the columns and not in the beams. The maximum deformation capacity of the building is controlled by the available rotation capacity of the columns in these critical stories and by the shear capacity of their corresponding beam-column joints.

The transverse reinforcement ratio (ρ_s) in the critical regions of these columns is 0.013 which is, in general, superior to that observed in buildings designed according to "pre-San Fernando" detailing requirements. The effectiveness of these hoops, however, for providing confinement to the core and therefore for increasing the rotation capacity of the columns, is not expected to be good because of the 90° hooks at the corners of the section (see Fig. 2.6). It has been observed that concrete columns with this detail do not exhibit good behavior, since when the concrete cover is lost the end of the hoop leg at the 90° hook moves away from the longitudinal bar it engages, resulting in complete loss of anchorage of the tie [24] and therefore there is a loss of confinement and restraining capacity against local buckling

of the longitudinal reinforcement. For the maximum deformation shown in Fig. 5.1, rotations in excess of 1.6% are observed in the fourth story columns.

When the roof displacement reaches 11 inches, computed joint shear stresses are 654 psi (10.35 $\sqrt{f'_c}$) similar to those measured at failure in recently tested beam-column connections that had little or no transverse reinforcement [25].

5.3 NONLINEAR STATIC-TO-COLLAPSE ANALYSIS IN THE TRANSVERSE (E-W) DIRECTION

In order to investigate the strength of the transverse direction of the building, a two-dimensional model was constructed. In this model, the exterior frames (frames 2 and 13 in Fig. 2.3) were lumped together by assuming a rigid floor diaphragm. Similarly, the two frames next to the elevator shaft (frames 7 and 8) and the moment-resisting frames (frames 3, 4, 5, 6, 9, 10, 11, and 12) were lumped together. The slab in these interior frames was modelled using the same assumptions previously made for the longitudinal direction. Shear walls were modelled as beam-column elements with rigid beams extending from the center line of the shear wall to each edge. The stiffness of the retaining walls in the basement was modelled by springs with zero tension capacity. The increase in axial load in the shear walls due to outrigger effects was included by adding nonlinear springs with stiffnesses equal to those of the beams framing perpendicularly into the shear walls. The complete mathematical model consisted of 121 nodes, 206 members, and 342 degrees of freedom.

As was done for the longitudinal direction of the building, load-deformation relations were determined using triangular and rectangular (uniform) lateral load patterns. Figure 5.10 shows the relationship between the base shear and the roof displacement for both loading patterns. These curves are characterized by a gradual loss in lateral stiffness due to yielding of the coupling girders, followed by a more drastic change in stiffness due to yielding of the shear walls. Strengths corresponding to the first significant yield (i.e., when yielding of the shear walls occurs) of 32% and 43% of the total weight of the building were computed for the triangular and uniform loading patterns, respectively. Also shown in the figure is the minimum strength required by the 1970 UBC (see Eq. 2.5). The building has an overstrength

even higher than that computed for the longitudinal direction. Computed ratios of maximum strength to code design strength in the transverse direction are 5.75 and 6.99 for the triangular and uniform loading patterns, respectively.

From Fig. 5.10 it can be seen that the maximum displacement of 1.16 inches (2.94 cm, see Table 4.2) in the transverse direction during the 1987 Whittier Narrows earthquake was not large enough to cause any significant damage in the building. However, analysis shows that some yielding must have occurred at the ends of the weak coupling beams of the four upper stories. It is not known if post-earthquake inspections [10, 11] included a careful inspection of these beams.

Displacement profiles of the building at different levels of deformation are shown in Figs. 5.11 and 5.12 for both the triangular and uniform loading patterns. From these figures it can be seen that for large levels of deformations (roof displacements larger than 4 inches) the presence of the shear walls produces a nearly uniform distribution of interstory displacements above the fourth story.

Figures 5.13 and 5.14 show the location of plastic hinges at large deformations for triangular and uniform loading patterns. The flat plate-column frames remain elastic for these levels of deformation because of their great lateral flexibility. Nonlinearities in frames 7 and 8 are characterized by yielding of the shear walls (throughout the 3rd and 4th stories) and by yielding of the slab adjacent to the shear walls in the upper floors. When the roof displacement reaches 7.5 inches the maximum average shear stress in the shear walls is 439 psi (6.9 $\sqrt{f'_c}$). Under this level of deformation it is expected that a combination of flexural and shear cracking would occur, but the web of the barbell-section shear wall should resist these levels of shear stress without a shear failure. Significant strength degradation could, however, occur under repeated large deformation cycles (roof displacements larger than 6.0 inches). For frames 2 and 13 nonlinearities are characterized by yielding of the weakly coupled shear walls and by yielding of the coupling beams. For a roof displacement of 7.5 inches, maximum average shear stresses in the coupled shear walls are 561 psi (8.8 $\sqrt{f'_c}$) which could initiate a shear failure of the web. Average shear stresses in the north-west wall

were computed as high as 755 psi (11.9 $\sqrt{f'_c}$). This is caused by the presence of a large opening (see Fig. 2.2) which accommodates the trash room door. Plastic rotations of up to 0.06 radian were computed for the coupling girders in the upper floors.

Because of their low flexural capacity, no shear failure is expected to occur in the coupling girders above the second floor (the maximum computed shear stress was 97 psi, or 1.8 $\sqrt{f'_c}$). However, a shear failure is expected to occur in the second floor coupling beam. The computed shear stress for this deep and flexurally strong beam was 885 psi (16 $\sqrt{f'_c}$) which is considerably higher than its shear capacity.
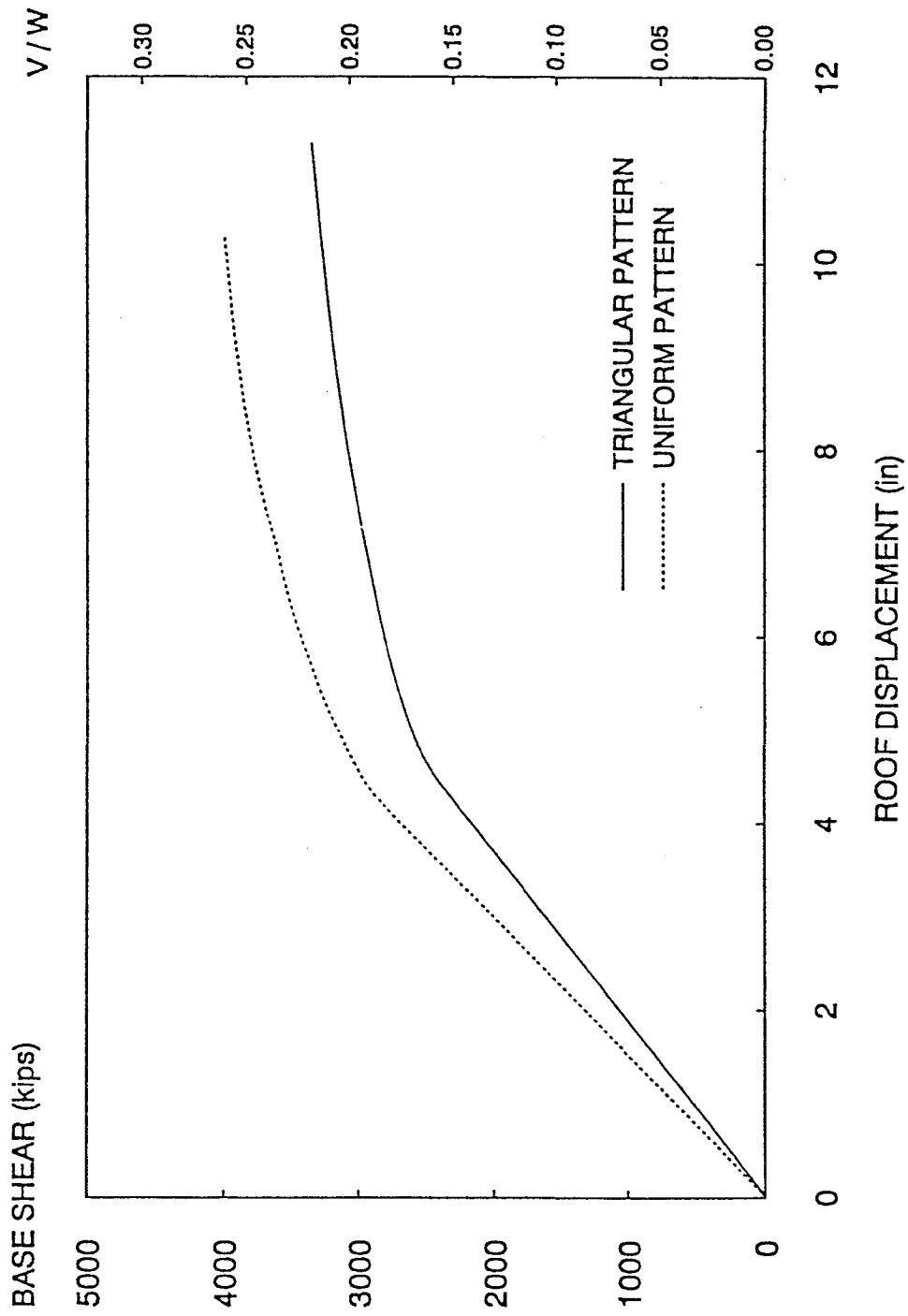
Figure 5. 1 - Load-deformation relations for the longitudinal direction of the building.
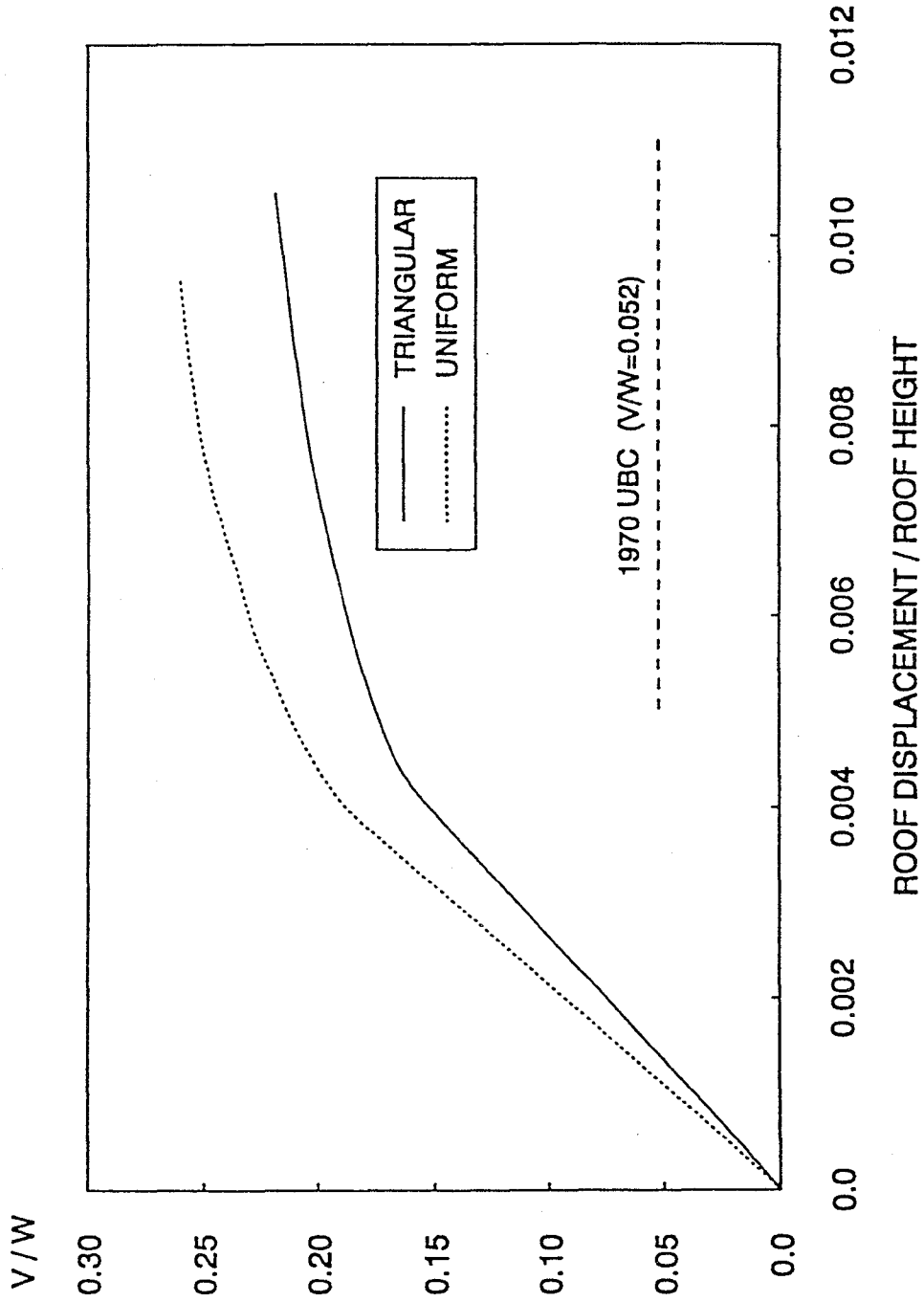
Figure 5. 2 - Comparison of computed strengths (for the longitudinal
direction of the building) and 1970 UBC minimum strength requirements
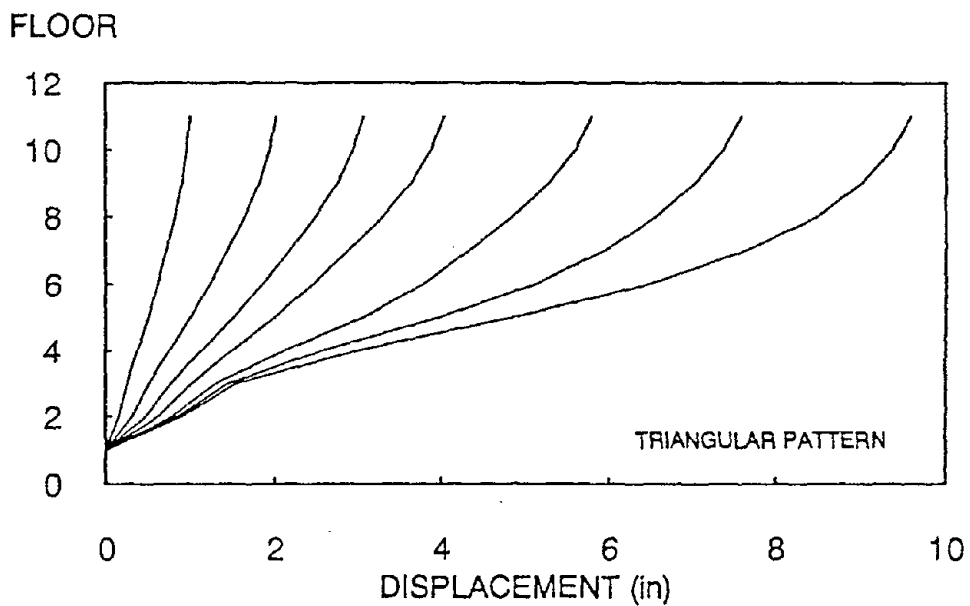
Figure 5. 3 - Longitudinal displacement profiles of the building at different levels of deformation when subjected to a triangular loading pattern
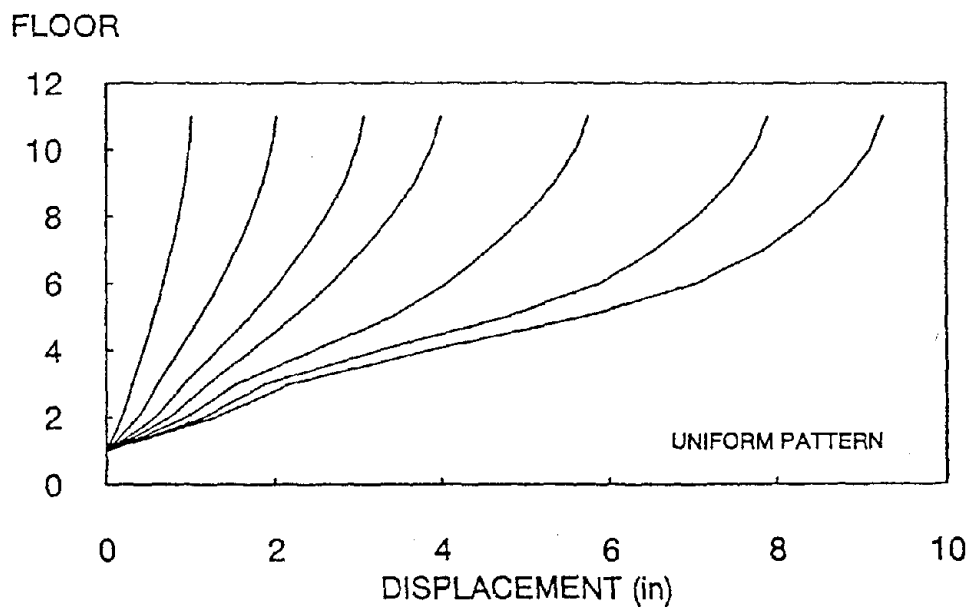
Figure 5. 4 - Longitudinal displacement profiles of the building at different levels of deformation when subjected to a uniform loading pattern
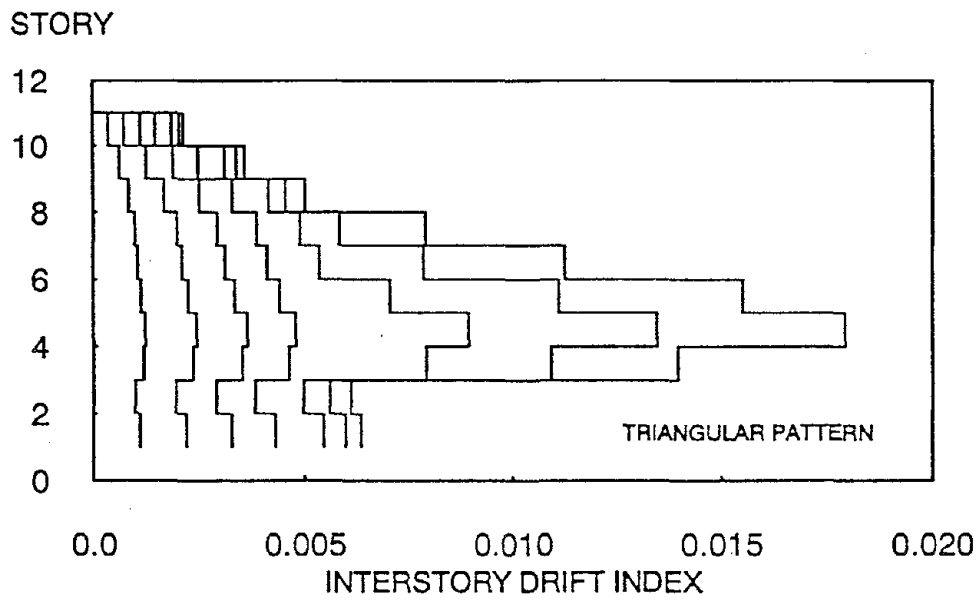
Figure 5. 5 - Interstory drift index profiles of the building at different levels of deformation when subjected to a triangular loading pattern
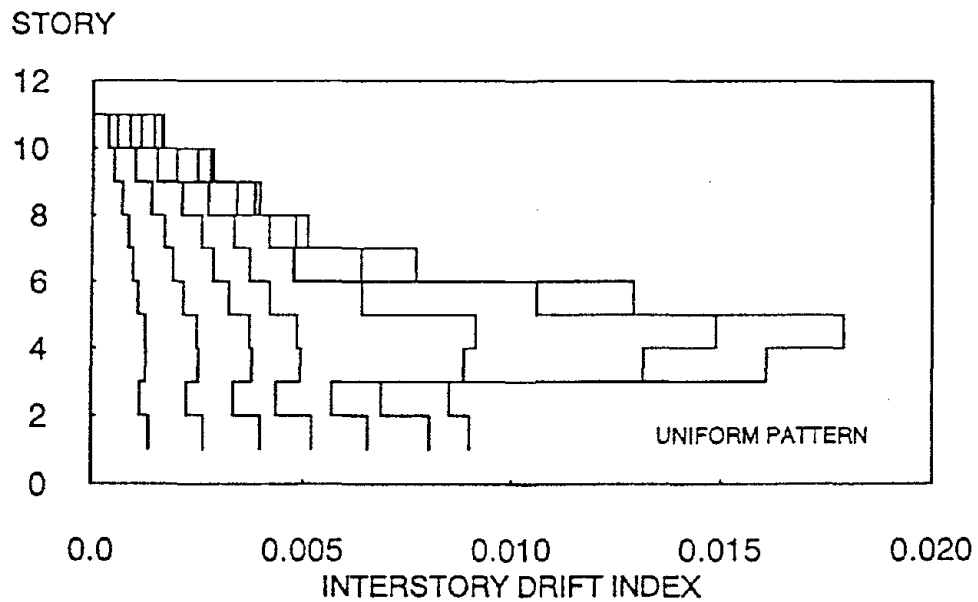
Figure 5. 6 - Interstory drift index profiles of the building at different levels of deformation when subjected to a uniform loading pattern.
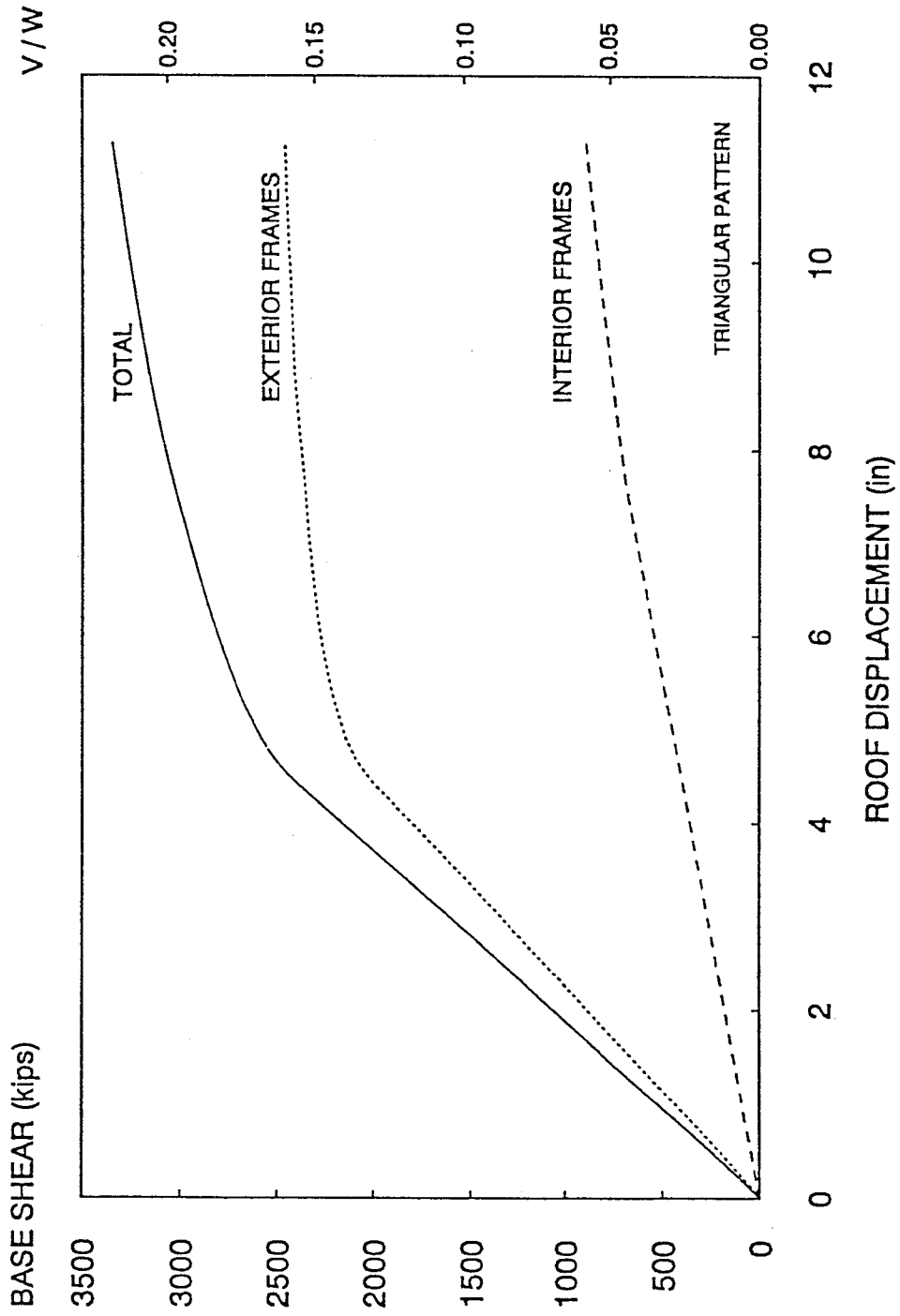
Figure 5. 7 - Contribution of exterior and interior frames to the total
lateral strength and stiffness of the building
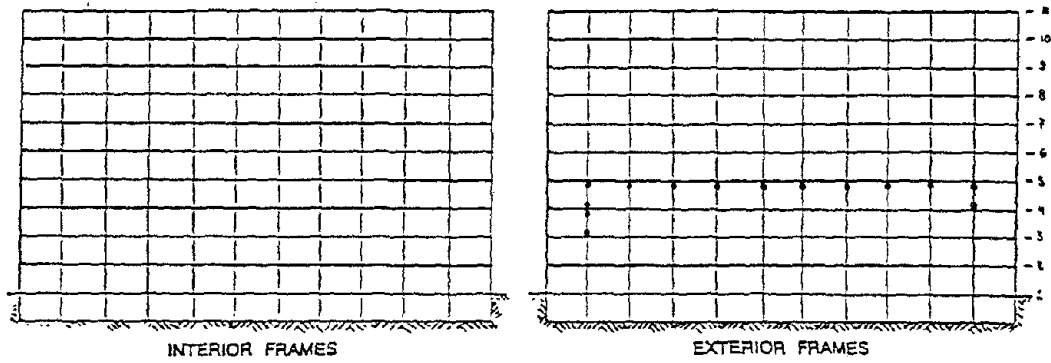
A) V_{base} = 2,454 kips $(\Delta_{roof}$ = 4.40 in)
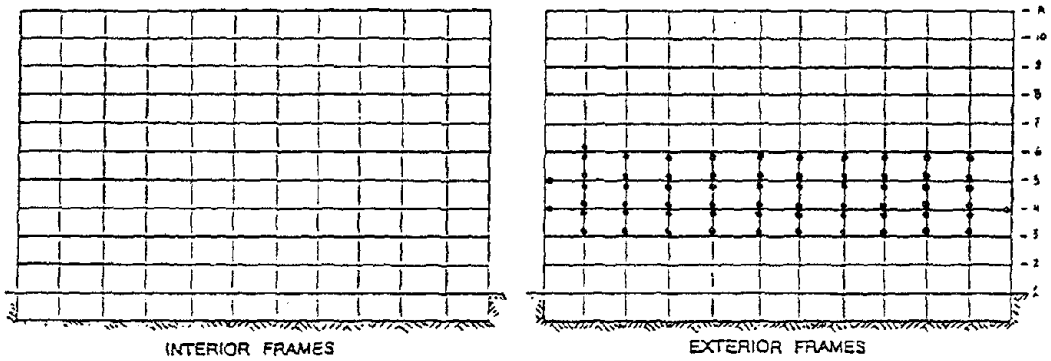
B) V_{base} = 2,789 kips $(\Delta_{roof}$ = 5.46 in)
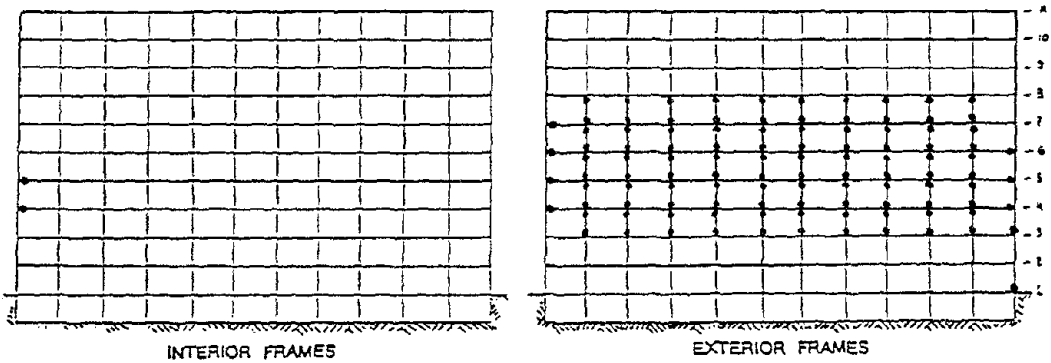
C) V_{base} = 3,114 kips $(\Delta_{roof}$ = 7.60 in)

Figure 5. 8 - Locations of plastic hinges in the building at three different levels of deformation when subjected to a triangular loading pattern
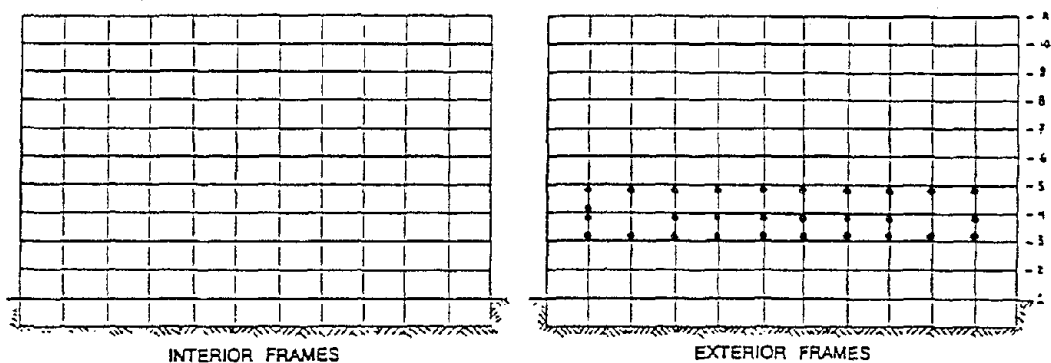
A) V_{base} = 2,881 kips (Δ_{roof} = 4.30 in)
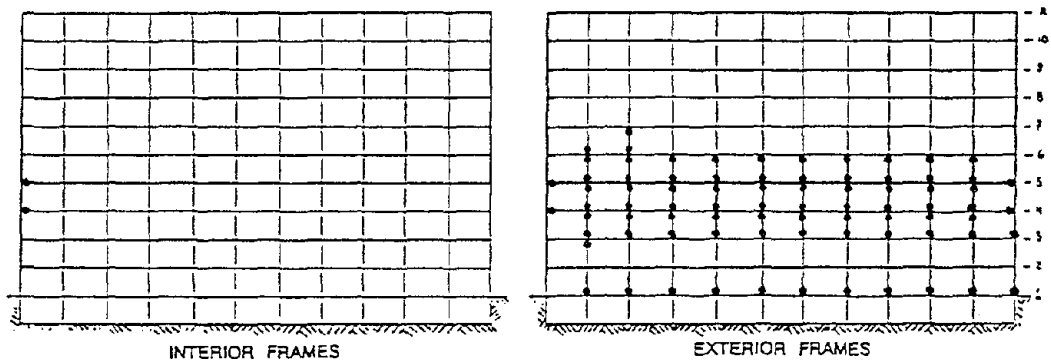
B) V_{base} = 3,560 kips (Δ_{roof} = 6.66 in)
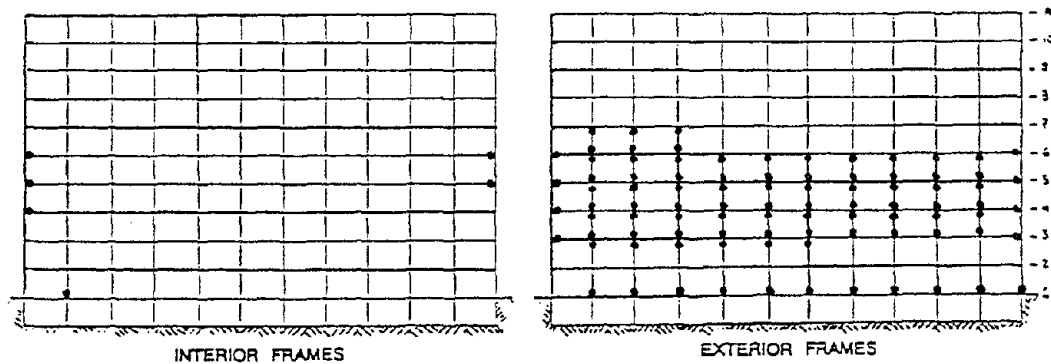
C) V_{base} = 3,920 kips (Δ_{roof} = 9.26 in)

Figure 5. 9 - Locations of plastic hinges in the building at three different levels of deformation when subjected to a uniform loading pattern
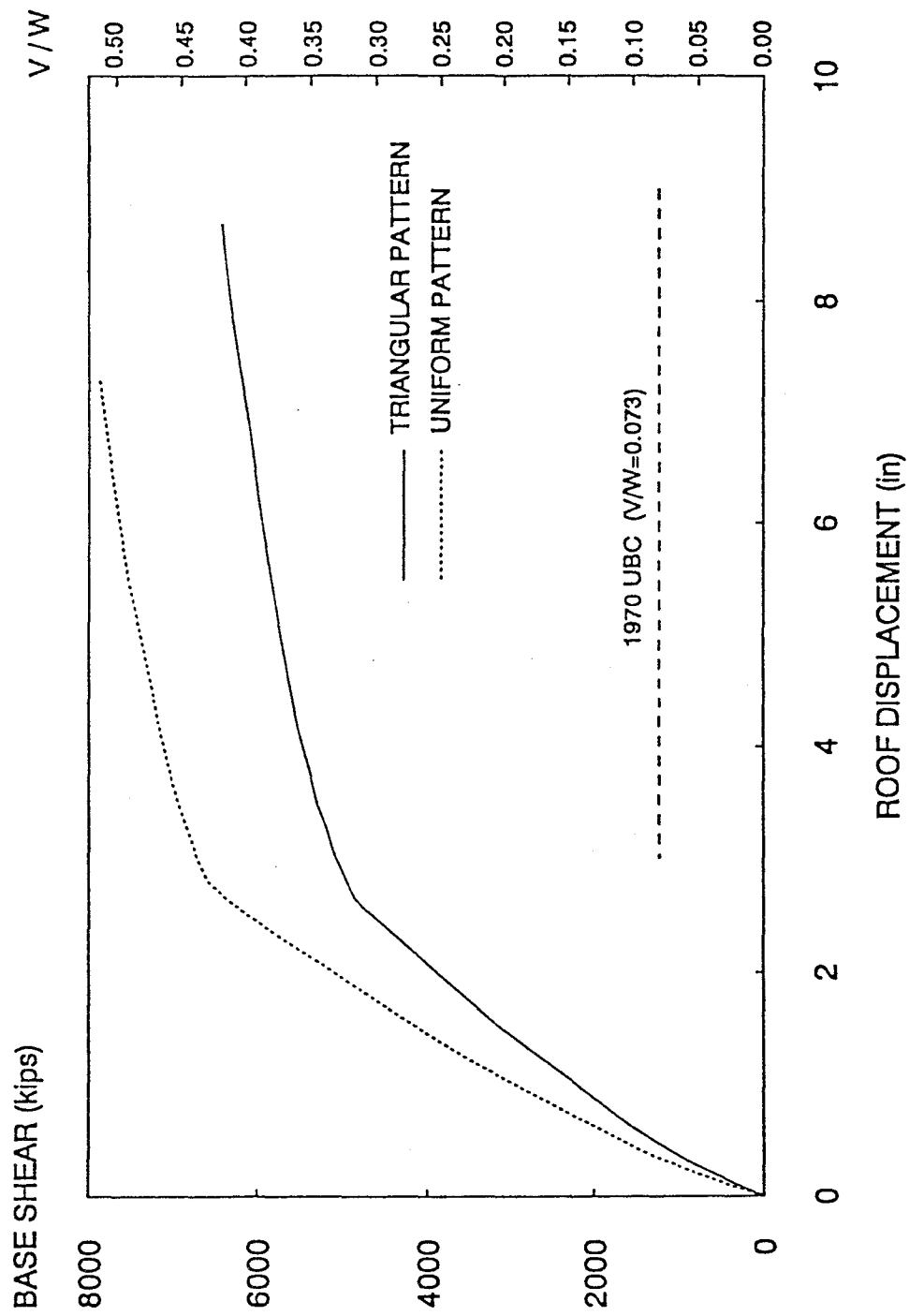
Figure 5. 10 - Load-deformation relation to the transverse direction of the building
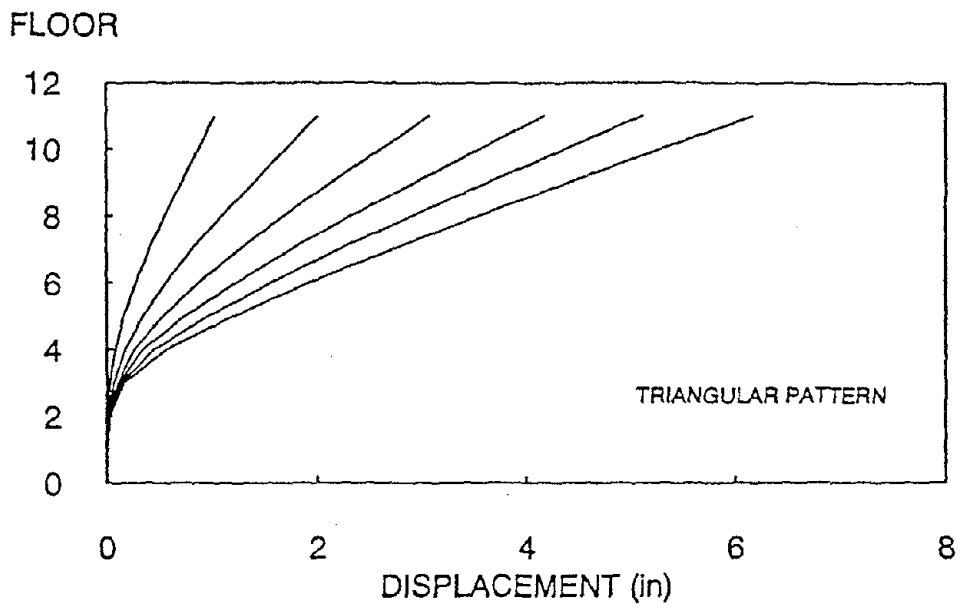
Figure 5. 11 - Transverse displacement profiles in the building at different levels of deformation when subjected to a triangular loading pattern
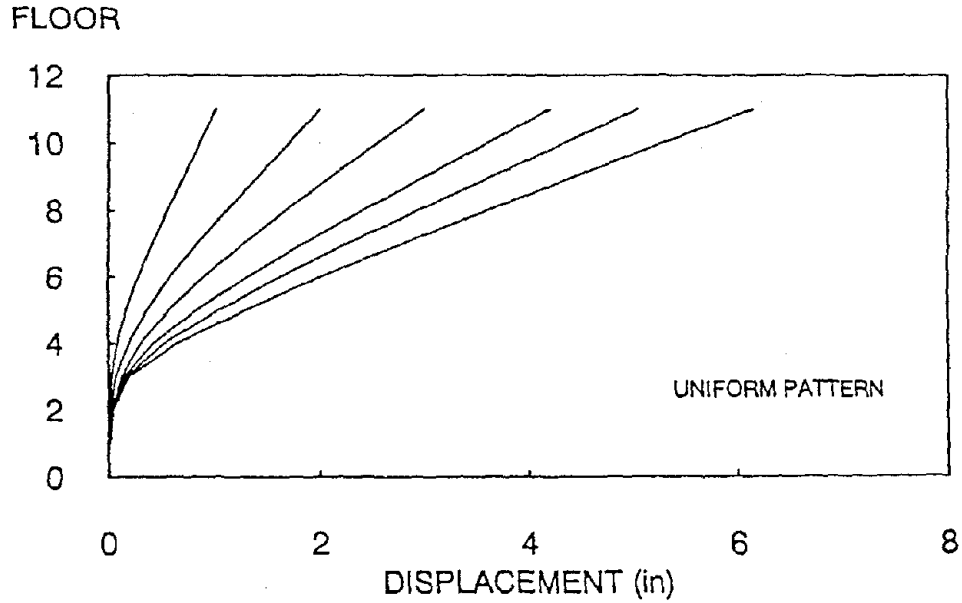
Figure 5. 12 - Transverse displacement profiles of the building at different levels of deformation when subjected to a uniform loading pattern

FRAMES 3, 4, 5, 6, 9, 10, 11, 12   FRAMES 7 & 8   FRAMES 2 & 13

V_{base} = 5,865 kips (Δ_{roof} = 5.63 in)
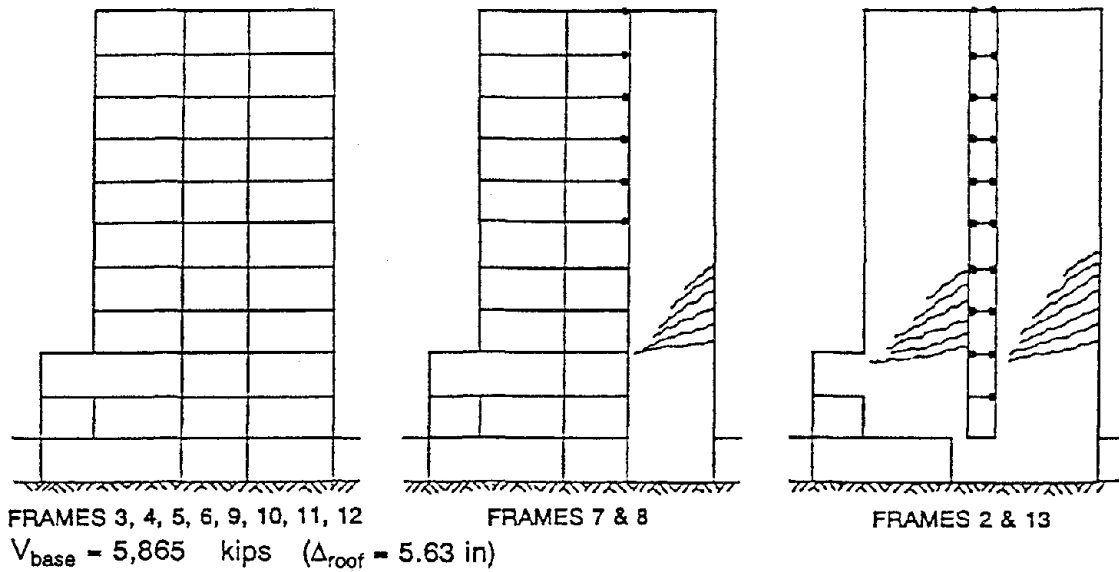
Figure 5. 13 - Locations of plastic hinges in the building when
subjected to a triangular loading pattern

FRAMES 3, 4, 5, 6, 9, 10, 11, 12   FRAMES 7 & 8   FRAMES 2 & 13

V_{base} = 7,874 kips (Δ_{roof} = 6.50 in)
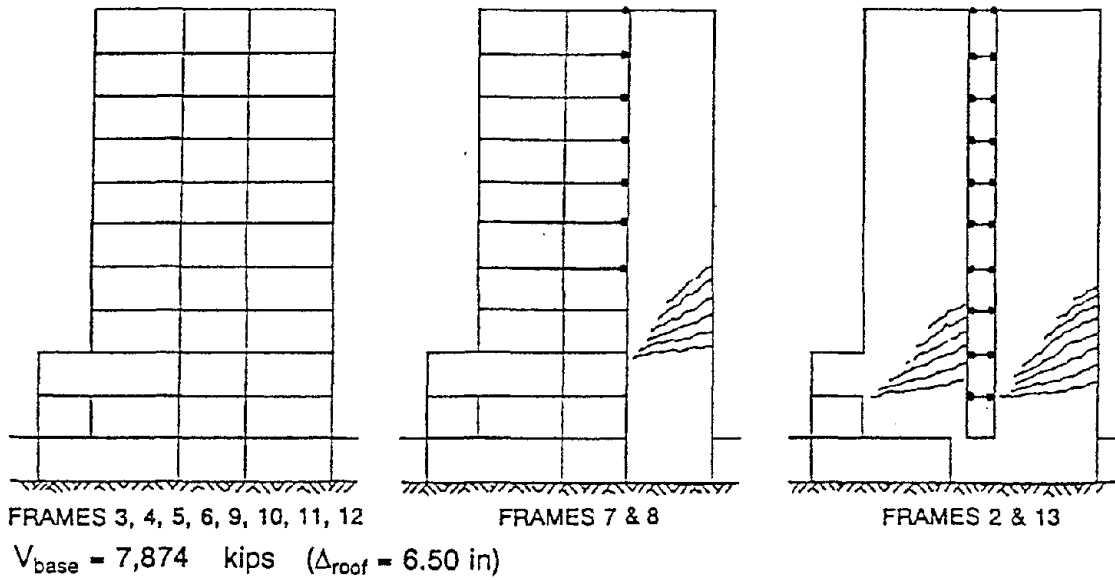
Figure 5. 14 - Locations of plastic hinges in the building when
subjected to a uniform loading pattern

6. NONLINEAR ANALYSES OF THE PERFORMANCE
OF THE BUILDING UNDER SAFETY LEVEL
EARTHQUAKE GROUND MOTIONS

6.1 SELECTION OF THE CRITICAL GROUND MOTIONS

A complex pattern of quaternary faults represents the earthquake hazard for this building, and in general for the Los Angeles region. The seismicity of this area is dominated by two seismically active fault systems -- the northwest-trending, right-lateral strike-slip San Andreas and its members (San Jacinto, Whittier-Elsinore, and Newport-Inglewood) and the west-trending, reverse faults of the Transverse Ranges (Santa Ynez, Santa Ana, San Cayetano, San Gabriel, San Fernando, Santa Monica, Cucamonga, etc). Details of the seismicity of these and many other smaller faults have been described by Ziony and Yerkes [26].

The San Andreas fault could be the source of the largest magnitude earthquake in this region. The San Andreas fault was the source of the 1857 Fort Tejon earthquake, the largest event known to have affected the Los Angeles region since the exploration of the area by the Spaniards in 1769. This earthquake is representative of the largest event likely to occur in the southern portion of the San Andreas fault [26]. Although this earthquake occurred before the advent of seismograph recordings, its magnitude has been estimated to be larger than the 1906 San Francisco earthquake [27].

The Mojave segment of the San Andreas fault has been attributed a 30% probability of producing a major earthquake between 1988 and 2018 [28]. Another study has attributed the probability of a major earthquake in southern California to be as high as 60% in the next 30 years [29].

The degree of damage that a specific building can undergo when subjected to major EQ ground motions can be predicted through nonlinear time-history analysis. This requires the availability of the full characterization of the acceleration time-history of the EQ ground motion, and particularly of the motion that will drive the structure to its critical response, i.e., the safety design EQ which is sometimes called the Maximum Credible EQ (MCEQ). This

critical EQ ground motion should be selected from all the possible ground motions that can occur during the service life of the structure [30]. Although an upper limit of about 8 for earthquakes in the Los Angeles region is compatible with the historical data [26], there are no acceleration records from earthquakes of magnitude larger than 7.7 in California. In this study, rather than taking into account what the EQ ground motions would be at the building site due to an EQ of M = 8 in the San Andreas fault zone, what is considered is the possible damage induced in the ten-story building by what are considered the two most critical recorded ground motions obtained on similar soil conditions in California.

The following two sections describe the results of time-history analyses conducted for the longitudinal direction of the building.

The soil conditions at the site consist of quaternary alluvium deposits of medium-grain sand sediments [31]. Two earthquake ground motions recorded in California on alluvium deposits and with relatively high input energies in the vicinity of the longitudinal fundamental period of the building (1.43 seconds) were selected as inputs for the time history analyses. The first ground motion is the north-south component of the Hollister record, obtained during the October 17, 1989 Loma Prieta earthquake (M_s = 7.1) in the city of Hollister (CSMIP Station No. 47524) approximately 48 km (29.8 miles) southeast of the epicenter [32]. The digitized record has a total duration of 40 seconds, a peak ground acceleration of 361.9 gals (0.37g), and a maximum incremental velocity of 121.6 cm/sec (47.9 in/sec).

The second ground motion is the S50W component of the James Road record, obtained during the October 15, 1979 Imperial Valley earthquake (M_L = 6.5) approximately 10 km (6.2 miles) north of the epicenter [33]. The digitized record has a total duration of 39.3 seconds, a peak ground acceleration of 360.4 gals (0.37g), and a maximum incremental velocity of 160.0 cm/sec (63.0 in/sec).

For both ground motions, only the initial 20 seconds of the records were employed in the time-history analyses. This portion of both acceleration times histories is shown in Fig. 6.1. The Hollister record is characterized by a low-frequency content and a long-duration

acceleration pulse (lasting 0.7 second) at approximately the 8 second mark and another (lasting 1.0 second) at approximately the 12 second mark. The James Road record is characterized by a long-duration acceleration pulse (lasting 1.6 seconds) at approximately the 6 second mark. The presence of long-duration pulses in records of the 1979 Imperial Valley EQ has been the subject of several detailed studies [34, 35].

6.2 BEHAVIOR UNDER THE HOLLISTER RECORD

Time-history analyses were conducted using DRAIN-2D with an integration time step of 0.02 second. Roof displacement and base shear time-histories computed in the building when subjected to the 1989 Hollister record are shown in Fig. 6.2. The maximum roof displacement and maximum base shear are 7.59 inches and 3,599 kips, respectively. These peaks both occur as a result of the long-duration acceleration pulse that occurs at the 8 second mark. Story load-deformation relations for the 1st to 8th stories are shown in Fig. 6.3. The inelastic deformations concentrate from the 3rd to 7th stories, with a maximum displacement ductility ratio of 3.15 in the fourth story. Columns in this story undergo four yield reversals and a maximum rotation of 0.02 radian. Computed response envelopes are shown in Fig. 6.4. The story deformations are significantly non-uniform, with the intermediate stories experiencing the highest demands.

6.3 BEHAVIOR UNDER THE JAMES ROAD RECORD

The time-history analysis for the James Road record was conducted using the same model and integration time step as that previously used for the Hollister record.

Roof displacement and base shear time-histories computed in the building when subjected to the 1979 James Road record are shown in Fig. 6.5. The response of the building is particularly sensitive to the long acceleration pulses in the record, particularly the one occurring at the 6 second mark. The maximum roof displacement is 7.71 inches while the maximum base shear is 3,433 kips. Local displacement ductility demands in the building can be observed in Fig. 6.6, where story load-deformation relations for the 1st to 8th stories are shown. The nonlinearities occur between the 2nd and 7th stories. The maximum

displacement ductility (3.03) again occurs in the fourth story. Nonlinearities in these stories have only one yield reversal. Computed response envelopes are shown in Fig. 6.7.

6.4 COMPARISON OF THE BEHAVIOR OF THE BUILDING UNDER THE HOLLISTER AND JAMES ROAD RECORDS

A summary of the maximum and minimum values of the main response parameters shown in Figs. 6.4 and 6.7 is presented in Table 6.1. From these results as well as from the comparison of the hysteretic behavior illustrated in Figs. 6.3 and 6.6 it can be concluded that the Hollister record appears to be more demanding than the James Road record. It is of interest to note that the results obtained in these analyses when compared with those obtained under the recorded motions at the basement (Chapters 3 and 4) give another good demonstration that Peak Ground Acceleration (PGA) is not a good parameter by which to judge damage potential. Although the PGA recorded at the basement, as shown in Table 2.2, was 0.60g in the E-W direction and 0.40g in the N-S direction, which is larger than the PGA of the Hollister and James Road records (approximately 0.37g), the damage potential of these last two records to the ten-story building is significantly larger than that of those recorded during the Whittier Narrows earthquake. This can be demonstrated easily by comparing the energy input spectra for the records.

The locations of plastic hinges in the building when subjected to these records are shown in Figs. 6.8 and 6.9. In the exterior frames most of the yielding occurs in the columns, while in the interior frames yielding is restricted to the slab.

6.5 SIMPLIFIED NONLINEAR ANALYSES
6.5.1 Estimation of Displacement Ductility Demands

Nonlinear static analyses, in addition to providing information about the strength and collapse mechanism of the structure, permit the establishment of a relationship between global (building) ductility ratio demands and local (story or member) ductility ratio demands [16]. Although, strictly speaking, "ductility" is not synonymous with "ductility ratio," in this report we will sometimes use the word "ductility" to mean "ductility ratio." Thus, the global ductility ratio is defined as the ratio of maximum deformation to yielding deformation at a

specific point in the building. For convenience, the reference point used here is the roof; therefore the global ductility ratio is defined as the ratio of the maximum displacement to the yielding roof displacement (see Fig. 6.10). Another convenient point to use would be an equivalent height H_e [16]. Such global-local ductility ratio demand relations are dependent on the imposed level of deformation and are strictly only valid for static loading under specific lateral loading patterns. They might, however, provide a way to obtain a good approximation of local demands under earthquake ground motions. A graphic representation of this relationship in the form of a 3D surface is shown in Fig. 6.11. When global ductility ratios larger than about 1.2 are imposed on the building, a concentration of local (story) demands is produced between the 3rd and 7th stories. A summary of relations between global and local (story) displacement ductility ratios computed using a triangular loading pattern is presented in Table 6.2 (for selected levels of deformation). It can be seen that for this building, a global ductility ratio of 2.0 can represent local (story) ductility ratio demands as high as 3.5.

Given the great uncertainties in the characteristics of future earthquake ground motions, gross estimates of the magnitude and distribution of local ductility (story and members of each story) demands in the building when subjected to a number of previously recorded ground motions might be sufficient when conducting the seismic evaluation of an existing building or for the design of a new building. These gross estimates can be obtained through simplified nonlinear analyses. These nonlinear analyses require the use of the relationships between global and local ductility demands, which are derived from the nonlinear static-to-collapse lateral loading, together with nonlinear analysis of an equivalent single degree-of-freedom system (SDOFS) [using inelastic response spectra (IRS) or time-history analysis] to predict the magnitude and distribution of local (story) displacement ductility ratio demands. The effectiveness of this simplified procedure is investigated below.

Nonlinear spectra computed for six levels of displacement ductility ratio, μ, were computed for both the Hollister and James Road records. These spectra, shown in Figs. 6.12 and 6.13, correspond to SDOFS with 5% damping and bilinear hysteretic behavior, characterized by a post-yielding stiffness that is 20% of the initial (elastic) stiffness. This post-yielding

stiffness is based on the observed behavior on the building under static loading (see Fig. 6.10). A comparison of story displacement ductility demands computed using DRAIN-2D and those estimated through the use of the global-local ductility relation derived from static-to-collapse loading (shown in Fig. 6.11) together with nonlinear spectra (shown in Figs. 6.12 and 6.13) are presented in Tables 6.3 and 6.4. The simplified analyses are able to capture both the magnitude and distribution of story displacement ductility demands well. For the Hollister record the simplified analysis predicts the maximum story displacement ductility demand (occurring in the fourth story) within 5.4%. For the James Road record, where the use of a triangular load distribution is more questionable given the presence of the very-long-duration acceleration pulse, the maximum story ductility demand is predicted within 16.4%. If the simplified analysis is based on a uniform load distribution instead of a triangular distribution, the difference is reduced to 5.0%.

Comparison of the results given in Tables 6.3 and 6.4 indicate that while the nonlinear time-history analyses under the Hollister record resulted in larger story displacement ductility demands than those demanded by the James Road record, the result is the opposite when simplified analyses are conducted. An explanation for this could be in the fact that the simplified analyses are based solely on the use of a single-degree-of-freedom model, i.e., neglect the influence of higher modes. Specifically, the values of the local story displacement ductility demands in the case of the simplified analyses have been obtained from the global ductility given by the nonlinear spectra for a single-degree-of-freedom model shown in Figs. 6.12 and 6.13, entering with $C_y \doteq 0.18$ (obtained from Fig. 6.10) and $T_1 = 1.43$ seconds (Table 3. 3) or $T_1 = 1.42$ seconds from Fig. 4.2. For these values, Fig. 6.12 shows $\mu_{global} \doteq 1.8$ and Fig. 6.13 shows $\mu_{global} \doteq 1.9$. Therefore it is clear that, the μ_{global} being larger for the James Road record than it is for the Hollister record, the local ductility should also be larger for the James Road record. However, the linear elastic analysis shows that the second mode with a T_2 of 0.48 second has a significant effect on the response of the building. This second mode has to affect the initiation and response in the inelastic range as well. A comparison of the spectral values in Figs. 6.12 and 6.13 for a $T_2 = 0.48$ second shows that for $C_y = 0.18$ the required global ductility for the Hollister record can be significantly larger than that required for the James Road record.

One of the main advantages of the use of the proposed approximate simplified analysis is the amount of time involved in the required computations. For the building analyzed here, and for records used in this study (with durations of 20 seconds and an integration time step of 0.02 second), the computational effort in a nonlinear dynamic time-history analysis (DRAIN-2D) is approximately 12 times greater than that for a nonlinear static-to-collapse analysis. Thus it is possible to conduct several simplified analyses rather than just one MDOFS nonlinear time-history analysis. As a result, simplified analyses can be used to analyze the sensitivities of the results if the assumed mechanical models are modified. Furthermore, it is easier to interpret results from a static-to-collapse lateral load analysis than from a dynamic time-history analysis.

6. 5. 2 Estimation of the Maximum Displacement and Interstory Drift Index

As is illustrated below, the simplified nonlinear analysis, or, in general, the results from nonlinear static-to-collapse analyses, together with the nonlinear (inelastic) spectra of Figs. 6.12 and 6. 13 can be used to estimate the maximum displacement as well as the maximum interstory drift.

Maximum Displacement of the Roof. Consider the ten-story building, with $T_1 = 1.43$ seconds subjected to the Hollister record, whose Inelastic Response Spectra (IRS) for different values of ductility are given in Fig. 6.12. According to Fig. 6.10, $C_y = V/W \doteq 0.18$. From Fig. 6.12, $\mu_{global} \doteq 1.8$. Therefore the displacement at yielding for the equivalent SDOFS would be approximately $0.18g (1.43/2\pi)^2 = 3.60$ in., and the maximum displacement for $\mu_{global} = 1.8$ would be 6.49 in. For the real MDOFS building, the maximum displacement will depend on the shape of the lateral deflection that is assumed in the derivation for the equivalent SDOFS. If this shape is assumed to be an inverted triangle, then the maximum displacement at the roof will be $(6.49 \text{ in}) \times 3/2 = 9.73$ in. This value is 28% larger than that obtained from the time-history analysis, i.e., 7.59 in. (see Table 6.1).

Maximum Interstory Drift Index (IDI). From analysis of the values given in Table 6.2 it is obvious that the maximum IDI will occur at the 4th story. The following two approaches can be used to estimate this maximum IDI: (1) from the estimated maximum displacement at the

roof, i.e., 9.73 in., the IDI at the 4th story will be approximately (9.73 in./1080 in.) (3.08/1.8)
= 0.015; (2) directly from the value of the $\mu_{local\ story}$ obtained from a simplified analysis, i.e.,
3.22 (see Table 6.3) and the value of the IDI at which yielding is initiated at the 4th story,
which is 0.005. Then the maximum IDI at the 4th story is 3.32 x 0.005 = 0.0166. (The value
of 0.005 is obtained from the static-to-collapse analysis of the 4th story. It can also be
obtained from Fig. 6.3). Comparison of the two above estimated values for the maximum
IDI with that obtained from the time-history analysis of the building, i.e., 0.0161 (see Table
6.1) shows good agreement for all practical purposes.

RESPONSE PARAMETER	HOLLISTER	JAMES ROAD
Max. Base Shear (kips)	3,599	3,433
Max. Displacement (in)	7.59	7.71
Max. IDI[(A)]	0.0161	0.0154
Min. Base Shear (kips)	-3,520	-2,752
Min. Displacement (in)	-7.46	-4.48
Min. IDI	-0.0132	-0.0078

(A) Interstory Drift Index

Table 6. 1   Summary of response parameters computed in nonlinear time history analyses.

STORY	GLOBAL DUCTILITY			
	0.8	1.2	1.6	2.0
1	0.55	0.71	0.78	0.82
2	0.59	0.79	0.90	0.97
3	0.86	1.56	2.16	2.76
4	0.88	1.76	2.66	3.51
5	0.82	1.40	2.25	3.07
6	0.77	1.04	1.60	2.24
7	0.72	0.94	1.17	1.55
8	0.63	0.82	0.91	1.00
9	0.47	0.61	0.67	0.71
10	0.28	0.36	0.40	0.42

Table 6. 2   Story ductilities for different levels of global deformation computed using nonlinear static analyses

STORY	STORY DISPLACEMENT DUCTILITY DEMAND	
	NONLINEAR TIME HISTORY ANALYSIS - DRAIN-2D	SIMPLIFIED ANALYSIS
10	0.59	0.44
9	0.92	0.73
8	1.10	1.01
7	1.77	1.55
6	2.36	2.22
5	2.61	2.60
4	3.15	3.32
3	2.64	2.66
2	0.96	0.96
1	0.88	0.84

Table 6. 3 Comparison of computed story displacement ductility demands for the Hollister record.

STORY	STORY DISPLACEMENT DUCTILITY DEMANDS	
	NONLINEAR TIME HISTORY ANALYSIS - DRAIN-2D	SIMPLIFIED ANALYSIS
10	0.51	0.45
9	0.81	0.74
8	1.06	1.02
7	1.32	1.56
6	1.52	2.25
5	2.23	3.09
4	3.03	3.52
3	2.61	2.76
2	0.99	0.99
1	0.83	0.83

Table 6. 4 Comparison of computed story displacement ductility demands for the James Road record.
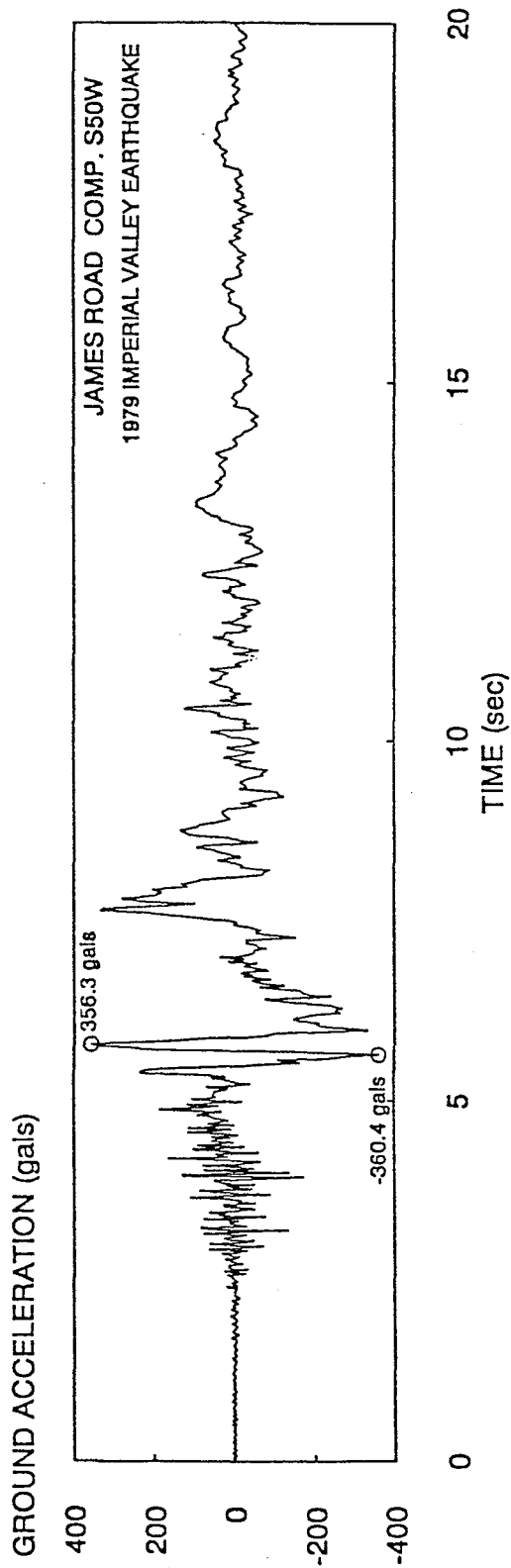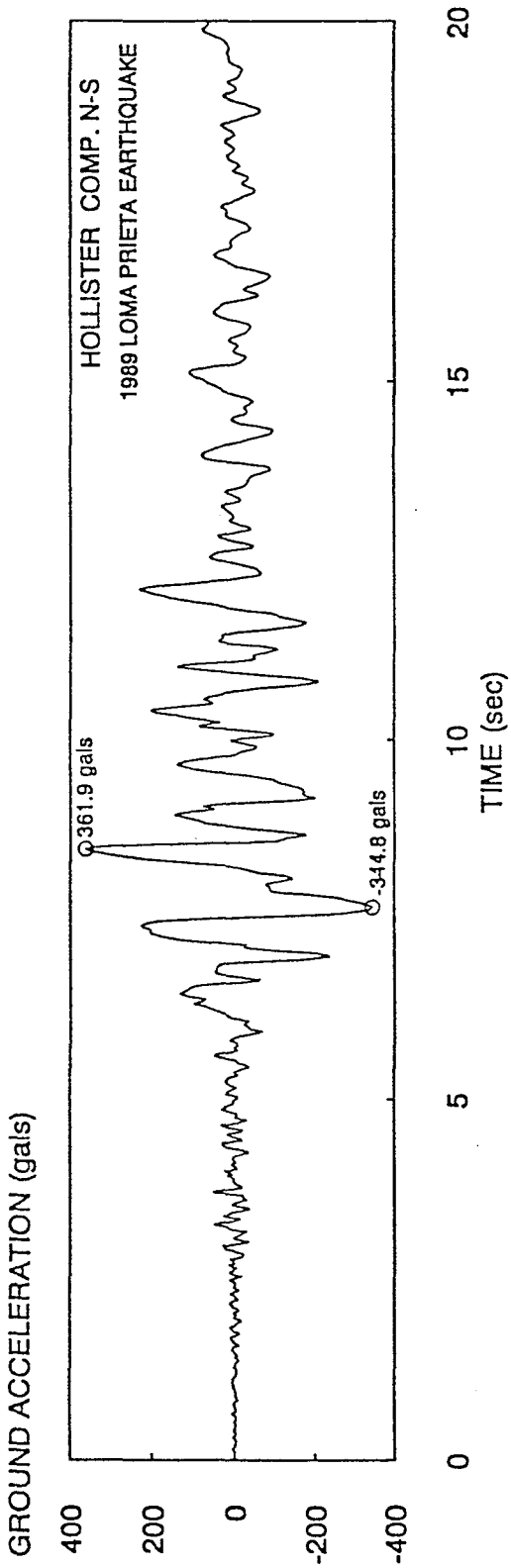
Figure 6. 1 - Acceleration time histories of the 1989 Hollister record and the 1979 James Road record.
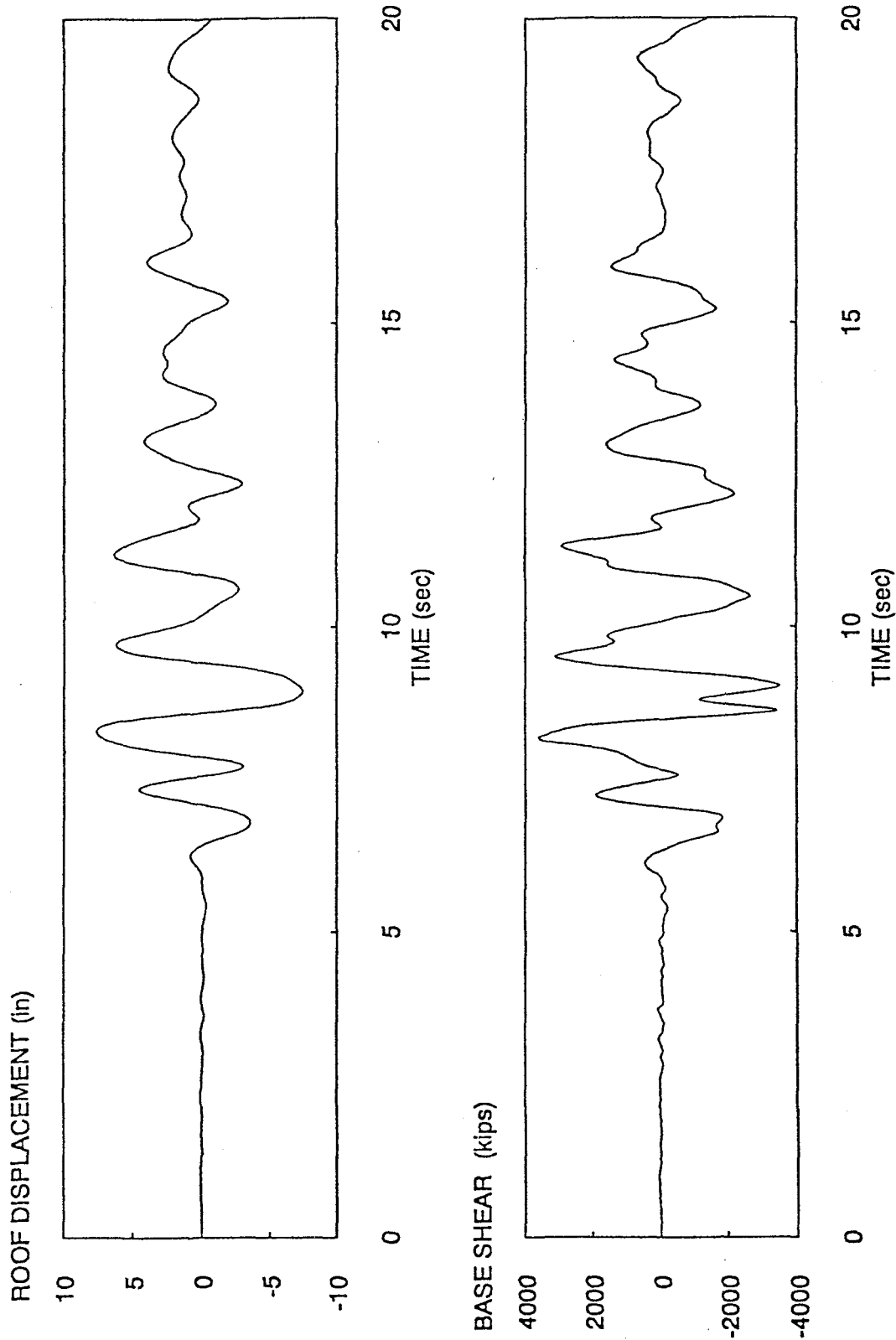
Figure 6. 2 - Roof displacement and base shear time histories computed in the building for the Hollister record.
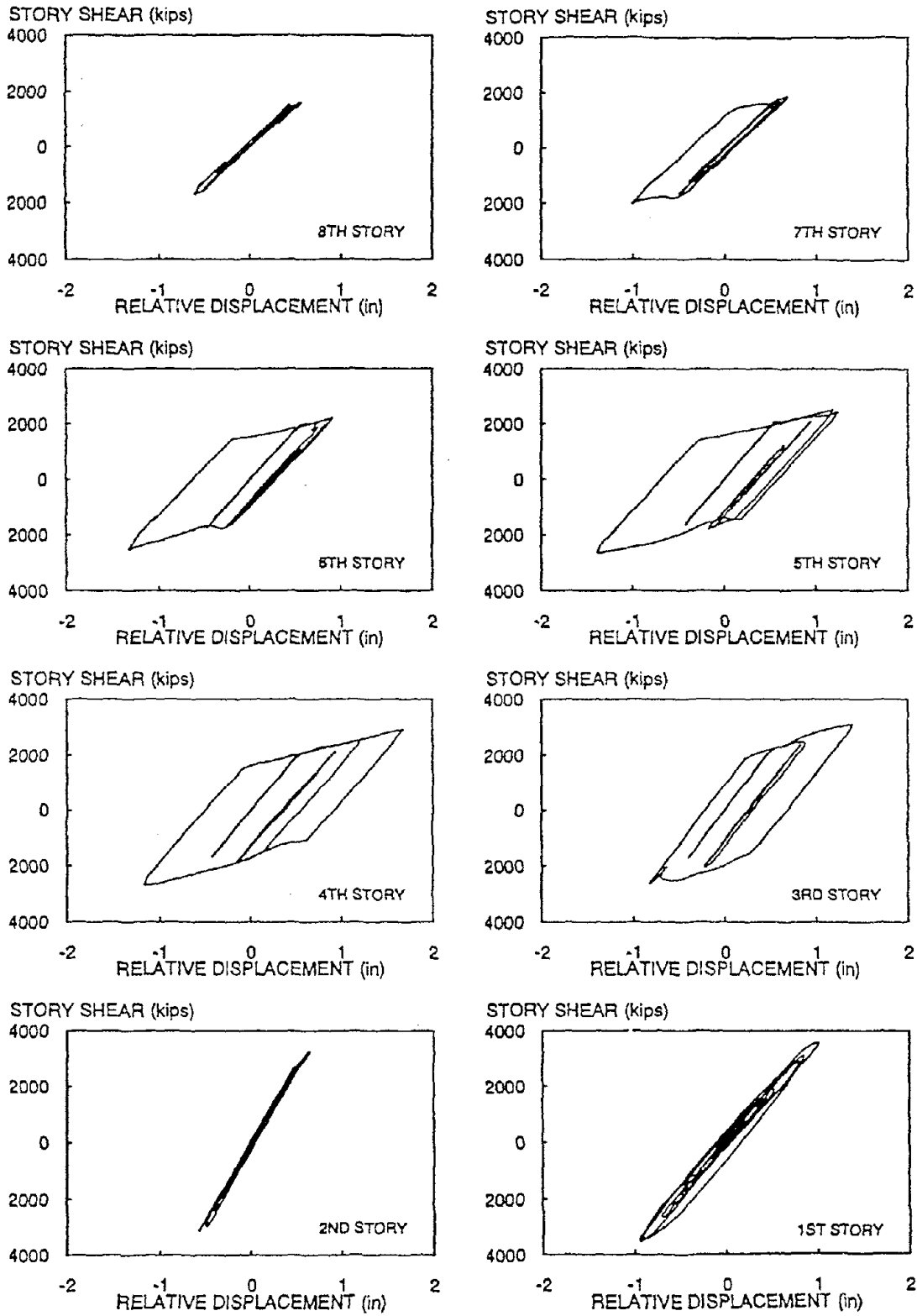
Figure 6. 3 - Story load-deformation relations computed in the building for the Hollister record
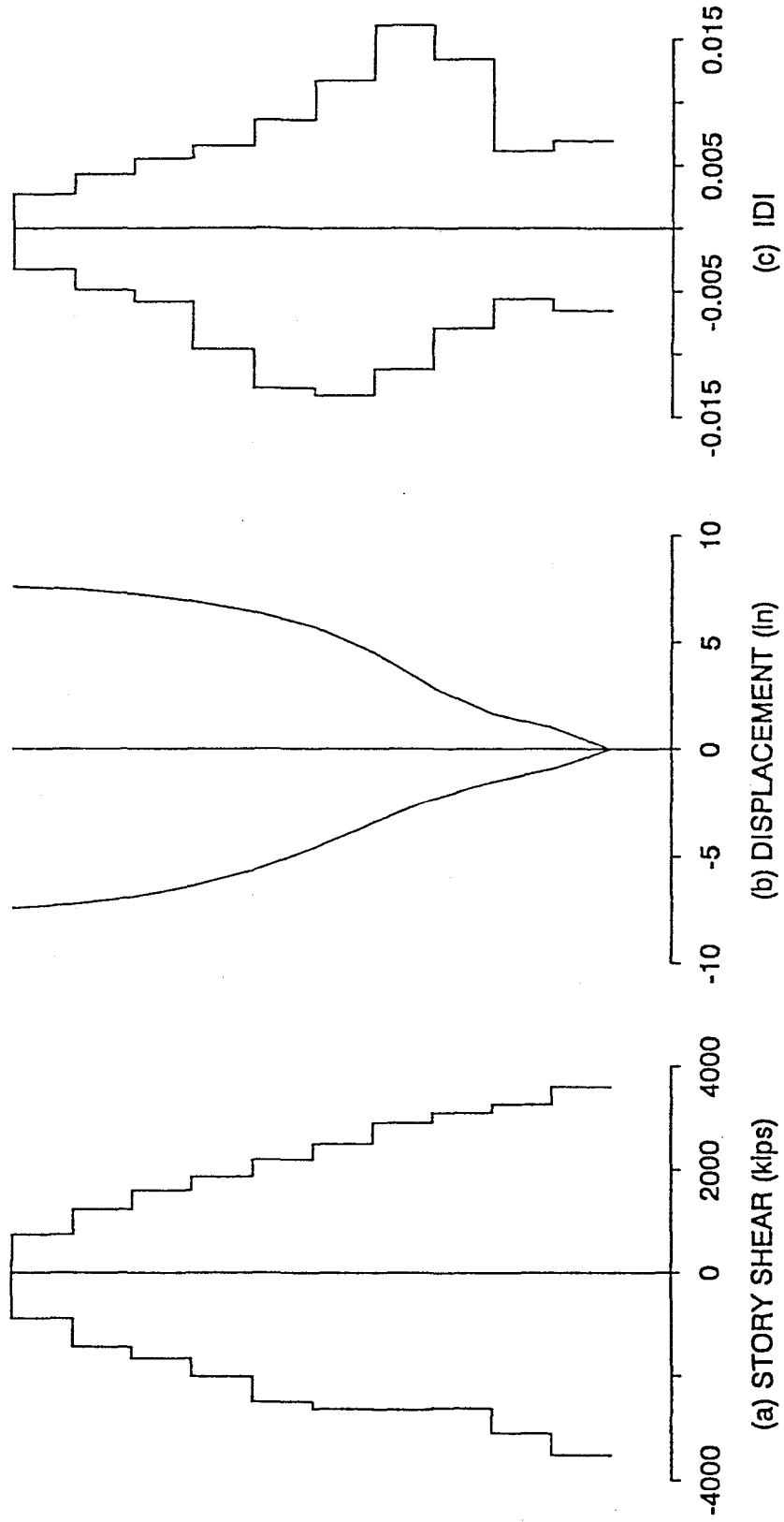
Figure 6. 4 - Computed response envelopes in the building for the Hollister record.

(a) STORY SHEAR (kips)

(b) DISPLACEMENT (in)

(c) IDI

ROOF DISPLACEMENT (in)

BASE SHEAR (kips)
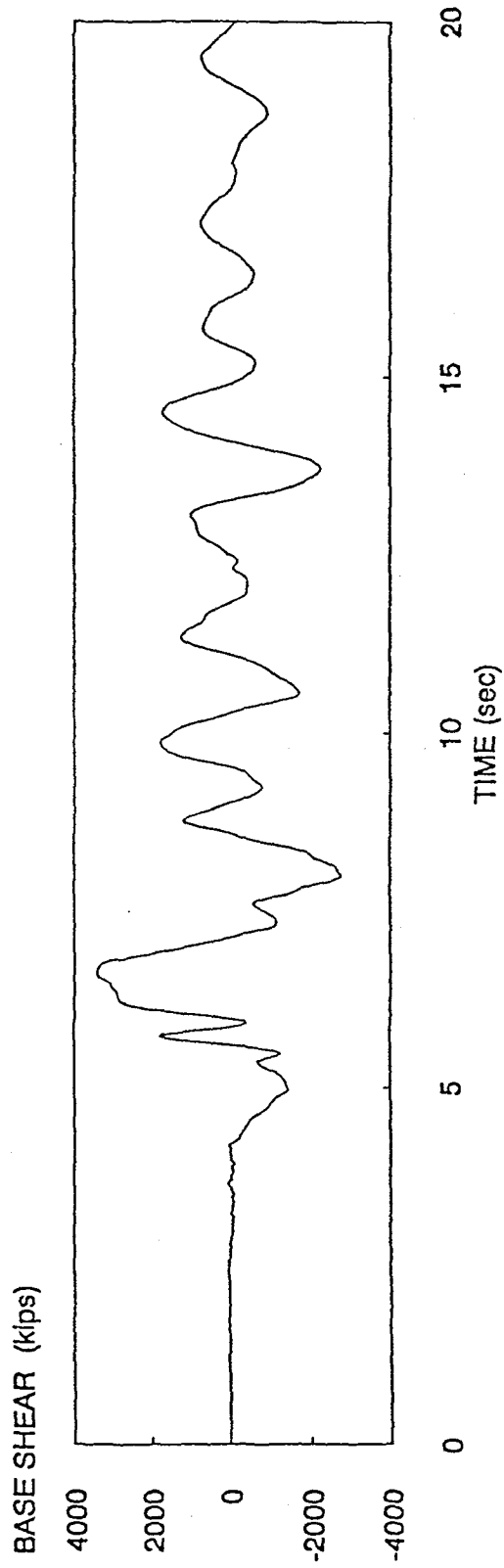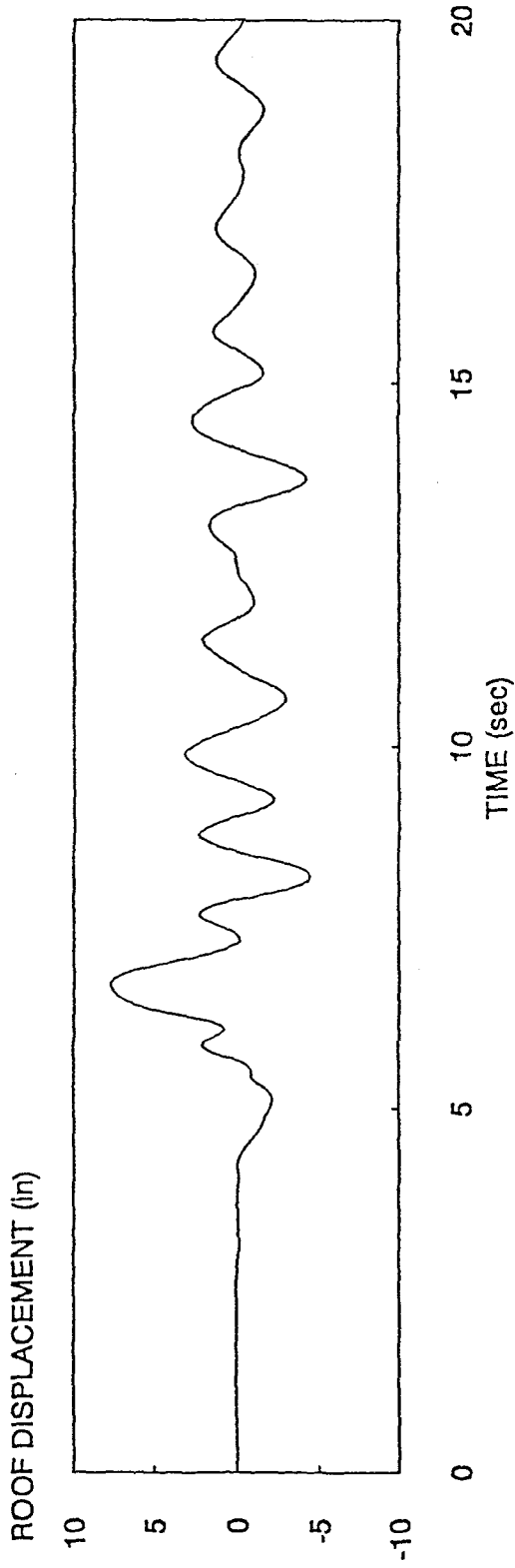
Figure 6. 5 - Roof displacement time histories computed in the building for the James Road record.
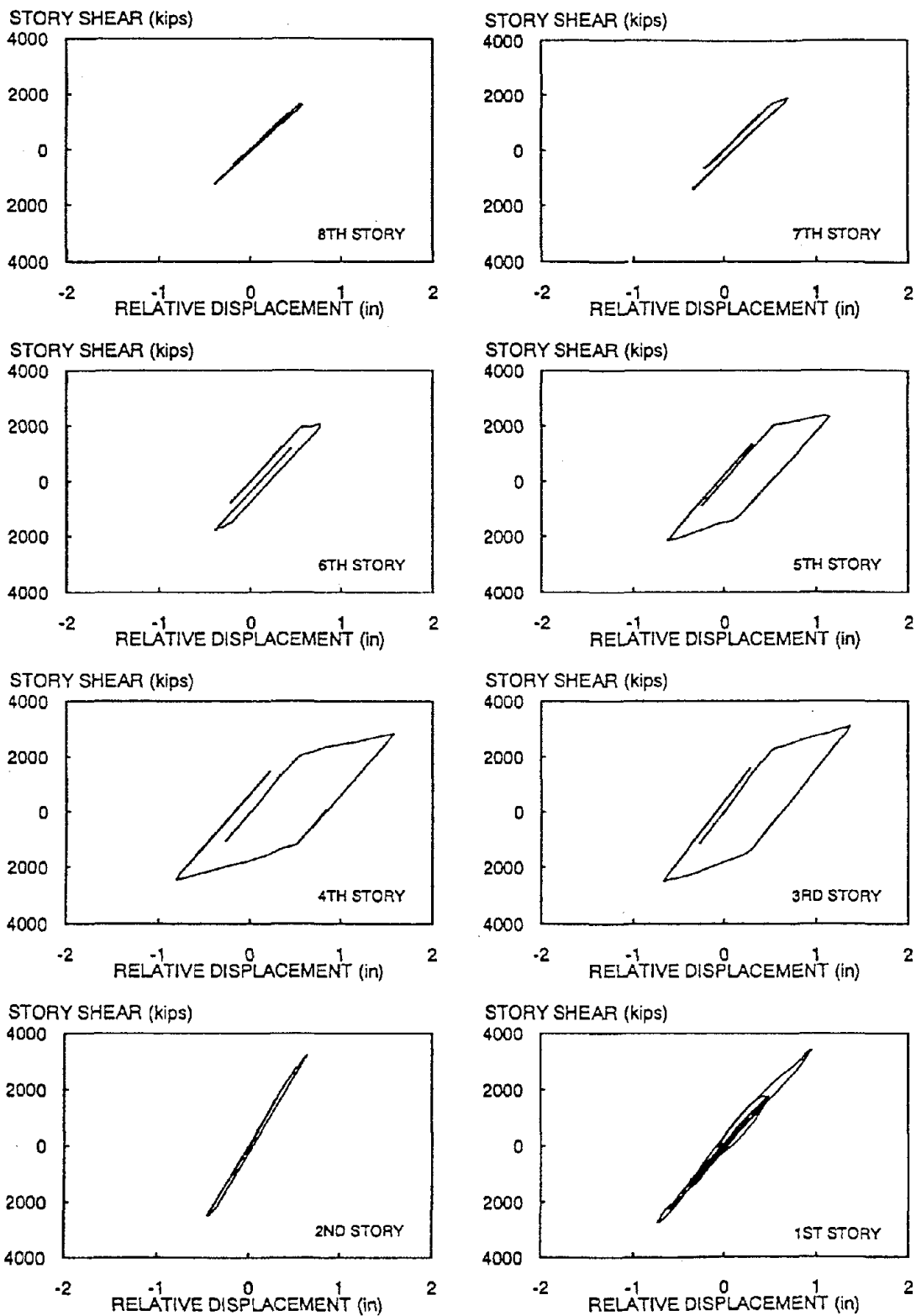
Figure 6. 6 - Story load-deformation relations computed in the building for the James Road record

(a) STORY SHEAR (kips)

(b) DISPLACEMENT (in)

(c) IDI
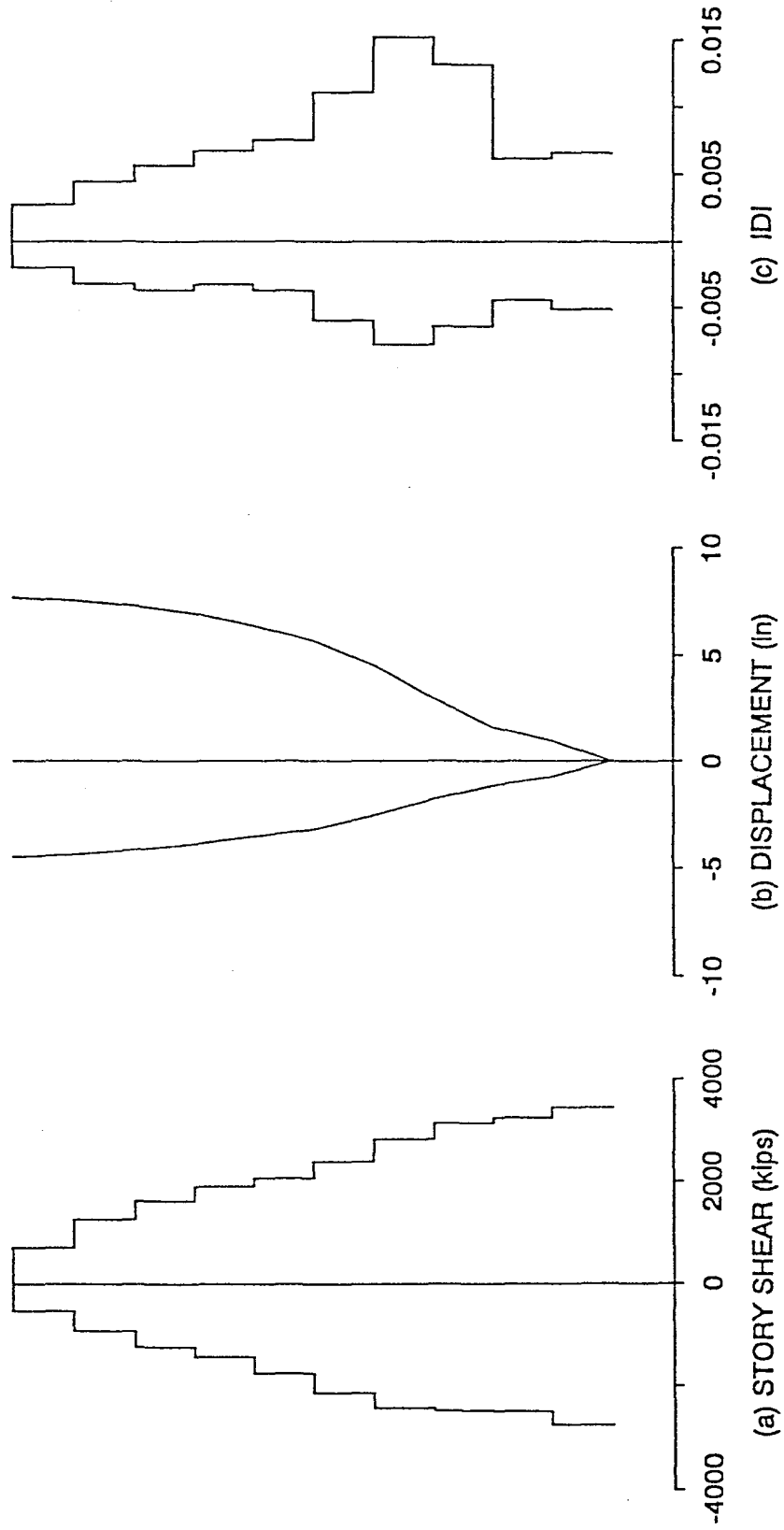
Figure 6. 7 - Computed response envelopes in the building for the James Road record.
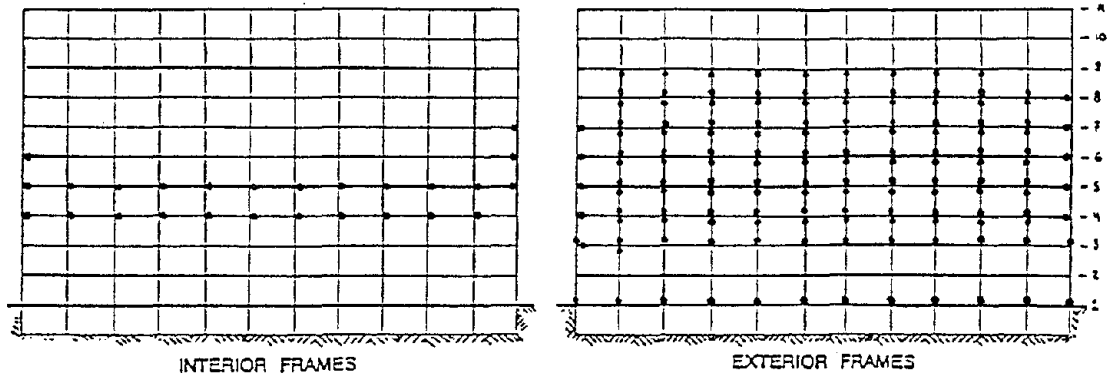
Figure 6. 8 - Locations of plastic hinges in the building for the Hollister record
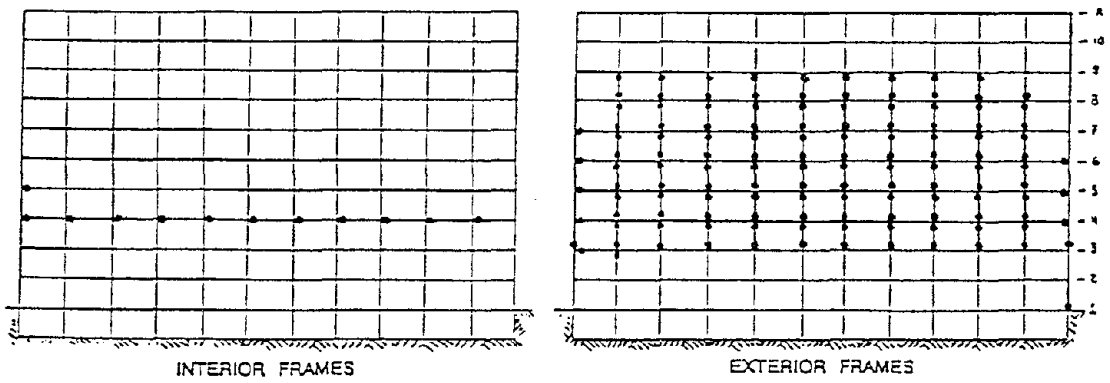
Figure 6. 9 - Locations of plastic hinges in the building for the James Road record

BASE SHEAR (kips)   V / W

$$\mu = \frac{\Delta_{max}}{\Delta_y}$$

——————— COMPUTED RESPONSE

- - - - - - IDEALIZED RESPONSE

TRIANGULAR PATTERN

ROOF DISPLACEMENT (in)
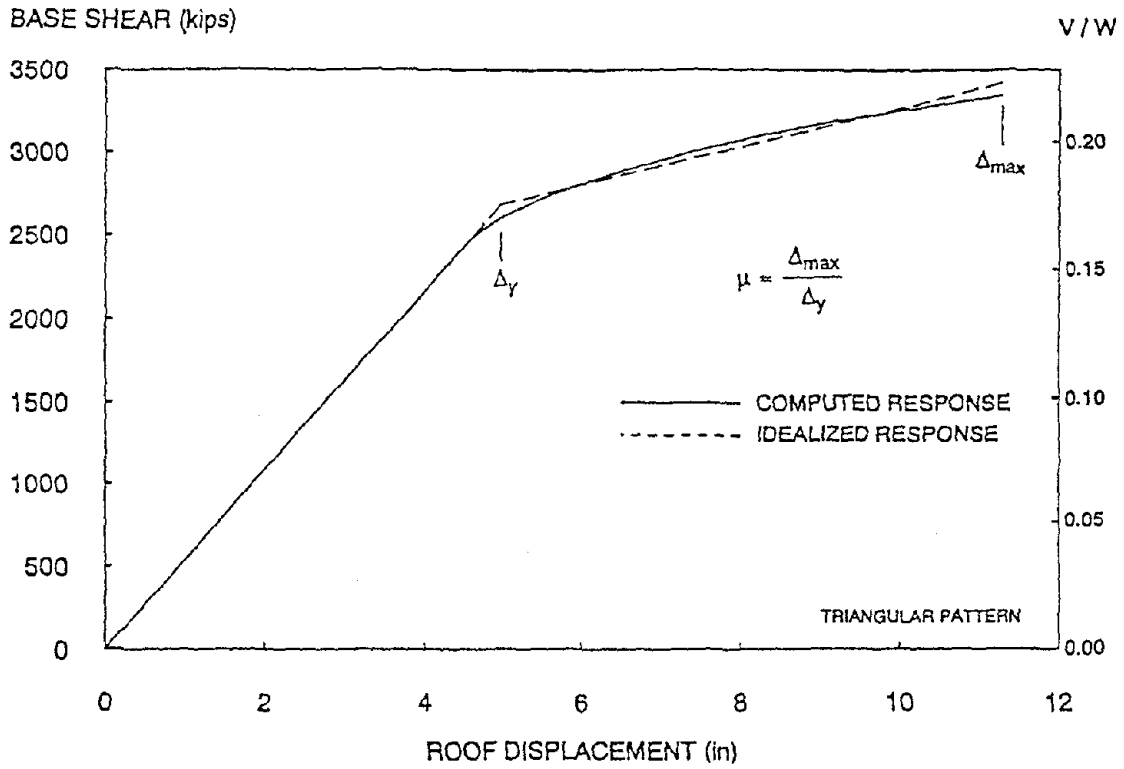
Figure 6. 10 - Comparison of computed response and idealized response used to define global ductility

STORY DUCTILITY
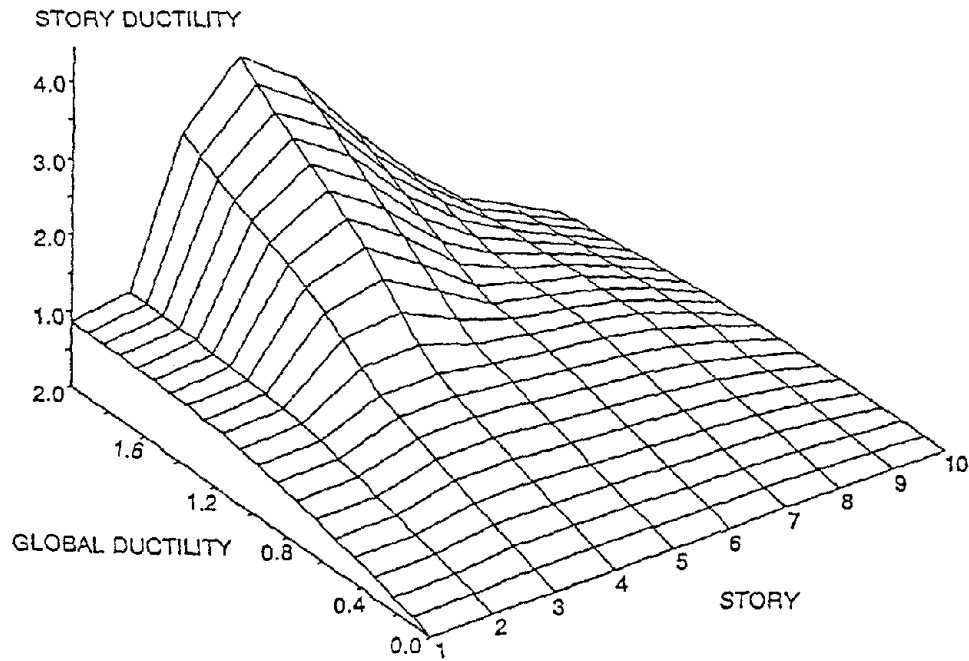
Figure 6. 11 - Relationship between global and local ductility demands for the longitudinal direction of the building
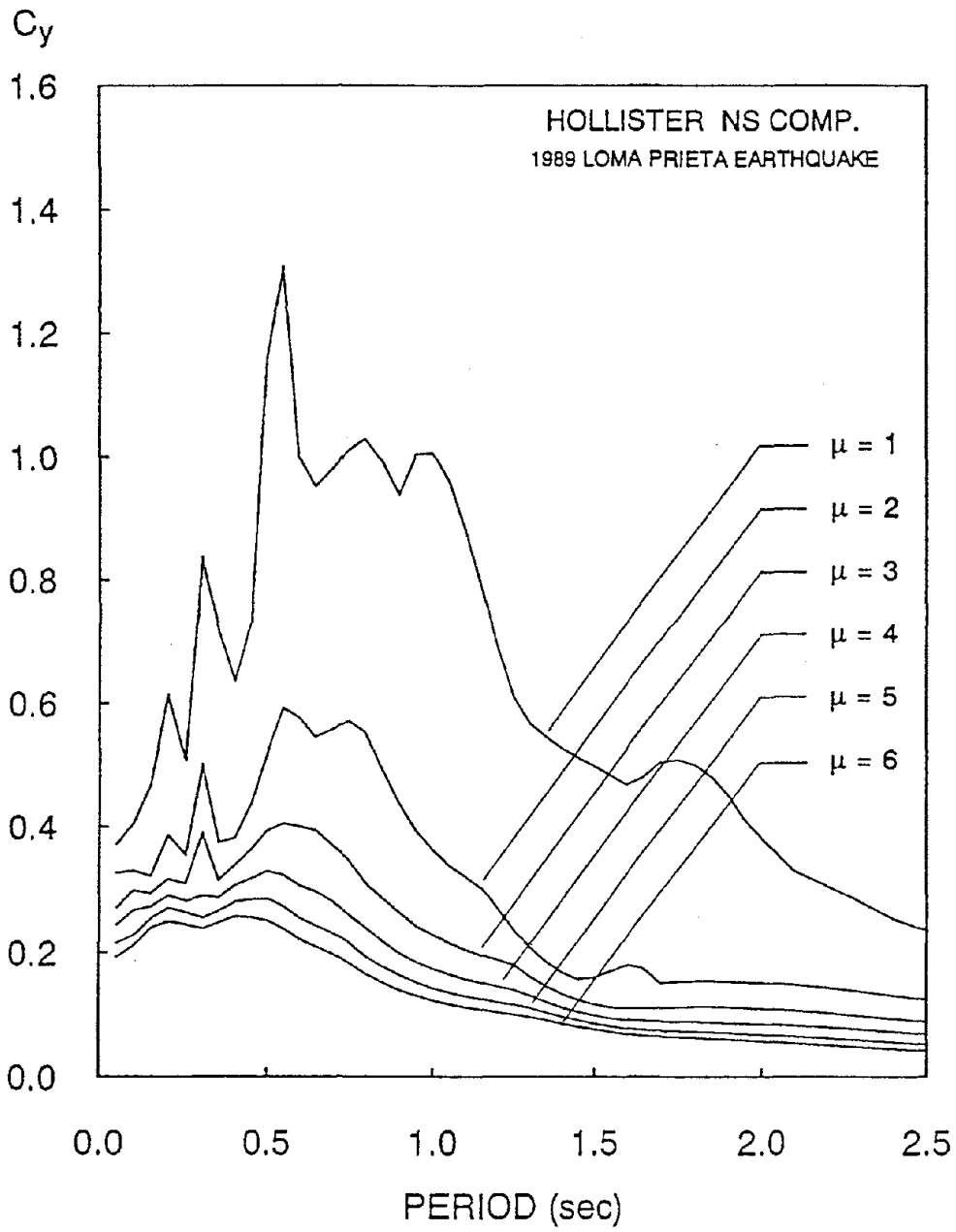
Figure 6. 12 - Nonlinear spectra for the 1989 Hollister record
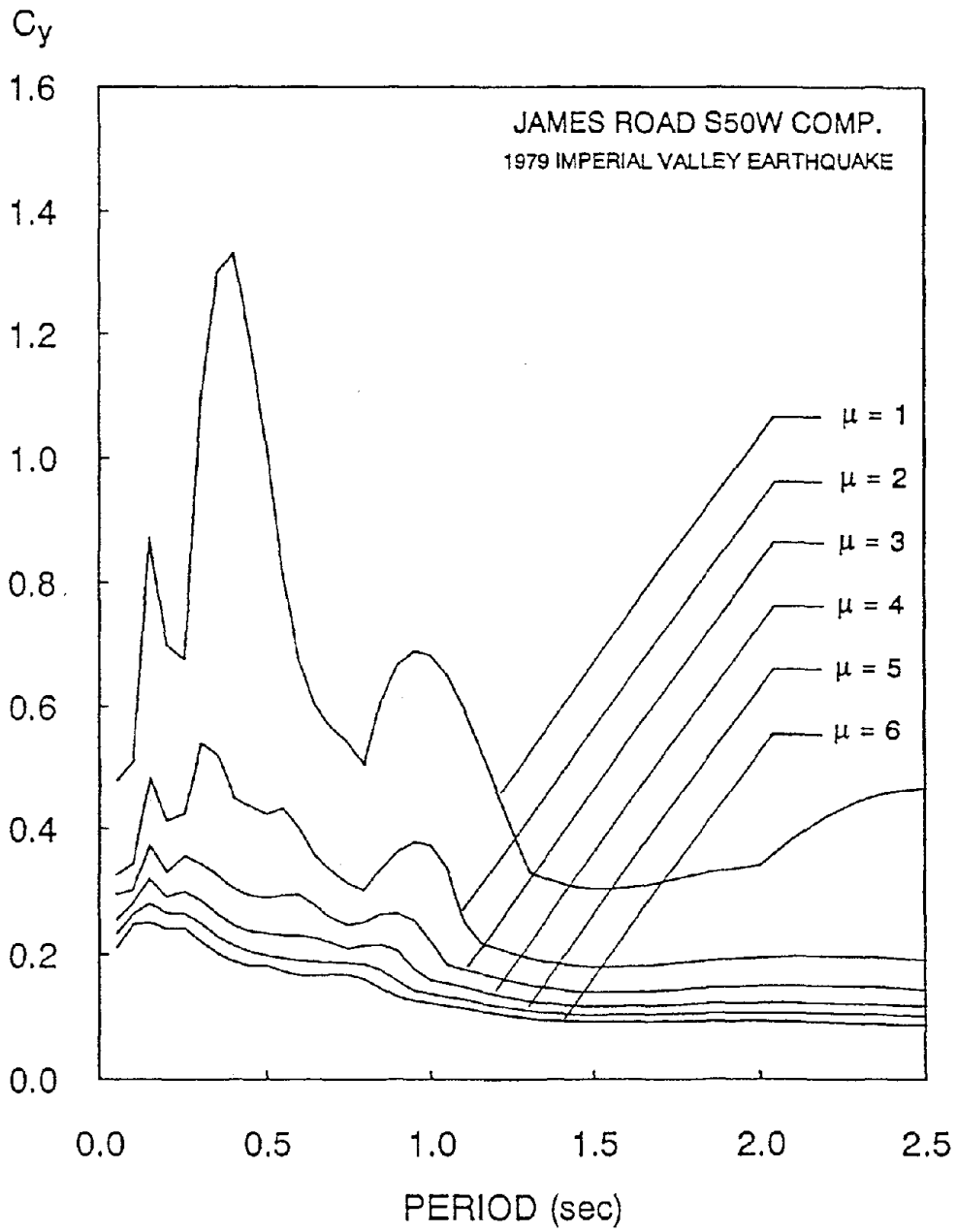
Figure 6. 13 - Nonlinear spectra of the 1979 James Road record

7. SUMMARY, CONCLUSIONS, IMPLICATIONS OF RESULTS AND RECOMMENDATIONS

7.1 SUMMARY AND CONCLUSIONS

An existing instrumented ten-story RC building, which was subjected to what can be considered as earthquake ground motions of moderate damage potential during the 1987 Whittier Narrows earthquake, was selected for detailed analytical studies to evaluate its seismic performance and to compare such performance with the observed (measured) response during that earthquake. This comparison has permitted an evaluation of the reliability of the analytical models and methods presently used in the analyses necessary for checking the preliminary designs of new structures and for the vulnerability assessment of existing buildings. The laterally-resistant structural system of the building consists of moment-resisting frames in the N-S direction and shear walls in the E-W direction. The building was designed according to the ACI strength method for a seismic design coefficient of 0.052 in the longitudinal (N-S) direction and 0.073 in the transverse (E-W) direction.

The dynamic characteristics of the building were identified using system identification techniques and the acceleration time histories recorded during the Whittier Narrows earthquake. The values of the identified vibration periods in the transverse direction agree with those identified from the 1976 Whittier earthquake records. On the other hand, the values of the identified period in the longitudinal direction are significantly higher, 81% for the first mode, than those identified from the 1976 earthquake records. A small change in fundamental period was observed during the earthquake for the transverse direction of the building. This would indicate that some extra damage [extra cracking or movement (rocking) of the foundation or both] had occurred. No changes in the longitudinal direction fundamental period were observed, indicating that no significant damage could have occurred in this direction during the response of the building to the recorded earthquake ground motions.

A three-dimensional, linear-elastic model of the building was calibrated using the dynamic characteristics previously identified. Using this model, time-history analyses were conducted

using as input the acceleration time histories recorded in the basement. These analyses had the following objectives: (i) to investigate the effectiveness of linear-elastic analyses to capture the response of the building under moderate ground motions; and (ii) to explain the absence of damage as a result of the Whittier Narrows earthquake despite the apparent severity of the recorded ground motions (i.e., the large peak ground accelerations in both directions: 0.60g and 0.40g, respectively, in the transverse and longitudinal directions.)

For both directions, the analyses that only took into account the fundamental mode failed to reproduce the recorded accelerations. When the first nine modes of vibration were considered, very good correlation between the measured and computed responses was obtained for both directions. Maximum computed interstory drift indices of 0.34% in the longitudinal direction and 0.21% in the transverse direction explain the absence of significant damage in the building. These results confirm once more that Peak Ground Accelerations of recorded ground motions are not a reliable parameter by which to judge the damage potential of such motions to a specific structure.

Nonlinear static-to-collapse lateral loading analyses were conducted to investigate the strength and deformation capacities of the building. Two lateral loading patterns, triangular and rectangular, were used. **Significant overstrengths were computed particularly in the transverse direction. For the longitudinal direction, the ratio between the base shear at first significant yielding and the ACI ultimate strength design base shear (0.052 W) was about 3.06 for the case of triangular loading and 3.62 for the rectangular loading. Because of plastic redistribution it was estimated that there was an additional overstrength: the ratio between the maximum base shear resistance and the base shear at first significant yielding was 1.38 for both lateral loading patterns. Therefore, the ratios between the maximum base shear resistance (0.22W and 0.26W) and the code (ultimate strength) design base shear (0.052W) were 4.23 and 5.0 for the triangular and the uniform lateral loads, respectively. These overstrengths were obtained assuming that the structure would be able to develop a global displacement ductility ratio of about 2.4 with a local ductility ratio of about 4 -- although it is doubtful that the existing detailing of the reinforcing will allow this to be developed. It should be noted that the**

above overstrengths are static overstrengths and that they are a lower bound of the dynamic overstrength [36]. For the transverse direction the overstrength ratios were higher than for the longitudinal direction. Base shear strengths corresponding to first significant yielding of the shear walls were 0.32W and 0.43W, respectively, for the triangular and rectangular load patterns. Considering that the structural system according to code requirements has to be designed for an ultimate strength of 0.073W (Eq. 2.5), the resulting strength ratios are 4.38 and 5.89. The maximum base shear strengths were computed to be 0.42W and 0.51W, respectively, for the triangular and rectangular load patterns, with the result that their ratios with the code design requirement of 0.073W were 5.75 and 6.99. These overstrengths were obtained assuming that the shear wall systems can develop a global displacement ductility ratio larger than 3 and near 2.5 for the triangular and rectangular patterns, respectively. It is doubtful that the detailing of the reinforcement in the coupling girders and walls could allow such a high global displacement ductility ratio to develop. Nonlinear time-history analyses were carried out for the longitudinal direction of the building using the Hollister and James Road records. In spite of the fact that these two records have peak ground accelerations smaller than those recorded at the basement of the building during the Whittier Narrows earthquake, large inelastic deformations along the 3rd to 7th stories were computed. The maximum base shear demanded was about 0.24W. The maximum displacement was 7.71 inches, and the maximum interstory drift index was 0.016, resulting in a maximum demanded story displacement ductility ratio of 3.15 in the 4th story. The number of yielding reversals was small, only four. The maximum rotation of the columns in the 4th story was 0.02 radian.

An approximate method was proposed and used to estimate local displacement ductility ratio demands. The method is based on the use of a relationship between global and local deformations obtained from static-to-collapse lateral loading, and the use of nonlinear (inelastic) spectra for SDOFS. Simplified earthquake analyses using this method were conducted for this building when subjected to the James Road and Hollister records. Results were then compared with those obtained using DRAIN-2D. For both records, the

simplified analysis method produced very good estimates of story displacement ductility ratio demands.

An attempt has also been made to estimate the maximum interstory drift index using the above approximate method. The results agree very well with those obtained from the nonlinear time-history of the building.

7.2 ASSESSMENT OF THE IMPLICATIONS OF THE RESULTS FOR EQ-RESISTANT DESIGN PRACTICE

The analyses conducted and the results obtained have clearly confirmed once more that there are uncertainties in the following areas.

● **Reliable estimation of the main dynamic characteristics of real buildings.** The estimation of the period for the moment-resistant frames using code provisions significantly underestimated the fundamental period identified from the records.

● **Analytical modelling of real buildings, particularly the foundation and the stiffnesses of the members and their connections.**

● **Selecting the critical EQ ground motions; particularly, the inadequacy of the peak ground acceleration as a parameter for measuring damage potential.**

● **Estimation of the demands resulting from selected EQ ground motions. The need to include all of the important modes.** The number of significant modes depends on the response parameter under study.

The studies conducted have also shown that RC structures designed and constructed according to building code regulations have significantly larger strength than that for which they have been designed. Not only does the constructed building have a significant first yielding overstrength, but it could also have developed a maximum strength significantly larger than the first yielding strength, provided that its members and their connections are provided with sufficient local ductility through proper detailing of their reinforcement. **There is a need to**

evaluate and consider the possible overstrength in the seismically-resistant design of structures.

The analysis of the detailing of the reinforcement used in the building considered herein shows clearly that the building cannot develop the local ductility ratio that would be demanded by the required global ductility ratio when it is subjected to safety level EQ ground motions. **This result points out clearly not only the severity of the problem created by many existing RC buildings with similar reinforcement detailing, but also the urgent need for proper seismic upgrading of buildings of this type located in regions of high seismicity.**

To identify the existing seismically hazardous buildings, as well as to improve the design of new buildings, there is an urgent need to develop and use a simplified nonlinear analysis procedure to estimate the maximum displacement, IDI, and global and local ductility that can be demanded of these buildings by safety level EQs. **The simplified method proposed herein, which is based on the use of nonlinear static-to-collapse lateral loading and nonlinear analysis of an equivalent SDOFS appears to be promising and should be investigated further.**

7.3 RECOMMENDATIONS FOR FUTURE RESEARCH AND DEVELOPMENTS

The analyses conducted in this case study of the ten-story RC building have shown the large number of uncertainties in the estimation of the demands, and that RC buildings designed according to the present codes have significant first yielding overstrength. Furthermore, if their members and connections are provided (constructed) with good local ductility ratios, the RC building structure can have significantly larger maximum overstrength. These overstrengths need to be considered in the design. The studies conducted have shown that to improve design methods for new structures and vulnerability assessment for existing buildings there is a need for the following research and developments.

● The estimation of realistic seismic demands on new or existing buildings depends on the consideration of the real strength and stiffness of the building. **There is a need**

to estimate the approximate overstrength of buildings according to their structural system and their height. Buildings having different structural systems and heights and located in regions of high seismic activity should be thoroughly instrumented.

●   It is recommended that in order to increase the reliability and transparency of current building code seismic design provisions, reductions in the required design strength due to inelastic behavior and overstrength should be considered explicitly. The reductions due to inelastic behavior must be dependent on the inelastic deformation capacity of the structure (which depends on the type of structural system and on the detailing of the elements and of their connections), on the fundamental period of the structure, and on local site conditions. Realistic estimates of displacement demands must also be considered explicitly in the design process. To achieve these estimations in practice it is necessary to develop simple but reliable analytic methods, such as the simplified method proposed and used in this study. Further work is needed to investigate the limitations and reliability of this method.

REFERENCES

[1] Abdel-Ghaffar, A.M., "Engineering Data and Analyses of the Whittier, California Earthquake of January 1, 1976," *Report EERL 77-05*. Earthquake Engineering Research Laboratory, California Institute of Technology, Pasadena, California, November, 1977.

[2] Etheredge, E., Porcella, R., "Strong-Motion Data from the October 1st, 1987 Whittier Narrow Earthquake," *Open-File Report 88-38*, Department of the Interior, U.S. Geological Survey, Menlo Park, California, January, 1988.

[3] Etheredge, E., Porcella, R., "Strong-Motion Data from the Whittier Narrows Aftershock of October 4, 1987," *Open-File Report 88-38*, Department of the Interior, U.S. Geological Survey, Menlo Park, California, January, 1988.

[4] Porcella, R., Etheredge, E., Maley, R., Switzer, J., "Strong-Motion Data from the July 8, 1986 North Palm Springs Earthquake and Aftershocks," *Open-File Report 87-155*, Department of the Interior, U.S. Geological Survey, Menlo Park, California, March, 1987.

[5] Etheredge, E.C., Acosta, A.V., Foote, L.J., Johnson, D.A., Maley, R.P., Porcella, R.L., and Switzer, J.C., "Strong-Motion Recordings from the $M_L = 5.5$ Upland, California Earthquake of February 28, 1990," *Open-File Report 90-311*, Department of the Interior, U.S. Geological Survey, Menlo Park, California, April, 1990.

[6] International Conference of Building Officials, "Uniform Building Code," 3rd Chapter, 1970 Edition, Whittier, California, 1970.

[7] Jones, L., Hakusson, E., "The Whittier Narrows Earthquake, California Earthquake of October 1, 1987 -- Seismology," *Earthquake Spectra*, Vol. 4, No. 1, pp.43-53, February, 1988.

[8]   Tierney, K., "The Whittier Narrows Earthquake, California Earthquake of October 1, 1987 -- Social Aspects," *Earthquake Spectra*, Vol. 4, No. 1, pp. 11-23, February, 1988.

[9]   Leyendecker, E.V., Highland, L.M., Hopper, M., Arnold, E.P., Thenhaus, P., and Powers, P., "The Whittier Narrows Earthquake, California Earthquake of October 1, 1987 -- Early Results of Isoseismal Studies and Damage Surveys," *Earthquake Spectra*, Vol. 4, No. 1, pp. 1-10, February, 1988.

[10]   Brady, A.G., Etheredge, E. C., Porcella, R.L., "The Whittier Narrows, California, Earthquake of October 1, 1987 -- Preliminary Assessment of Strong Motion Records," *Earthquake Spectra*, Vol. 4, No. 1, pp. 55-74, February, 1988.

[11]   Hart, G.C., Thurston, S.J., Englekirk, R.E., "Seismic Evaluation of a Tall Reinforced Concrete Frame Building," Seismic Engineering: Research and Practice," *Proceedings of the ASCE Structures Conference '89*, San Francisco, California, pp. 277-286, May, 1989.

[12]   Hudson, D.E., *Reading and Interpreting Strong-Motion Accelerograms*, Earthquake Engineering Research Institute, Special Monograph, Berkeley, California, 1979.

[13]   Trifunac, M.D., and Lee, V.W., "A Note on the Accuracy of Computed Ground Displacements from Strong-Motion Accelerograms," *Bulletin of the Seismological Society of America*, Vol. 64, No. 4, pp. 1209-1219, August, 1974.

[14]   Nigam, N.C., and Jennings, P.C., "Calculation of Response Spectra from Strong-Motion Records," *Bulletin of the Seismological Society of America*, Vol. 59, No. 2, pp. 909-922, 1969.

[15] Anderson, J.C., Miranda, E., and Bertero, V.V., "Evaluation of Seismic Performance of a Thirty-Story Building," Report on Tasks 3, 4, and 5 of the CUREe Kajima Project on Design Guidelines for Ductility and Drift Limits, Earthquake Engineering Research Center, University of California, Berkeley, California, July, 1991.

[16] Miranda, E., "Seismic Evaluation and Upgrading of Existing Buildings," Thesis (Ph.D.), 482 p., University of California, Berkeley, California, 1991.

[17] Berg, G.V., *Seismic Design Codes and Procedures*" Earthquake Engineering Research Institute, Special Monograph, Berkeley, California, 1983.

[18] Bertero, V.V., Bendimerad, F.M., Shah, H.C., "Fundamental Period of Reinforced Concrete Moment-Resisting Frame Structures," *Report No. 87*, The John A. Blume Earthquake Engineering Center, Stanford University, Stanford, October, 1988.

[19] Haviland, R., Biggs, J.M., and Vanmarcke, E.H., "A Study of the Uncertainties in the Fundamental Translational Periods and Damping Values for Real Buildings," *Publication No. R76-12*, Massachusetts Institute of Technology, February, 1976.

[20] Wilson, E.L., Habibullah, A., *SAP-90 A Series of Computer Programs for the Static and Dynamic Finite Element Analysis of Structures*, User's Manual, Computer and Structures, Berkeley, California, 1989.

[21] Shakal, A., "Variability in Strong Motion Processing Results Due to Noise Removal Techniques," *Proceedings, 1989 EERI Annual Meeting*, Earthquake Engineering Research Institute, San Francisco, California, February, 1989.

[22] Kanaan, A.E., and Powell, G.H., "Drain-2D A General Purpose Computer Program for Dynamic Analysis of Inelastic Plane Structures," *Report No. EERC/UCB-72/22*,

Earthquake Engineering Research Center, University of California, Berkeley, California, April, 1973.

[23] Moehle, J.P., and Diebold, J.W., "lateral Load Response of Flat-Plane Frame," *Journal of Structural Engineering*, Vol. 111, No.10, pp. 2149-2164, October 1985.

[24] Park, R., "Detailing of Transverse Reinforcement in Concrete Columns for Ductility," *Proceedings of the Fourth U.S. National Conference on Earthquake Engineering*, Vol. 2, pp. 1037-1046, Palm Springs, California, May, 1990.

[25] Pessiki, S.P., Conley, C., White, R.N., and Gergely, P., "Seismic Behavior of the Beam-Column Connection Region in Lightly-Reinforced Concrete Frame Structures," *Proceedings of the Fourth U.S. National Conference on Earthquake Engineering*, Vol. 2, pp. 707-716, Palm Springs, California, May 1990.

[26] Ziony, J.I., and Yerkes, R.F., "Evaluating Earthquake and Surface-Faulting Potential," *Professional Paper 1360*, Evaluating Earthquake Hazards in the Los Angeles Region - - An Earth-Science Perspective, Department of the Interior, U.S. Geological Survey, pp. 43-91, Washington, D.C., 1985.

[27] Hanks, T.C., and Kanamori, H., "A Moment Magnitude Scale," *Journal of Geophysical Research*, Vol. 84, No. B5, pp. 2348-2350, 1979.

[28] Working Group on California Earthquake Probabilities, "Probabilities of Large Earthquakes Occurring in California on the San Andreas Fault," *Geological Survey Open-File Report*, U.S. Department of the Interior, Geological Survey, U.S. Printing Office, 1988.

[29] Governor's Board of Inquiry on the October 17, 1989 Loma Prieta Earthquake, *"Competing Against Time,"* State of California, May, 1990.

[30] Anderson, J.C., and Bertero, V.V., "Uncertainties in Establishing Design Earthquakes," *Journal of Structural Engineering*, Vol. 113, No. 8, pp. 1709-1724, August, 1987.

[31] Tinley, J.C, and Funal, T.E., "Mapping Quaternary Sedimentary Deposits for Areal Variations in Shaking Response," *Professional Paper 1360*, Evaluating Earthquake Hazards in the Los Angeles Region -- An Earth-Science Perspective, Department of the Interior, U.S. Geological Survey, pp. 101-126, Washington D.C., 1985.

[32] Shakal, A.M., Huang, M., Reichle, M., Ventura, C., Cao, T., Sherburne, R., Savage, M., Darragh, R., and Petersen, C., "CSMIP Strong-Motion Records from the Santa Cruz Mountains (Loma Prieta), California Earthquake of October 17, 1989," *Report No. OSMS 89-06*, California Division of Mines and Geology, California Strong Motion Instrumentation Program, Sacramento, California, 1989.

[33] Brady, A.G., Perez, V., and Mork, P.N., "The Imperial Valley Earthquake, October 15, 1979 Digitization and Processing of Accelerograph Records," *Earthquake Spectra*, Vol. 1, No. 4, pp. 55-74, February, 1988.

[34] Kanamori, H., and Regan, J., "Long-Period Surface Waves in the Imperial Valley, California, Earthquake of October 15, 1979," *Professional Paper 1254*, Department of the Interior, U.S. Geological Survey, pp. 55-58, 1982.

[35] Singh, J.P., "Earthquake Ground Motions: Implications for Designing Structures and Reconciling Structural Damage," *Earthquake Spectra*, Vol. 1, No. 2, pp. 239-270, February, 1985.

[36] Bertero, V.V., "Strength and Deformation Capacities of Buildings Made Under Extreme Environments," Structural Engineering and Structural Mechanics, ed. K. Pister, Prentice Hall, Inc., pp. 188-237, 1980.

EARTHQUAKE ENGINEERING RESEARCH CENTER REPORT SERIES

UCB/EERC-81/01   "Control of Seismic Response of Piping Systems and Other Structures by Base Isolation," by Kelly, J.M., January 1981, (PB81 200 735)A05.

UCB/EERC-81/02   "OPTNSR- An Interactive Software System for Optimal Design of Statically and Dynamically Loaded Structures with Nonlinear Response," by Bhatti, M.A., Ciampi, V. and Pister, K.S., January 1981, (PB81 218 851)A09.

UCB/EERC-81/03   "Analysis of Local Variations in Free Field Seismic Ground Motions," by Chen, J.-C., Lysmer, J. and Seed, H.B., January 1981, (AD-A099508)A13.

UCB/EERC-81/04   "Inelastic Structural Modeling of Braced Offshore Platforms for Seismic Loading," by Zayas, V.A., Shing, P.-S.B., Mahin, S.A. and Popov, E.P., January 1981, INEL4, (PB82 138 777)A07.

UCB/EERC-81/05   "Dynamic Response of Light Equipment in Structures," by Der Kiureghian, A., Sackman, J.L. and Nour-Omid, B., April 1981, (PB81 218 497)A04.

UCB/EERC-81/06   "Preliminary Experimental Investigation of a Broad Base Liquid Storage Tank," by Bouwkamp, J.G., Kollegger, J.P. and Stephen, R.M., May 1981, (PB82 140 385)A03.

UCB/EERC-81/07   "The Seismic Resistant Design of Reinforced Concrete Coupled Structural Walls," by Aktan, A.E. and Bertero, V.V., June 1981, (PB82 113 358)A11.

UCB/EERC-81/08   "Unassigned," by Unassigned, 1981.

UCB/EERC-81/09   "Experimental Behavior of a Spatial Piping System with Steel Energy Absorbers Subjected to a Simulated Differential Seismic Input," by Stiemer, S.F., Godden, W.G. and Kelly, J.M., July 1981, (PB82 201 898)A04.

UCB/EERC-81/10   "Evaluation of Seismic Design Provisions for Masonry in the United States," by Sveinsson, B.I., Mayes, R.L. and McNiven, H.D., August 1981, (PB82 166 075)A08.

UCB/EERC-81/11   "Two-Dimensional Hybrid Modelling of Soil-Structure Interaction," by Tzong, T.-J., Gupta, S. and Penzien, J., August 1981, (PB82 142 118)A04.

UCB/EERC-81/12   "Studies on Effects of Infills in Seismic Resistant R/C Construction," by Brokken, S. and Bertero, V.V., October 1981, (PB82 166 190)A09.

UCB/EERC-81/13   "Linear Models to Predict the Nonlinear Seismic Behavior of a One-Story Steel Frame," by Valdimarsson, H., Shah, A.H. and McNiven, H.D., September 1981, (PB82 138 793)A07.

UCB/EERC-81/14   "TLUSH: A Computer Program for the Three-Dimensional Dynamic Analysis of Earth Dams," by Kagawa, T., Mejia, L.H., Seed, H.B. and Lysmer, J., September 1981, (PB82 139 940)A06.

UCB/EERC-81/15   "Three Dimensional Dynamic Response Analysis of Earth Dams," by Mejia, L.H. and Seed, H.B., September 1981, (PB82 137 274)A12.

UCB/EERC-81/16   "Experimental Study of Lead and Elastomeric Dampers for Base Isolation Systems," by Kelly, J.M. and Hodder, S.B., October 1981, (PB82 166 182)A05.

UCB/EERC-81/17   "The Influence of Base Isolation on the Seismic Response of Light Secondary Equipment," by Kelly, J.M., April 1981, (PB82 255 266)A04.

UCB/EERC-81/18   "Studies on Evaluation of Shaking Table Response Analysis Procedures," by Blondet, J. M., November 1981, (PB82 197 278)A10.

UCB/EERC-81/19   "DELIGHT.STRUCT: A Computer-Aided Design Environment for Structural Engineering," by Balling, R.J., Pister, K.S. and Polak, E., December 1981, (PB82 218 496)A07.

UCB/EERC-81/20   "Optimal Design of Seismic-Resistant Planar Steel Frames," by Balling, R.J., Ciampi, V. and Pister, K.S., December 1981, (PB82 220 179)A07.

UCB/EERC-82/01   "Dynamic Behavior of Ground for Seismic Analysis of Lifeline Systems," by Sato, T. and Der Kiureghian, A., January 1982, (PB82 218 926)A05.

UCB/EERC-82/02   "Shaking Table Tests of a Tubular Steel Frame Model," by Ghanaat, Y. and Clough, R.W., January 1982, (PB82 220 161)A07.

UCB/EERC-82/03   "Behavior of a Piping System under Seismic Excitation: Experimental Investigations of a Spatial Piping System supported by Mechanical Shock Arrestors," by Schneider, S., Lee, H.-M. and Godden, W. G., May 1982, (PB83 172 544)A09.

UCB/EERC-82/04   "New Approaches for the Dynamic Analysis of Large Structural Systems," by Wilson, E.L., June 1982, (PB83 148 080)A05.

UCB/EERC-82/05   "Model Study of Effects of Damage on the Vibration Properties of Steel Offshore Platforms," by Shahrivar, F. and Bouwkamp, J.G., June 1982, (PB83 148 742)A10.

UCB/EERC-82/06   "States of the Art and Pratice in the Optimum Seismic Design and Analytical Response Prediction of R/C Frame Wall Structures," by Aktan, A.E. and Bertero, V.V., July 1982, (PB83 147 736)A05.

UCB/EERC-82/07   "Further Study of the Earthquake Response of a Broad Cylindrical Liquid-Storage Tank Model," by Manos, G.C. and Clough, R.W., July 1982, (PB83 147 744)A11.

UCB/EERC-82/08   "An Evaluation of the Design and Analytical Seismic Response of a Seven Story Reinforced Concrete Frame," by Charney, F.A. and Bertero, V.V., July 1982, (PB83 157 628)A09.

UCB/EERC-82/09   "Fluid-Structure Interactions: Added Mass Computations for Incompressible Fluid," by Kuo, J.S.-H., August 1982, (PB83 156 281)A07.

UCB/EERC-82/10   "Joint-Opening Nonlinear Mechanism: Interface Smeared Crack Model," by Kuo, J.S.-H., August 1982, (PB83 149 195)A05.

UCB/EERC-82/11   "Dynamic Response Analysis of Techi Dam," by Clough, R.W., Stephen, R.M. and Kuo, J.S.-H., August 1982, (PB83 147 496)A06.

UCB/EERC-82/12   "Prediction of the Seismic Response of R/C Frame-Coupled Wall Structures," by Aktan, A.E., Bertero, V.V. and Piazzo, M., August 1982, (PB83 149 203)A09.

UCB/EERC-82/13   "Preliminary Report on the Smart 1 Strong Motion Array in Taiwan," by Bolt, B.A., Loh, C.H., Penzien, J. and Tsai, Y.B., August 1982, (PB83 159 400)A10.

UCB/EERC-82/14   "Seismic Behavior of an Eccentrically X-Braced Steel Structure," by Yang, M.S., September 1982, (PB83 260 778)A12.

UCB/EERC-82/15   "The Performance of Stairways in Earthquakes," by Roha, C., Axley, J.W. and Bertero, V.V., September 1982, (PB83 157 693)A07.

UCB/EERC-82/16   "The Behavior of Submerged Multiple Bodies in Earthquakes," by Liao, W.-G., September 1982, (PB83 158 709)A07.

UCB/EERC-82/17   "Effects of Concrete Types and Loading Conditions on Local Bond-Slip Relationships," by Cowell, A.D., Popov, E.P. and Bertero, V.V., September 1982, (PB83 153 577)A04.

UCB/EERC-82/18   "Mechanical Behavior of Shear Wall Vertical Boundary Members: An Experimental Investigation," by Wagner, M.T. and Bertero, V.V., October 1982, (PB83 159 764)A05.

UCB/EERC-82/19   "Experimental Studies of Multi-support Seismic Loading on Piping Systems," by Kelly, J.M. and Cowell, A.D., November 1982, (PB90 262 684)A07.

UCB/EERC-82/20   "Generalized Plastic Hinge Concepts for 3D Beam-Column Elements," by Chen, P. F.-S. and Powell, G.H., November 1982, (PB83 247 981)A13.

UCB/EERC-82/21   "ANSR-II: General Computer Program for Nonlinear Structural Analysis," by Oughourlian, C.V. and Powell, G.H., November 1982, (PB83 251 330)A12.

UCB/EERC-82/22   "Solution Strategies for Statically Loaded Nonlinear Structures," by Simons, J.W. and Powell, G.H., November 1982, (PB83 197 970)A06.

UCB/EERC-82/23   "Analytical Model of Deformed Bar Anchorages under Generalized Excitations," by Ciampi, V., Eligehausen, R., Bertero, V.V. and Popov, E.P., November 1982, (PB83 169 532)A06.

UCB/EERC-82/24   "A Mathematical Model for the Response of Masonry Walls to Dynamic Excitations," by Sucuoglu, H., Mengi, Y. and McNiven, H.D., November 1982, (PB83 169 011)A07.

UCB/EERC-82/25   "Earthquake Response Considerations of Broad Liquid Storage Tanks," by Cambra, F.J., November 1982, (PB83 251 215)A09.

UCB/EERC-82/26   "Computational Models for Cyclic Plasticity, Rate Dependence and Creep," by Mosaddad, B. and Powell, G.H., November 1982, (PB83 245 829)A08.

UCB/EERC-82/27   "Inelastic Analysis of Piping and Tubular Structures," by Mahasuverachai, M. and Powell, G.H., November 1982, (PB83 249 987)A07.

UCB/EERC-83/01   "The Economic Feasibility of Seismic Rehabilitation of Buildings by Base Isolation," by Kelly, J.M., January 1983, (PB83 197 988)A05.

UCB/EERC-83/02   "Seismic Moment Connections for Moment-Resisting Steel Frames.," by Popov, E.P., January 1983, (PB83 195 412)A04.

UCB/EERC-83/03   "Design of Links and Beam-to-Column Connections for Eccentrically Braced Steel Frames," by Popov, E.P. and Malley, J.O., January 1983, (PB83 194 811)A04.

UCB/EERC-83/04   "Numerical Techniques for the Evaluation of Soil-Structure Interaction Effects in the Time Domain," by Bayo, E. and Wilson, E.L., February 1983, (PB83 245 605)A09.

UCB/EERC-83/05   "A Transducer for Measuring the Internal Forces in the Columns of a Frame-Wall Reinforced Concrete Structure," by Sause, R. and Bertero, V.V., May 1983, (PB84 119 494)A06.

UCB/EERC-83/06   "Dynamic Interactions Between Floating Ice and Offshore Structures," by Croteau, P., May 1983, (PB84 119 486)A16.

UCB/EERC-83/07   "Dynamic Analysis of Multiply Tuned and Arbitrarily Supported Secondary Systems," by Igusa, T. and Der Kiureghian, A., July 1983, (PB84 118 272)A11.

UCB/EERC-83/08   "A Laboratory Study of Submerged Multi-body Systems in Earthquakes," by Ansari, G.R., June 1983, (PB83 261 842)A17.

UCB/EERC-83/09   "Effects of Transient Foundation Uplift on Earthquake Response of Structures," by Yim, C.-S. and Chopra, A.K., June 1983, (PB83 261 396)A07.

UCB/EERC-83/10   "Optimal Design of Friction-Braced Frames under Seismic Loading," by Austin, M.A. and Pister, K.S., June 1983, (PB84 119 288)A06.

UCB/EERC-83/11   "Shaking Table Study of Single-Story Masonry Houses: Dynamic Performance under Three Component Seismic Input and Recommendations," by Manos, G.C., Clough, R.W. and Mayes, R.L., July 1983, (UCB/EERC-83/11)A08.

UCB/EERC-83/12   "Experimental Error Propagation in Pseudodynamic Testing," by Shiing, P.B. and Mahin, S.A., June 1983, (PB84 119 270)A09.

UCB/EERC-83/13   "Experimental and Analytical Predictions of the Mechanical Characteristics of a 1/5-scale Model of a 7-story R/C Frame-Wall Building Structure," by Aktan, A.E., Bertero, V.V., Chowdhury, A.A. and Nagashima, T., June 1983, (PB84 119 213)A07.

UCB/EERC-83/14   "Shaking Table Tests of Large-Panel Precast Concrete Building System Assemblages," by Oliva, M.G. and Clough, R.W., June 1983, (PB86 110 210/AS)A11.

UCB/EERC-83/15   "Seismic Behavior of Active Beam Links in Eccentrically Braced Frames," by Hjelmstad, K.D. and Popov, E.P., July 1983, (PB84 119 676)A09.

UCB/EERC-83/16   "System Identification of Structures with Joint Rotation," by Dimsdale, J.S., July 1983, (PB84 192 210)A06.

UCB/EERC-83/17   "Construction of Inelastic Response Spectra for Single-Degree-of-Freedom Systems," by Mahin, S. and Lin, J., June 1983, (PB84 208 834)A05.

UCB/EERC-83/18   "Interactive Computer Analysis Methods for Predicting the Inelastic Cyclic Behaviour of Structural Sections," by Kaba, S. and Mahin, S., July 1983, (PB84 192 012)A06.

UCB/EERC-83/19   "Effects of Bond Deterioration on Hysteretic Behavior of Reinforced Concrete Joints," by Filippou. F.C., Popov, E.P. and Bertero, V.V., August 1983, (PB84 192 020)A10.

UCB/EERC-83/20 "Correlation of Analytical and Experimental Responses of Large-Panel Precast Building Systems," by Oliva, M.G., Clough, R.W., Velkov, M. and Gavrilovic, P., May 1988, (PB90 262 692)A06.

UCB/EERC-83/21 "Mechanical Characteristics of Materials Used in a 1/5 Scale Model of a 7-Story Reinforced Concrete Test Structure," by Bertero, V.V., Aktan, A.E., Harris, H.G. and Chowdhury, A.A., October 1983, (PB84 193 697)A05.

UCB/EERC-83/22 "Hybrid Modelling of Soil-Structure Interaction in Layered Media," by Tzong, T.-J. and Penzien, J., October 1983, (PB84 192 178)A08.

UCB/EERC-83/23 "Local Bond Stress-Slip Relationships of Deformed Bars under Generalized Excitations," by Eligehausen, R., Popov, E.P. and Bertero, V.V., October 1983, (PB84 192 848)A09.

UCB/EERC-83/24 "Design Considerations for Shear Links in Eccentrically Braced Frames," by Malley, J.O. and Popov, E.P., November 1983, (PB84 192 186)A07.

UCB/EERC-84/01 "Pseudodynamic Test Method for Seismic Performance Evaluation: Theory and Implementation," by Shing, P.-S.B. and Mahin, S.A., January 1984, (PB84 190 644)A08.

UCB/EERC-84/02 "Dynamic Response Behavior of Kiang Hong Dian Dam," by Clough, R.W., Chang, K.-T., Chen, H.-Q. and Stephen, R.M., April 1984, (PB84 209 402)A08.

UCB/EERC-84/03 "Refined Modelling of Reinforced Concrete Columns for Seismic Analysis," by Kaba, S.A. and Mahin, S.A., April 1984, (PB84 234 384)A06.

UCB/EERC-84/04 "A New Floor Response Spectrum Method for Seismic Analysis of Multiply Supported Secondary Systems," by Asfura, A. and Der Kiureghian, A., June 1984, (PB84 239 417)A06.

UCB/EERC-84/05 "Earthquake Simulation Tests and Associated Studies of a 1/5th-scale Model of a 7-Story R/C Frame-Wall Test Structure," by Bertero, V.V., Aktan, A.E., Charney, F.A. and Sause, R., June 1984, (PB84 239 409)A09.

UCB/EERC-84/06 "Unassigned," by Unassigned, 1984.

UCB/EERC-84/07 "Behavior of Interior and Exterior Flat-Plate Connections subjected to Inelastic Load Reversals," by Zee, H.L. and Moehle, J.P., August 1984, (PB86 117 629/AS)A07.

UCB/EERC-84/08 "Experimental Study of the Seismic Behavior of a Two-Story Flat-Plate Structure," by Moehle, J.P. and Diebold, J.W., August 1984, (PB86 122 553/AS)A12.

UCB/EERC-84/09 "Phenomenological Modeling of Steel Braces under Cyclic Loading," by Ikeda, K., Mahin, S.A. and Dermitzakis, S.N., May 1984, (PB86 132 198/AS)A08.

UCB/EERC-84/10 "Earthquake Analysis and Response of Concrete Gravity Dams," by Fenves, G. and Chopra, A.K., August 1984, (PB85 193 902/AS)A11.

UCB/EERC-84/11 "EAGD-84: A Computer Program for Earthquake Analysis of Concrete Gravity Dams," by Fenves, G. and Chopra, A.K., August 1984, (PB85 193 613/AS)A05.

UCB/EERC-84/12 "A Refined Physical Theory Model for Predicting the Seismic Behavior of Braced Steel Frames," by Ikeda, K. and Mahin, S.A., July 1984, (PB85 191 450/AS)A09.

UCB/EERC-84/13 "Earthquake Engineering Research at Berkeley - 1984," by EERC, August 1984, (PB85 197 341/AS)A10.

UCB/EERC-84/14 "Moduli and Damping Factors for Dynamic Analyses of Cohesionless Soils," by Seed, H.B., Wong, R.T., Idriss, I.M. and Tokimatsu, K., September 1984, (PB85 191 468/AS)A04.

UCB/EERC-84/15 "The Influence of SPT Procedures in Soil Liquefaction Resistance Evaluations," by Seed, H.B., Tokimatsu, K., Harder, L.F. and Chung, R.M., October 1984, (PB85 191 732/AS)A04.

UCB/EERC-84/16 "Simplified Procedures for the Evaluation of Settlements in Sands Due to Earthquake Shaking," by Tokimatsu, K. and Seed, H.B., October 1984, (PB85 197 887/AS)A03.

UCB/EERC-84/17 "Evaluation of Energy Absorption Characteristics of Highway Bridges Under Seismic Conditions - Volume I (PB90 262 627)A16 and Volume II (Appendices) (PB90 262 635)A13," by Imbsen, R.A. and Penzien, J., September 1986.

UCB/EERC-84/18 "Structure-Foundation Interactions under Dynamic Loads," by Liu, W.D. and Penzien, J., November 1984, (PB87 124 889/AS)A11.

UCB/EERC-84/19 "Seismic Modelling of Deep Foundations," by Chen, C.-H. and Penzien, J., November 1984, (PB87 124 798/AS)A07.

UCB/EERC-84/20 "Dynamic Response Behavior of Quan Shui Dam," by Clough, R.W., Chang, K.-T., Chen, H.-Q., Stephen, R.M., Ghanaat, Y. and Qi, J.-H., November 1984, (PB86 115177/AS)A07.

UCB/EERC-85/01 "Simplified Methods of Analysis for Earthquake Resistant Design of Buildings," by Cruz, E.F. and Chopra, A.K., February 1985, (PB86 112299/AS)A12.

UCB/EERC-85/02 "Estimation of Seismic Wave Coherency and Rupture Velocity using the SMART 1 Strong-Motion Array Recordings," by Abrahamson, N.A., March 1985, (PB86 214 343)A07.

UCB/EERC-85/03 "Dynamic Properties of a Thirty Story Condominium Tower Building," by Stephen, R.M., Wilson, E.L. and Stander, N., April 1985, (PB86 118965/AS)A06.

UCB/EERC-85/04 "Development of Substructuring Techniques for On-Line Computer Controlled Seismic Performance Testing," by Dermitzakis, S. and Mahin, S., February 1985, (PB86 132941/AS)A08.

UCB/EERC-85/05 "A Simple Model for Reinforcing Bar Anchorages under Cyclic Excitations," by Filippou, F.C., March 1985, (PB86 112 919/AS)A05.

UCB/EERC-85/06 "Racking Behavior of Wood-framed Gypsum Panels under Dynamic Load," by Oliva, M.G., June 1985, (PB90 262 643)A04.

UCB/EERC-85/07 "Earthquake Analysis and Response of Concrete Arch Dams," by Fok, K.-L. and Chopra, A.K., June 1985, (PB86 139672/AS)A10.

UCB/EERC-85/08 "Effect of Inelastic Behavior on the Analysis and Design of Earthquake Resistant Structures," by Lin, J.P. and Mahin, S.A., June 1985, (PB86 135340/AS)A08.

UCB/EERC-85/09 "Earthquake Simulator Testing of a Base-Isolated Bridge Deck," by Kelly, J.M., Buckle, I.G. and Tsai, H.-C., January 1986, (PB87 124 152/AS)A06.

UCB/EERC-85/10   "Simplified Analysis for Earthquake Resistant Design of Concrete Gravity Dams," by Fenves, G. and Chopra, A.K., June 1986, (PB87 124 160/AS)A08.

UCB/EERC-85/11   "Dynamic Interaction Effects in Arch Dams," by Clough, R.W., Chang, K.-T., Chen, H.-Q. and Ghanaat, Y., October 1985, (PB86 135027/AS)A05.

UCB/EERC-85/12   "Dynamic Response of Long Valley Dam in the Mammoth Lake Earthquake Series of May 25-27, 1980," by Lai, S. and Seed, H.B., November 1985, (PB86 142304/AS)A05.

UCB/EERC-85/13   "A Methodology for Computer-Aided Design of Earthquake-Resistant Steel Structures," by Austin, M.A., Pister, K.S. and Mahin, S.A., December 1985, (PB86 159480/AS)A10 .

UCB/EERC-85/14   "Response of Tension-Leg Platforms to Vertical Seismic Excitations," by Liou, G.-S., Penzien, J. and Yeung, R.W., December 1985, (PB87 124 871/AS)A08.

UCB/EERC-85/15   "Cyclic Loading Tests of Masonry Single Piers: Volume 4 - Additional Tests with Height to Width Ratio of 1," by Sveinsson, B., McNiven, H.D. and Sucuoglu, H., December 1985.

UCB/EERC-85/16   "An Experimental Program for Studying the Dynamic Response of a Steel Frame with a Variety of Infill Partitions," by Yanev, B. and McNiven, H.D., December 1985, (PB90 262 676)A05.

UCB/EERC-86/01   "A Study of Seismically Resistant Eccentrically Braced Steel Frame Systems," by Kasai, K. and Popov, E.P., January 1986, (PB87 124 178/AS)A14.

UCB/EERC-86/02   "Design Problems in Soil Liquefaction," by Seed, H.B., February 1986, (PB87 124 186/AS)A03.

UCB/EERC-86/03   "Implications of Recent Earthquakes and Research on Earthquake-Resistant Design and Construction of Buildings," by Bertero, V.V., March 1986, (PB87 124 194/AS)A05.

UCB/EERC-86/04   "The Use of Load Dependent Vectors for Dynamic and Earthquake Analyses," by Leger, P., Wilson, E.L. and Clough, R.W., March 1986, (PB87 124 202/AS)A12.

UCB/EERC-86/05   "Two Beam-To-Column Web Connections," by Tsai, K.-C. and Popov, E.P., April 1986, (PB87 124 301/AS)A04.

UCB/EERC-86/06   "Determination of Penetration Resistance for Coarse-Grained Soils using the Becker Hammer Drill," by Harder, L.F. and Seed, H.B., May 1986, (PB87 124 210/AS)A07.

UCB/EERC-86/07   "A Mathematical Model for Predicting the Nonlinear Response of Unreinforced Masonry Walls to In-Plane Earthquake Excitations," by Mengi, Y. and McNiven, H.D., May 1986, (PB87 124 780/AS)A06.

UCB/EERC-86/08   "The 19 September 1985 Mexico Earthquake: Building Behavior," by Bertero, V.V., July 1986.

UCB/EERC-86/09   "EACD-3D: A Computer Program for Three-Dimensional Earthquake Analysis of Concrete Dams," by Fok, K.-L., Hall, J.F. and Chopra, A.K., July 1986, (PB87 124 228/AS)A08.

UCB/EERC-86/10   "Earthquake Simulation Tests and Associated Studies of a 0.3-Scale Model of a Six-Story Concentrically Braced Steel Structure," by Uang, C.-M. and Bertero, V.V., December 1986, (PB87 163 564/AS)A17.

UCB/EERC-86/11   "Mechanical Characteristics of Base Isolation Bearings for a Bridge Deck Model Test," by Kelly, J.M., Buckle, I.G. and Koh, C.-G., November 1987, (PB90 262 668)A04.

UCB/EERC-86/12   "Effects of Axial Load on Elastomeric Isolation Bearings," by Koh, C.-G. and Kelly, J.M., November 1987.

UCB/EERC-87/01   "The FPS Earthquake Resisting System: Experimental Report," by Zayas, V.A., Low, S.S. and Mahin, S.A., June 1987.

UCB/EERC-87/02   "Earthquake Simulator Tests and Associated Studies of a 0.3-Scale Model of a Six-Story Eccentrically Braced Steel Structure," by Whittaker, A., Uang, C.-M. and Bertero, V.V., July 1987.

UCB/EERC-87/03   "A Displacement Control and Uplift Restraint Device for Base-Isolated Structures," by Kelly, J.M., Griffith, M.C. and Aiken, I.D., April 1987.

UCB/EERC-87/04   "Earthquake Simulator Testing of a Combined Sliding Bearing and Rubber Bearing Isolation System," by Kelly, J.M. and Chalhoub, M.S., 1987.

UCB/EERC-87/05   "Three-Dimensional Inelastic Analysis of Reinforced Concrete Frame-Wall Structures," by Moazzami, S. and Bertero, V.V., May 1987.

UCB/EERC-87/06   "Experiments on Eccentrically Braced Frames with Composite Floors," by Ricles, J. and Popov, E., June 1987.

UCB/EERC-87/07   "Dynamic Analysis of Seismically Resistant Eccentrically Braced Frames," by Ricles, J. and Popov, E., June 1987.

UCB/EERC-87/08   "Undrained Cyclic Triaxial Testing of Gravels-The Effect of Membrane Compliance," by Evans, M.D. and Seed, H.B., July 1987.

UCB/EERC-87/09   "Hybrid Solution Techniques for Generalized Pseudo-Dynamic Testing," by Thewalt, C. and Mahin, S.A., July 1987.

UCB/EERC-87/10   "Ultimate Behavior of Butt Welded Splices in Heavy Rolled Steel Sections," by Bruneau, M., Mahin, S.A. and Popov, E.P., September 1987.

UCB/EERC-87/11   "Residual Strength of Sand from Dam Failures in the Chilean Earthquake of March 3, 1985," by De Alba, P., Seed, H.B., Retamal, E. and Seed, R.B., September 1987.

UCB/EERC-87/12   "Inelastic Seismic Response of Structures with Mass or Stiffness Eccentricities in Plan," by Bruneau, M. and Mahin, S.A., September 1987, (PB90 262 650)A14.

UCB/EERC-87/13   "CSTRUCT: An Interactive Computer Environment for the Design and Analysis of Earthquake Resistant Steel Structures," by Austin, M.A., Mahin, S.A. and Pister, K.S., September 1987.

UCB/EERC-87/14   "Experimental Study of Reinforced Concrete Columns Subjected to Multi-Axial Loading," by Low, S.S. and Moehle, J.P., September 1987.

UCB/EERC-87/15   "Relationships between Soil Conditions and Earthquake Ground Motions in Mexico City in the Earthquake of Sept. 19, 1985," by Seed, H.B., Romo, M.P., Sun, J., Jaime, A. and Lysmer, J., October 1987.

UCB/EERC-87/16   "Experimental Study of Seismic Response of R. C. Setback Buildings," by Shahrooz, B.M. and Moehle, J.P., October 1987.

UCB/EERC-87/17   "The Effect of Slabs on the Flexural Behavior of Beams," by Pantazopoulou, S.J. and Moehle, J.P., October 1987, (PB90 262 700)A07.

UCB/EERC-87/18   "Design Procedure for R-FBI Bearings," by Mostaghel, N. and Kelly, J.M., November 1987, (PB90 262 718)A04.

UCB/EERC-87/19   "Analytical Models for Predicting the Lateral Response of R C Shear Walls: Evaluation of their Reliability," by Vulcano, A. and Bertero, V.V., November 1987.

UCB/EERC-87/20   "Earthquake Response of Torsionally-Coupled Buildings," by Hejal, R. and Chopra, A.K., December 1987.

UCB/EERC-87/21   "Dynamic Reservoir Interaction with Monticello Dam," by Clough, R.W., Ghanaat, Y. and Qiu, X-F., December 1987.

UCB/EERC-87/22   "Strength Evaluation of Coarse-Grained Soils," by Siddiqi, F.H., Seed, R.B., Chan, C.K., Seed, H.B. and Pyke, R.M., December 1987.

UCB/EERC-88/01   "Seismic Behavior of Concentrically Braced Steel Frames," by Khatib, I., Mahin, S.A. and Pister, K.S., January 1988.

UCB/EERC-88/02   "Experimental Evaluation of Seismic Isolation of Medium-Rise Structures Subject to Uplift," by Griffith, M.C., Kelly, J.M., Coveney, V.A. and Koh, C.G., January 1988.

UCB/EERC-88/03   "Cyclic Behavior of Steel Double Angle Connections," by Astaneh-Asl, A. and Nader, M.N., January 1988.

UCB/EERC-88/04   "Re-evaluation of the Slide in the Lower San Fernando Dam in the Earthquake of Feb. 9, 1971," by Seed, H.B., Seed, R.B., Harder, L.F. and Jong, H.-L., April 1988.

UCB/EERC-88/05   "Experimental Evaluation of Seismic Isolation of a Nine-Story Braced Steel Frame Subject to Uplift," by Griffith, M.C., Kelly, J.M. and Aiken, I.D., May 1988.

UCB/EERC-88/06   "DRAIN-2DX User Guide.," by Allahabadi, R. and Powell, G.H., March 1988.

UCB/EERC-88/07   "Theoretical and Experimental Studies of Cylindrical Water Tanks in Base-Isolated Structures," by Chalhoub, M.S. and Kelly, J.M., April 1988.

UCB/EERC-88/08   "Analysis of Near-Source Waves: Separation of Wave Types using Strong Motion Array Recordings," by Darragh, R.B., June 1988.

UCB/EERC-88/09   "Alternatives to Standard Mode Superposition for Analysis of Non-Classically Damped Systems," by Kusainov, A.A. and Clough, R.W., June 1988.

UCB/EERC-88/10   "The Landslide at the Port of Nice on October 16, 1979," by Seed, H.B., Seed, R.B., Schlosser, F., Blondeau, F. and Juran, I., June 1988.

UCB/EERC-88/11   "Liquefaction Potential of Sand Deposits Under Low Levels of Excitation," by Carter, D.P. and Seed, H.B., August 1988.

UCB/EERC-88/12   "Nonlinear Analysis of Reinforced Concrete Frames Under Cyclic Load Reversals," by Filippou, F.C. and Issa, A., September 1988.

UCB/EERC-88/13   "Implications of Recorded Earthquake Ground Motions on Seismic Design of Building Structures," by Uang, C.-M. and Bertero, V.V., November 1988.

UCB/EERC-88/14   "An Experimental Study of the Behavior of Dual Steel Systems," by Whittaker, A.S. , Uang, C.-M. and Bertero, V.V., September 1988.

UCB/EERC-88/15   "Dynamic Moduli and Damping Ratios for Cohesive Soils," by Sun, J.I., Golesorkhi, R. and Seed, H.B., August 1988.

UCB/EERC-88/16   "Reinforced Concrete Flat Plates Under Lateral Load: An Experimental Study Including Biaxial Effects," by Pan, A. and Moehle, J., October 1988.

UCB/EERC-88/17   "Earthquake Engineering Research at Berkeley - 1988," by EERC, November 1988.

UCB/EERC-88/18   "Use of Energy as a Design Criterion in Earthquake-Resistant Design," by Uang, C.-M. and Bertero, V.V., November 1988.

UCB/EERC-88/19   "Steel Beam-Column Joints in Seismic Moment Resisting Frames," by Tsai, K.-C. and Popov, E.P., November 1988.

UCB/EERC-88/20   "Base Isolation in Japan, 1988," by Kelly, J.M., December 1988.

UCB/EERC-89/01   "Behavior of Long Links in Eccentrically Braced Frames," by Engelhardt, M.D. and Popov, E.P., January 1989.

UCB/EERC-89/02   "Earthquake Simulator Testing of Steel Plate Added Damping and Stiffness Elements," by Whittaker, A., Bertero, V.V., Alonso, J. and Thompson, C., January 1989.

UCB/EERC-89/03   "Implications of Site Effects in the Mexico City Earthquake of Sept. 19, 1985 for Earthquake-Resistant Design Criteria in the San Francisco Bay Area of California," by Seed, H.B. and Sun, J.I., March 1989.

UCB/EERC-89/04   "Earthquake Analysis and Response of Intake-Outlet Towers," by Goyal, A. and Chopra, A.K., July 1989.

UCB/EERC-89/05   "The 1985 Chile Earthquake: An Evaluation of Structural Requirements for Bearing Wall Buildings," by Wallace, J.W. and Moehle, J.P., July 1989.

UCB/EERC-89/06   "Effects of Spatial Variation of Ground Motions on Large Multiply-Supported Structures," by Hao, H., July 1989.

UCB/EERC-89/07   "EADAP - Enhanced Arch Dam Analysis Program: Users's Manual," by Ghanaat, Y. and Clough, R.W., August 1989.

UCB/EERC-89/08   "Seismic Performance of Steel Moment Frames Plastically Designed by Least Squares Stress Fields," by Ohi, K. and Mahin, S.A., August 1989.

UCB/EERC-89/09   "Feasibility and Performance Studies on Improving the Earthquake Resistance of New and Existing Buildings Using the Friction Pendulum System," by Zayas, V., Low, S., Mahin, S.A. and Bozzo, L., July 1989.

UCB/EERC-89/10   "Measurement and Elimination of Membrane Compliance Effects in Undrained Triaxial Testing," by Nicholson, P.G., Seed, R.B. and Anwar, H., September 1989.

UCB/EERC-89/11   "Static Tilt Behavior of Unanchored Cylindrical Tanks," by Lau, D.T. and Clough, R.W., September 1989.

UCB/EERC-89/12   "ADAP-88: A Computer Program for Nonlinear Earthquake Analysis of Concrete Arch Dams," by Fenves, G.L., Mojtahedi, S. and Reimer, R.B., September 1989.

UCB/EERC-89/13   "Mechanics of Low Shape Factor Elastomeric Seismic Isolation Bearings," by Aiken, I.D., Kelly, J.M. and Tajirian, F.F., November 1989.

UCB/EERC-89/14   "Preliminary Report on the Seismological and Engineering Aspects of the October 17, 1989 Santa Cruz (Loma Prieta) Earthquake," by EERC, October 1989.

UCB/EERC-89/15   "Experimental Studies of a Single Story Steel Structure Tested with Fixed, Semi-Rigid and Flexible Connections," by Nader, M.N. and Astaneh-Asl, A., August 1989, (PB91 229 211/AS)A10.

UCB/EERC-89/16   "Collapse of the Cypress Street Viaduct as a Result of the Loma Prieta Earthquake," by Nims, D.K., Miranda, E., Aiken, I.D., Whittaker, A.S. and Bertero, V.V., November 1989, (PB91 217 935/AS)A05.

UCB/EERC-90/01   "Mechanics of High-Shape Factor Elastomeric Seismic Isolation Bearings," by Kelly, J.M., Aiken, I.D. and Tajirian, F.F., March 1990.

UCB/EERC-90/02   "Javid's Paradox: The Influence of Preform on the Modes of Vibrating Beams," by Kelly, J.M., Sackman, J.L. and Javid, A., May 1990, (PB91 217 943/AS)A03.

UCB/EERC-90/03   "Earthquake Simulator Testing and Analytical Studies of Two Energy-Absorbing Systems for Multistory Structures," by Aiken, I.D. and Kelly, J.M., October 1990.

UCB/EERC-90/04   "Damage to the San Francisco-Oakland Bay Bridge During the October 17, 1989 Earthquake," by Astaneh, A., June 1990.

UCB/EERC-90/05   "Preliminary Report on the Principal Geotechnical Aspects of the October 17, 1989 Loma Prieta Earthquake," by Seed, R.B., Dickenson, S.E., Riemer, M.F., Bray, J.D., Sitar, N., Mitchell, J.K., Idriss, I.M., Kayen, R.E., Kropp, A., Harder, L.F., Jr. and Power, M.S., April 1990.

UCB/EERC-90/06   "Models of Critical Regions in Reinforced Concrete Frames Under Seismic Excitations," by Zulfiqar, N. and Filippou, F., May 1990.

UCB/EERC-90/07   "A Unified Earthquake-Resistant Design Method for Steel Frames Using ARMA Models," by Takewaki, I., Conte, J.P., Mahin, S.A. and Pister, K.S., June 1990.

UCB/EERC-90/08   "Soil Conditions and Earthquake Hazard Mitigation in the Marina District of San Francisco," by Mitchell, J.K., Masood, T., Kayen, R.E. and Seed, R.B., May 1990.

UCB/EERC-90/09   "Influence of the Earthquake Ground Motion Process and Structural Properties on Response Characteristics of Simple Structures," by Conte, J.P., Pister, K.S. and Mahin, S.A., July 1990.

UCB/EERC-90/10   "Experimental Testing of the Resilient-Friction Base Isolation System," by Clark, P.W. and Kelly, J.M., July 1990.

UCB/EERC-90/11   "Seismic Hazard Analysis: Improved Models, Uncertainties and Sensitivities," by Araya, R. and Der Kiureghian, A., March 1988.

UCB/EERC-90/12   "Effects of Torsion on the Linear and Nonlinear Seismic Response of Structures," by Sedarat, H. and Bertero, V.V., September 1989.

UCB/EERC-90/13   "The Effects of Tectonic Movements on Stresses and Deformations in Earth Embankments," by Bray, J. D., Seed, R. B. and Seed, H. B., September 1989.

UCB/EERC-90/14   "Inelastic Seismic Response of One-Story, Asymmetric-Plan Systems," by Goel, R.K. and Chopra, A.K., October 1990.

UCB/EERC-90/15   "Dynamic Crack Propagation: A Model for Near-Field Ground Motion.," by Seyyedian, H. and Kelly, J.M., 1990.

UCB/EERC-90/16   "Sensitivity of Long-Period Response Spectra to System Initial Conditions," by Blasquez, R., Ventura, C. and Kelly, J.M., 1990.

UCB/EERC-90/17   "Behavior of Peak Values and Spectral Ordinates of Near-Source Strong Ground-Motion over a Dense Array," by Niazi, M., June 1990.

UCB/EERC-90/18   "Material Characterization of Elastomers used in Earthquake Base Isolation," by Papoulia, K.D. and Kelly, J.M., 1990.

UCB/EERC-90/19   "Cyclic Behavior of Steel Top-and-Bottom Plate Moment Connections," by Harriott, J.D. and Astaneh, A., August 1990, (PB91 229 260/AS)A05.

UCB/EERC-90/20   "Seismic Response Evaluation of an Instrumented Six Story Steel Building," by Shen, J.-H. and Astaneh, A., December 1990.

UCB/EERC-90/21   "Observations and Implications of Tests on the Cypress Street Viaduct Test Structure," by Bollo, M., Mahin, S.A., Moehle, J.P., Stephen, R.M. and Qi, X., December 1990.

UCB/EERC-91/01   "Experimental Evaluation of Nitinol for Energy Dissipation in Structures," by Nims, D.K., Sasaki, K.K. and Kelly, J.M., 1991.

UCB/EERC-91/02   "Displacement Design Approach for Reinforced Concrete Structures Subjected to Earthquakes," by Qi, X. and Moehle, J.P., January 1991.

UCB/EERC-91/03   "Shake Table Tests of Long Period Isolation System for Nuclear Facilities at Soft Soil Sites," by Kelly, J.M., March 1991.

UCB/EERC-91/04   "Dynamic and Failure Characteristics of Bridgestone Isolation Bearings," by Kelly, J.M., April 1991.

UCB/EERC-91/05   "Base Sliding Response of Concrete Gravity Dams to Earthquakes," by Chopra, A.K. and Zhang, L., May 1991.

UCB/EERC-91/06   "Computation of Spatially Varying Ground Motion and Foundation-Rock Impedance Matrices for Seismic Analysis of Arch Dams," by Zhang, L. and Chopra, A.K., May 1991.

UCB/EERC-91/07   "Estimation of Seismic Source Processes Using Strong Motion Array Data," by Chiou, S.-J., July 1991.

UCB/EERC-91/08   "A Response Spectrum Method for Multiple-Support Seismic Excitations," by Der Kiureghian, A. and Neuenhofer, A., August 1991.

UCB/EERC-91/09   "A Preliminary Study on Energy Dissipating Cladding-to-Frame Connection," by Cohen, J.M. and Powell, G.H., September 1991.

UCB/EERC-91/10   "Evaluation of Seismic Performance of a Ten-Story RC Building During the Whittier Narrows Earthquake," by Miranda, E. and Bertero, V.V., October 1991.